ENGINEERING EVALUATION of the LORAN - C NAVIGATION SYSTEM

FINAL REPORT

SEPTEMBER 30, 1959

by

W. T. Dickinson

JANSKY & BAILEY, INC.

PREPARED FOR

THE UNITED STATES COAST GUARD

U.S. COAST GUARD CONTRACT
NO. Tcg-40547 (CG-40,502-A)

ABSTRACT

Loran-C is a pulsed low frequency long-range system of radionavigation. It operates in the frequency band 90-110 kc which was allocated on a world-wide basis by the International Telecommunications Union Conference in 1947 for the development of a long distance radionavigation system. The first Loran-C system was installed on the U.S. East Coast for the U.S. Navy in 1957. This reports gives the results of tests in the ground wave service area, the results of limited tests and observations in the sky wave area, and theoretical considerations concerning the range and accuracy of Loran-C in both the ground wave area and sky wave areas.

The results indicate that Loran-C systems can provide long distance radionavigation service with a probable error of one-tenth to two-tenths of a microsecond at the extreme limit of the ground wave area. For a system having 1000 kw peak radiated power the maximum ground wave range is about 1700 nautical miles in the daytime and about 1200 nautical miles at night on over-water paths in many areas of the world. The maximum range will be greater or less than this, depending upon the level of atmospheric noise in the receiving area. Ranges over land are slightly less than over water.

Results to date are most encouraging for using sky waves for radionavigation with probable errors of 1 to 1.5 microseconds. Nighttime sky wave ranges of about 2800 nautical miles are indicated for systems of 1000 kw peak radiated power. Daytime ranges of 2000 to 2600 nautical miles, depending upon the season of the year and transmitter power, can be expected.

TABLE OF CONTENTS

SECTION I
INTRODUCTORY BACKGROUND

A. INTRODUCTION

Loran-C is a pulsed low frequency long-range system of hyperbolic navigation. It operates in the frequency band 90-110 kc which was allocated on a world-wide basis for long distance radionavigation by the International Telecommunications Union Conference in 1947.

The first Loran-C navigation system was installed on the U.S. East Coast in 1957 by the Sperry Gyroscope Company, under supervision of the U.S. Coast Guard, to provide special purpose navigation service for the U.S. Navy. Under a separate contract with the U.S. Coast Guard, Jansky & Bailey, Inc. has performed engineering consultatory services for the purpose of evaluating the Loran-C system as a long-range navigation aid. The evaluation is based on analysis of data obtained from the East Coast Chain, measurements made to determine the extent of ground wave and sky wave coverage, and theoretical considerations of equipment design and radio wave propagation.

B. HISTORICAL BACKGROUND

1. Low Frequency Loran in World War II

The range, area coverage, accuracy and reliability of Standard Loran were thoroughly demonstrated during the Second World War. A system with longer baselines and greater 24-hour overland range than Standard Loran was desired for assistance in the East Asia land and sea war against Japan. An experimental Low Frequency Loran triad was installed with transmitting stations at Cape Cod, Mass., Cape Fear, N.C. and Key Largo, Fla. The triad operated during the summer of 1945 at 180 kc. Monitoring stations were operated at Bermuda, Puerto Rico, Trinidad and the Azores for observations of overwater transmission. The signals over land were observed by fixed monitors at Wright Field and Little Falls, Minn. and aboard an aircraft used to examine the range and accuracy of the system. Additional fixed monitors were operated by the U.S. Army at Eatontown, N.J. and Mobile, Ala. The Canadian Navy operated a monitor station at Halifax (Comperdown), Nova Scotia. The Bermuda monitor was operated by the U.S. Coast Guard.

For the most part, the equipment was converted from Standard Loran equipment and was designed for operating techniques similar to those used in Standard Loran. The receiver indicators at the slave stations displayed the individual cycles of the master and slave signals. By superimposing the individual cycles in addition to the envelopes of the master and slave pulses, synchronization of the slaves could be maintained with several times the precision of

Standard Loran except for an occasional mismatch of one or two whole cycles. Envelope and cycle matching was accomplished visually and manually. When the signal strength was well above the noise, the cycles of the ground wave pulses could be matched by the slave station operators with a probable error of about 0.15 microsecond. The operators were assisted in the selection of the correct pair of cycles by knowing in advance the correct time difference between master and slave envelopes. This advantage was not available to operators of the airborne receivers, and no method was found to avoid errors of one or more whole cycles when the correct envelope time difference was not known by the operators. Before the techniques of cycle matching in L.F. Loran could be thoroughly developed, the war in the Pacific ended. Nevertheless, the tests demonstrated that an L.F. Loran triad could (a) operate successfully with baselines about twice the lengths used in a Standard triad, (b) provide a 24-hour service area over land about two-thirds that over water and (c) provide several times the timing accuracy at greater range than Standard Loran if the problems of cycle ambiguity were solved.

2. The Cyclan and Cytac Systems

In 1946, the Sperry Gyroscope Company under contract with the U.S. Air Force, Air Materiel Command, began the development of automatic cycle identification and phase measuring techniques as part of the Cyclan project. Field tests of the Cyclan system in 1951 indicated that solution of the problem of cycle ambiguity was feasible. The Cyclan system emitted pulses on two radio frequencies 20 kc apart. (These were 160 kc and 180 kc). This led to duplications of certain transmitting and receiving equipments and precluded the possibility of relocating the signals within the 90-110 kc radionavigation band. These and other considerations led to the development of the 100 kc Loran system designated Cytac.

Cytac was developed by the Sperry Gyroscope Company, beginning in 1952, for the U.S. Air Force, WADC, to demonstrate the feasibility of completely automatic guidance of aircraft with high accuracy at a range of 1000 nautical miles.

The master station was located at Cape Fear (Carolina Beach, N.C.) and the two slaves were located at Forestport, N.Y. and Carrabella, Fla. The transmitters were modifications of the AN/FPN-15 L.F. Loran transmitters which in turn were modified Standard Loran transmitters. The transmitter synchronizers and ground monitor receivers were constructed in the physical form of experimental laboratory equipment to facilitate circuit design changes. The experimental airborne receivers were substantially identical to the ground monitor receivers except for a more compact construction.

The Cytac receivers, including the receiver portions of the transmitter synchronizers, were designed to use only the leading edge of the received pulses in the measurement of time differences. In this way it was expected that the measurements could be made on the ground wave component of the pulse before arrival of the skywaves. The receivers were designed to compare the phase of the cycles within the master pulse with the slave cycles and to measure the time difference between master and slave pulse envelopes. The cycle phase difference, or time difference, would then be a precise indication of difference in time of arrival of master and slave signals except for an uncertainty of the exact number of whole cycles by which the master pulse preceded the slave pulse at the receiver. The cycle (or phase) ambiguity was to be resolved by the envelope time difference measurements.

At the beginning of the test program it was not certain whether or not the effects of propagation on the pulse would make cycle identification unreliable. The attenuation and phase shift of the ground wave is a function of frequency and causes some distortion of the pulse shape. It was conceived to be possible that this distortion might introduce enough error in the envelope time difference measurements to cause errors in cycle identification. However, in field tests from September 1954 to October 1955, it was found that distortion of the pulse caused by dispersion of the ground wave had negligible effects on cycle identification. At fixed monitoring points the correct cycles could be identified continuously over long periods of time with an input signal-to-noise ratio of about 1 to 1.

Sky wave interference was almost completely eliminated by sampling the pulses with a two-microsecond sampling gate which occurred about 30 microseconds after the beginning of the pulse and before arrival of the first-hop sky wave.

In the Cytac system each station transmitted groups of eight closely spaced pulses instead of the single pulses used in Standard Loran. Other things being equal, the average power over a complete pulse repetition period was increased by a factor of eight. Pulses within the group were spaced at equal intervals of 1200 microseconds. (The spacing was later changed to either 500 or 1000 microseconds in the Loran-C system.)

Near the end of the Cytac field test program a technique was employed for phase-modulating the 100 kc radio frequency excitation of the Cytac transmitters according to a predetermined code. An identical code was generated in the receiver and was used to phase modulate the receiver's 100 kc reference. This technique reduced the effectiveness of synchronous interference by 12 db. The phase coding technique also reduced the probability of interference from long-delayed sky waves (500 to 1200 microseconds).

The Cytac tests demonstrated conclusively that automatic instrumentation could be developed to measure time differences in a 100 kc Loran system with an average error of a few tenths of a microsecond when the signal-to-noise ratio is at least 1 to 1 and the ratio of ground wave-to-sky wave amplitude is at least 1 to 10.

3. <u>The U. S. East Coast Loran-C System</u>

In 1957, less than a year after completion of field tests of the experimental Cytac system, an operational requirement of the U.S. Navy called for a system of radionavigation which would provide wide area coverage, like Standard Loran, but with an accuracy approaching an order of magnitude greater than Standard Loran at 1000 nautical miles. The results of the Cytac tests, which were obtained principally over land, indicated that the new requirements could be satisfied with the navigation portion of the Cytac system. With very little modification, the navigation portion of the Cytac system became the first Loran-C radionavigation system. In order to meet an early on-air date, maximum use was made of existing equipment and facilities, with the realization that full system reliability, stability and accuracy would not be obtained.

Loran-C slave stations were established at Martha's Vineyard, Mass. and Jupiter Inlet, Fla. to operate with the existing master station at Cape Fear (Carolina Beach, N.C.). Temporary buildings were erected to house the equipment. Primary power was obtained from the nearest commercial sources. Primary power lines and transformers could not supply standby transmitting equipment under full load. No emergency power was provided except for antenna tower lights.

Antennas for the slaves are 625 foot guyed towers with twenty-four 600 foot top loading elements anchored at a radius of 850 feet from the base of the antenna. Prior to September, 1958, the master station antenna was a self-supported 625 foot top-loaded structure. The electrical characteristics of the three transmitting antennas were sufficiently similar for satisfactory operation.

A Loran-C receiver, mounted within a trailer van, was located near each of the slave baseline extensions, one at Cape Cod, Mass. and another at West Palm Beach, Fla. Another van-mounted Loran-C receiver was located at Bermuda. The two baseline monitor receivers were used, initially, to assist in system calibration. Later, they were used to assist in evaluation of system synchronization stability. The Bermuda monitor, being well out into the ground wave service area, is used to observe overall system stability, including stability of radio wave propagation.

A portion of the ground wave service area of the U.S. East Coast Loran-C system is shown in Figure 1. The heavy solid curved line is the contour of 1000-foot fix errors for 0.2 microsecond time difference errors on both MX and MY pairs. The fix error for a given time difference error depends upon the crossing angle of the hyperbolic lines of position. The lines of position extend over most of the eastern one-third of the United States (not shown) and intersect at angles only slightly less favorable than over the Atlantic.

SECTION II

RANGE AND ACCURACY OF LORAN-C
- PROPAGATION CONSIDERATIONS -

A. GENERAL

Certain of the factors which affect the range and accuracy of Loran-C are either independent of frequency or are associated with frequency only indirectly. Some of these factors have the same application to Loran-C that they have to Standard Loran. For example, the geometry of the hyperbolic lines of position has the same relationship to fix accuracy in both systems. In general, however, the range and accuracy of either system is greatly affected by the operating frequency.

It is the purpose of this Section to examine the factors affecting the range and accuracy of Loran-C systems. Reception in both the ground wave and sky wave areas is considered. Particular attention is given to those factors which, because of their frequency dependence, are considerably different for the 100 kc Loran-C system as compared to the 2 mc Standard Loran systems.

B. GROUND WAVE RANGE AND ACCURACY

Radio signals may be detected at distances much greater than the maximum range at which satisfactory service can be obtained. In the Loran-C system, for example, the ground wave may be detected at very great distances in the presence of atmospheric noise. Theoretically, at least, the signal-to-noise ratio can be increased by increasing the radiated signal power. Interference from the sky wave components of the signal, however, is independent of transmitter power and thus has a significant effect on the maximum useful ground wave range.

Other radio signals in the 90-110 kc radionavigation band may interfere with Loran-C under certain circumstances. These other signals affect Loran-C service only when they greatly exceed the strength of the Loran-C signals. The use of synchronous detection and filtering greatly reduces the susceptibility of the Loran-C receiver to non-synchronous interference.

Each of the factors which limits the maximum range of Loran-C also affects the accuracy at extended range. In addition, accuracy at all ranges is affected by variations in velocity of radio wave propagation. The principal factors affecting velocity of the low radio frequency ground wave are the refractivity of the atmosphere and the conductivity of the earth.

To summarize, the principal factors of radio wave propagation which affect the range and accuracy of Loran-C in the ground wave area are the following:

(1) amplitude ratio of ground wave to sky wave and sky wave delay,

(2) signal-to-noise ratio,

(3) interference,

(4) refractivity of the earth's atmosphere, and

(5) conductivity of the earth.

1. Sky Wave Amplitude and Delay

The maximum practical ground wave range of Loran-C is limited, particularly at night, by the first-hop sky wave. At 1500 nautical miles, the first-hop nighttime sky wave over sea water has 40 times the amplitude of the ground wave (32 db). Beyond this distance the ratio of ground wave-to-first-hop sky wave remains almost constant. On a winter day, the ratio of sky wave-to-ground wave is about 10-to-1 (20 db) for all ranges greater than about 1300 nautical miles over sea water. On a summer day, the sky wave amplitude is considerably lower. The ratio of sky wave-to-ground wave amplitude is approximately 3-to-1 (10 db) over sea water on a summer day for all ranges greater than 1300 nautical miles.

Curves of sky wave field strength over sea water are given in Figures 29, 30 and 31.

Interference from the sky wave is not a problem to ground wave working when the sky wave is less than about 10 times the ground wave amplitude. This is the situation at all ranges during the daytime, regardless of the season of the year. Ground wave operation of the Loran-C receiver at night, however, is complicated by the extremely large first-hop sky wave at ranges greater than about 1000 nautical miles (ratio equal 10-to-1 or 20 db).

The ability of the Loran-C receiver to operate on the ground wave in the presence of a much greater sky wave depends upon the fact that the ground wave component arrived at the receiver slightly ahead of the sky wave. Theoretically, at least, interference from the sky wave can be eliminated by sampling the received signal ahead of arrival of the first-hop sky wave. In practice, however, it is necessary to allow the received pulse to build up to a suitable signal-to-noise ratio before sampling.

Interference from the greater nighttime sky wave amplitude is partially offset by the greater nighttime sky wave delay. Over sea water the nighttime sky wave delay approaches a minimum of about 54 microseconds at and beyond about 1340 nautical miles. In the daytime, the sky wave delay over sea water approaches a minimum of about 39 microseconds at and beyond about 1200 nautical miles. Over land of average conductivity (0.005 mhos per meter), the sky wave delay is about 7 microseconds less than over sea water both at day and night.

2. Signal-to-Noise Ratio

The accuracy of cycle time difference measurement is practically independent of atmospheric noise for signal-to-noise ratios greater than 1-to-1 (zero db). At much lower signal-to-noise ratios the mean indicated cycle time difference is unaffected by noise even though the short-term deviations from the mean increase in magnitude. Figure 38 shows the manner in which the standard deviation of cycle time difference varies with random noise. Certain special purpose applications of Loran-C, such as mapping and surveying, can be accomplished satisfactorily with signal-to-noise ratios as low as -20 db. At these low values of signal-to-noise ratio, cycle accuracy can be obtained by averaging the indicated cycle time difference for a few minutes. Reliable measurements of envelope time difference, however, require a higher signal-to-noise ratio. Envelope time difference measurements with an accuracy of ± 4 microseconds 90 to 95 percent of the time can be made with signal-to-noise ratios of about 1-to-1 at the sampling point.

The level of atmospheric noise varies greatly from one area of the earth to another and from one season and time of day to the other. In general, atmospheric noise is greater at night than in the daytime. Seasonal variations are not great and have more to do with the relative lengths of day-and-night than to the seasons as such.

Table 1 gives the median values of atmospheric noise expected at seven widely separated receiving locations in the northern hemisphere. The daytime values are for the four-hour time block from 0800 to 1200. The nighttime values are for 2000 to 0400 hours. It is apparent, from Table 1 that there is not much variation in atmospheric noise on a winter day from one location to another in the northern hemisphere. On a summer day, however, the atmospheric noise is 30 db (31.6 times) greater in the Panama Canal area than in the area of the Norwegian Sea.

Table 2 gives the distances from the transmitters at which the ground wave signal strength at the 50 percent sampling point equals the median atmospheric noise when the radiated power at the peak of the pulse is 100 kw and the receiver bandwidth is 25 kc. If the transmitter power is multiplied by 10 times (1 megawatt radiated at peak of pulse), about 260 nautical miles can be added to all ranges shown in Table 2.

It should be pointed out that the values of atmospheric noise given in Table 1 are median values. The actual values observed during any four-hour time block will exceed the median value for about 10 percent of the time by about 14 db during the daytime and by about 9 db at night. No reduction in range of Loran-C service for variation of

Receiver Location	Lat.	Long.	Atmospheric Noise in db above 1 microvolt-per-meter			
			Winter		Summer	
			Day	Night	Day	Night
Norwegian Sea	65°N	0°E	26	32	16	37
Mediterranean Sea	35°N	30°E	24	41	20	41
Bermuda	30°N	60°W	24	37	24	41
Arabian Sea	20°N	60°E	24	41	20	45
Hawaiian Islands	20°N	155°W	24	41	18	37
Panama Canal	10°N	80°W	24	45	46	61
Sea of Japan	40°N	135°E	20	37	24	41

TABLE 1

EXPECTED MEDIAN VALUES OF RADIO NOISE IN DECIBELS ABOVE 1 MICROVOLT-PER-METER RMS IN A 25 KC BANDWIDTH CENTERED AT 100 KC

Receiver Location	Lat.	Long.	Range in Nautical Miles For 1-to-1 Signal-to-Noise Ratio			
			Winter		Summer	
			Day	Night	Day	Night
Norwegian Sea	65°N	0°E	1260	1090	1570	960
Mediterranean Sea	35°N	30°E	1350	870	1440	870
Bermuda	30°N	60°W	1350	960	1350	870
Arabian Sea	20°N	60°E	1350	870	1440	740
Hawaiian Islands	20°N	155°W	1350	870	1480	960
Panama Canal	10°N	80°W	1350	740	740	390
Sea of Japan	40°N	135°E	1440	960	1350	870

TABLE 2

RANGE IN NAUTICAL MILES AT WHICH LORAN-C GROUND WAVE SIGNAL-TO-NOISE RATIO IS 1-TO-1 AT 50 PERCENT SAMPLING POINT FOR 100 KW RADIATED AT PEAK OF PULSE atmospheric noise about the median is required beyond that given in Table 2, however. This is true because the observed requirement for 1-to-1 signal-to-noise ratio is based upon median values of noise.

3. Interference From Other Radio Services

The use of synchronous detection and synchronous filtering greatly reduces the disturbing effects of non-synchronous signals on the performance of the Loran-C receiver. When the amplitude of the undesired signals is sufficiently greater than the Loran-C signals, however, the desired signals at the output of the R.F. amplifier become distorted and normal operation of the receiver is impaired.

Several techniques for minimizing interference from non-synchronous signals in or near the 90-110 kc radio-navigation band are well known. Some of these techniques are employed in existing Loran-C receivers. Others are planned for new equipment.

The basic principles of synchronous detection and synchronous filtering afford a considerable measure of immunity to non-synchronous interference. Figure 39 shows the results of a test of the AN/SPN-28(XZ-1) Loran-C receiver. The test shows that the indicated cycle time difference is unaffected by one or two signals located within the 90-110 kc band when the signal-to-interference ratio S/J is less than -20 db (undesired signal 10-times the

Loran-C signal amplitude).

In practice, the amplitude of the undesired signal at 91.9 kc could be reduced greatly by a notch filter located ahead of the receiver input. The notch filter would have very little effect on either the amplitude or shape of the Loran-C pulses. If the notch frequency were located at 98.5 kc, however, some distortion of the pulse envelope would occur. There would be some elongation of both the ground wave and sky wave pulses following the notch filter. This would have the effect of reducing the apparent delay between sky wave and ground wave envelopes and would make sky wave discrimination more difficult.

The pass band of the radio frequency amplifier is made quite broad to minimize elongation of the received pulses. The bandwidths between 3 db and 6 db points are approximately 25 kc and 33 kc, respectively. An auxiliary band pass filter having an adjustable band width has been used successfully to reduce interference from signals located closely adjacent to the 90-110 kc band. Limited operational experience with band pass filters indicates that Loran-C receivers can operate successfully with much smaller band widths than expected. The subject has not been adequately investigated experimentally. However, new receiver equipment is being furnished with auxiliary band pass and notch filters.

4. Refractivity of the Atmosphere

Transmission time of a pulse from the Loran-C transmitter to the receiver depends upon the velocity of radio wave propagation. The factors which affect propagation velocity of the low-frequency ground wave are, principally, the index of refraction of the earth's atmosphere and the conductivity of the earth's surface. A very complete description of the phase of the low radio frequency ground wave is given in Reference 1. A brief review of certain of the considerations and results contained in Reference 1 is given below.

It is convenient to express the total vertical electric field intensity E_r as the product of two factors: (a) the primary field or free-space field E_{pr} and (b) the secondary factor F_r. Thus, the total vertical electric field intensity is

$$E_r = E_{pr} \cdot F_r \qquad (1)$$

The total field can be expressed in terms of the total magnitude and the total phase as follows:

$$E_r = |E_{pr}| \cdot |F_r| \cdot \exp\left\{ i \left[\phi' + \phi_c - \omega t\right] \right\}, \qquad (2)$$

where

$$\phi' = \frac{\omega\ n_s\ d}{C} \quad \text{(radians)} \tag{3}$$

$$\phi_c = \arg F_r \quad \text{(radians).} \tag{4}$$

In the above expressions, ω is the frequency in radians per second; n_s is the index of refraction of the atmosphere, at the surface of the earth; C is the free-space velocity of light in meters per second and d is the distance from the source in meters. Neglecting the time function ωt, the total phase ϕ of the vertical electric field is the sum of the primary phase ϕ' and the secondary phase ϕ_c,

$$\phi = \phi' + \phi_c \tag{5}$$

It is convenient to express the phase, ϕ, at a time, t, as follows:

$$t = \frac{\phi}{\omega} \cdot 10^6 \text{ (microseconds).} \tag{6}$$

It follows from the additive properties of the phase that the total phase, t, is the sum of the phase t' of the primary field or free space field E_{pr} and the phase, t_c, of the secondary factor F_r. Thus, the total phase (in microseconds) is the sum of two parts as follows:

$$t = t' + t_c \tag{7}$$

Before continuing into the discussion of transmission time of the Loran-C pulses, it is appropriate to point out that the physical significance of the phase is a subject that requires very careful consideration. Reference 1 gives a number of interpretations of the physical significance of the signal velocity, v_s, the phase velocity, v_c, and the group velocity, v_g. At great distances from the source, the total phase, t, (in microseconds) may be interpreted as the time for the signal to propagate to the observer.

Transmission time of the primary wave can be expressed very simply as follows:

$$t' = \frac{n_s\, d}{C} \cdot 10^6 \text{ (microseconds)} \tag{8}$$

where

n_s = index of refraction of the atmosphere at the surface of the earth.

d = distance between source and observer in meters.

C = velocity of light in free-space in meters per second.

The quantity t' can be interpreted as the transmission time of the signal in a "free-space" having a uniform index of refraction equal to that at the surface of the earth. Actually, the index of refraction of the earth's atmosphere usually decreases with height above sea level. The effects of the vertical gradient of the refractive index are included in the phase, t_c, of the secondary factor along with the effects of the earth's conductivity and dielectric constant. Reference 1 gives numerous curves of the phase, t_c of the secondary factor, F_r, in addition to the formulas and procedures used for computation.

Since the index of refraction, n, departs from unity by only a few parts in 10^{-4}, it is convenient to describe n in terms of the refractivity, N, which is defined

$$N = (n - 1) \cdot 10^6 \tag{9}$$

The phase, t', of the primary wave is computed as if the refractivity, N, were constant throughout all space at the surface value N_s. The effect of the vertical gradient of refractivity is accounted for in the phase, t_c, of the secondary factor. The refractivity is assumed to decrease linearly from the surface value, N_s, to the value N_1 at a height of 1 km above the surface. Thus, the vertical lapse in ΔN units per kilometer is

$$\Delta N = N_s - N_1 \; . \qquad (10)$$

The values of ΔN may be determined from radiosonde observations. Fortunately, ΔN may be predicted with good accuracy from N_s and, in the absence of radiosonde observations, the following emperical formula may be used to determine the predicted value of $\Delta N'$:

$$\Delta N' = 7.32 \exp\left\{0.005577 N_s\right\} . \qquad (11)$$

Reference 2 gives maps which may be used to estimate the value of N_s averaged throughout the day for the months of February and August at any geographical location in the world, together with a map of the annual range of N_s.

An example of the variations of mean monthly transmission times between August and February over the two baselines and over the paths from the transmitter to Bermuda is given in Table 3.

If it is assumed that the slaves operated with constant coding delays (which was the standard operating procedure), the predicted variations in mean monthly time difference at Bermuda can be computed as follows:

$$\Delta T_x(\text{Bermuda}) = \Delta t_{mx} + \Delta t_{xb} - \Delta t_{mb}, \tag{12}$$

$$\Delta T_y(\text{Bermuda}) = \Delta t_{my} + \Delta t_{yb} - \Delta t_{mb}. \tag{13}$$

If the slave coding delay had been adjusted to maintain a constant time interval between emission of master and slave pulses (the basis for the Loran-C Table), the variations in time differences at Bermuda would be computed as follows:

$$\Delta T_x(\text{Bermuda}) = \Delta t_{xb} - \Delta t_{mb}, \tag{14}$$

$$\Delta T_y(\text{Bermuda}) = \Delta t_{yb} - \Delta t_{mb}. \tag{15}$$

Predicted values of the changes in mean monthly time differences between the months of August and February are given in Table 4.

Quantity	Identification of Path				
	MX	XB	MY	YB	MB
N_s (Feb.)	337	342	317	322	330
N_s (Aug.)	375	380	365	370	375
$\Delta N'$ (Feb.)	48	49	43	44	46
$\Delta N'$ (Aug.)	59	61	56	58	59
N_s (Aug.) - N_s (Feb.)	38	36	48	48	45
$\frac{d}{c}$ (microseconds)	2700	5280	3400	3800	4100
$\Delta t'$ (microseconds)					
$= 10^{-6} \frac{d}{c} \left[N_s(Aug) - N_s(Feb)\right]$	.10	.19	.16	.18	.18
Δt_c (microseconds)					
$= t_c(Aug) - t_c(Feb)$	-.03	-.10	-.05	-.06	-.05
$\Delta t = \Delta t' + \Delta t_c$	+.07	+.09	+.11	+.12	+.13

TABLE 3

VARIATIONS OF TRANSMISSION TIMES OVER THE BASELINES AND OVER THE PATHS TO BERMUDA DUE TO VARIATIONS OF MEAN MONTHLY VALUES OF REFRACTIVITY

Receiver Location and Rate	Variation of Time Difference (Mean August Minus Mean February) For Two Methods of Coding Delay Adjustments	
	Constant Coding Delay	Constant Time Interval Between Master and Slave Pulses
ΔT_x (Bermuda)	+.03	-.04
ΔT_y (Bermuda)	+.10	-.01
ΔT_x (Master)	+.14	+.07
ΔT_y (Master)	+.22	+.11
ΔT_x (x BLE)	0	-.07
ΔT_y (y BLE)	0	-.11

TABLE 4

PREDICTED CHANGE IN MEAN MONTHLY TIME DIFFERENCE
DUE TO CHANGES IN MEAN MONTHLY
SURFACE REFRACTIVITY N_s (AUGUST MINUS FEBRUARY)

Changes, Δt_c, in the phase of the secondary factor as a function of the vertical atmospheric lapse, ΔN, have not been published in the literature for over water paths. Reference 1 gives curves of Δt_c as a function of ΔN for over land paths (conductivity, σ = 0.005 mhos/meter). The values of Δt_c in Table 3 were estimated for over water paths (σ = 5 mhos/meter).

The effect of changes in the vertical atmospheric lapse, ΔN, on the phase, t_c, of the secondary factor is several times greater over land than over water. On an all water path variations, Δt_c, in the phase of the secondary factor due to changes in ΔN are, generally, less than (one-third to one-half) the changes, $\Delta t'$, in the phase of the primary wave. Changes in the surface value of refractivity, N_s, and changes in the vertical atmospheric lapse, ΔN, have a greater effect on the phase of the secondary factor over all land paths than over all water paths.

5. Conductivity of the Earth

a. General

No other factor has a greater effect on the phase of the low frequency ground wave than does the conductivity of the earth. When the service area is predominantly over land, as over the continental U.S.A., for example, conductivities of the surface paths are far from homogeneous. This causes the observed lines-of-position to be distorted from the lines-of-position which might be computed for a homogeneous surface.

When the paths are entirely over sea water, the effects of surface conductivity can be predicted with great accuracy, and variations in the phase of the low-frequency ground wave are caused almost entirely by variations in the refractivity of the atmosphere. However, it is not always possible to locate the transmitting stations at positions which provide all water paths to the service area or between transmitters.

The phase of the ground wave over mixed paths can be computed by the use of a modification of Millington's method (References 3, 4, 5). In this method, the rate of change of phase, t_c of the secondary factor with distance along any portion of the surface path is assumed to be independent of the nature of other parts of the total path between source and observer. The method gives a different value for the phase in the forward and reverse directions of propagation over unsymmetrical paths. This conflict with the principles of reciprocity is resolved by assuming that the actual phase is the arithmetic average of the values computed for the forward and reverse directions. An example of the method is given in Table 5. The importance of the land conductivity can be illustrated by working through the example several times with a different value of land

FORWARD DIRECTION

Path Part No.	Conductivity mhos/meter	Distance to Start St. Miles	Distance to End St. Miles	Partial Secondary Factor Microseconds		
				At Start	At End	Δt_c (end-start)
1	5	0	100	-	.20	+ .20
2	.001	100	300	2.70	4.75	2.05
3	5	300	600	0.70	1.70	+1.00

$$t_c \text{ (Forward)} = \Sigma\Delta t_c \text{ (Forward)} = +3.25$$

REVERSE DIRECTION

Path Part No.	Conductivity mhos/meter	Distance to Start St. Miles	Distance to End St. Miles	Partial Secondary Factor Microseconds		
				At Start	At End	Δt_c (end-start)
3	5	0	300	-	0.70	0.70
2	.001	300	500	4.75	6.50	1.75
1	5	500	600	1.35	1.70	0.35

$$t_c \text{ (Reverse)} = \Sigma\Delta t_c \text{ (Reverse)} = 2.80$$

$$t_c = \frac{t_c \text{ (Forward)} + t_c \text{ (Reverse)}}{2} = 3.02 \text{ microseconds}$$

TABLE 5

SAMPLE COMPUTATION OF PHASE, t_c, OF THE SECONDARY FACTOR FOR A MIXED PATH conductivity each time. This has been done for four different values of conductivity. The results are shown in Table 6.

Conductivity of Land Portion of the Path (mhos/meter)	Phase, t_c, of Secondary Factor (microseconds)
.001	3.02
.002	2.90
.005	2.08
5.0 (all water)	1.70

TABLE 6

THE PHASE, t_c, FOR THE MIXED PATH ILLUSTRATED IN TABLE 5 AS A FUNCTION OF CONDUCTIVITY OF THE LAND PORTION

C. SKY WAVE RANGE AND ACCURACY

1. General

Most of the factors which affect ground wave range and accuracy are important in the consideration of sky waves. Some of the factors have almost the same relationship to range and accuracy for either ground wave or sky wave working. For example, a certain minimum signal-to-noise (or interference) ratio is required for satisfactory operation by either mode. Most of the propagation factors, however, have entirely different effects on sky wave and ground wave operation. For this reason, certain of the propagation factors previously considered in connection with ground wave range and accuracy are discussed below with particular reference to sky wave working.

2. Contamination By Other Modes

Just as the first hop sky wave may interfere with ground wave operation, so may the second hop interfere with first hop operation of the receiver. In general, it is always necessary to consider the amplitude of the next higher mode. It is also possible to have interference from the next lower mode. The duration of the Loran-C pulse (about 200 microseconds) is greater than the delay between successive hops at all distances beyond the normal ground wave range. Thus, some portion of the (N-1)-th hop pulse will overlap the leading edge of the N-th hop pulse at the receiver. This could cause distortion of the composite pulse envelope and malfunctions of the envelope time difference circuits of the receiver. Even relatively small contamination by the lower mode could cause errors in phase measurement (cycle time difference).

The maximum phase error for a certain ratio of desired mode to interfering mode can be determined easily. However, the ability of the receiver to make reliable envelope time difference measurements in the presence of an interfering lower mode is not known exactly. On the basis of a limited number of tests, it is assumed that N-th hop signal (desired signal) should have at least twice the amplitude of the (N-1) hop signal (interfering mode) when the amplitudes are measured at the sampling point of the desired signal. For modes up to and including the fourth hop, the (N-1)-th hop arrives at the receiver about 30 to 80 microseconds earlier than the desired N-th hop (for all distances at which aky waves are likely to be employed). The interfering (N-1)-th hop pulse will have an appreciable amplitude when the receiver samples the desired N-th hop signal. Thus, it is desirable for the N-th hop signal to have at least four times the amplitude of the undesired (N-1)-th hop signal (12 db) in order to insure a 2-to-1 ratio at the instant of sampling. On a summer day, the successive hops differ in amplitude by only about 10 db at large distances (see

Figure 31). For this reason, in the examples which follow, the amplitude of the N-th hop is required to be at least 10 db greater than the (N-1)-th hop before the N-th hop can be used. Under these conditions, contamination of the N-th hop by the (N-1)-th hop would cause a maximum phase error of 0.9 microsecond. The maximum phase error occurs when the undesired (N-1)-th hop arrived at the receiver ± 90 degrees out of phase with respect to the desired N-th hop. The maximum phase error would be 0.32 microsecond if the ratio of desired-to-undesired signal were 20 db.

Table 7 gives the minimum distance at which the amplitude of the N-th hop sky wave is 10 db greater than the next lower mode.

No. Hops N	Nautical Miles			
	Winter		Summer	
	Day	Night	Day	Night
Gnd (0)	0	0	0	0
1	870	610	1300	610
2	2180	1900	3200	1900
3	3050	3200	4300	3200

TABLE 7

MINIMUM DISTANCE IN NAUTICAL MILES FOR THE AMPLITUDE OF THE N-TH HOP SKY WAVE TO BE 10 DB GREATER THAN THE (N-1)-TH HOP

3. Sky Wave Amplitude

It should be emphasized that all of the sky wave field strengths referred to here are median values. Even though the amplitude of the low frequency sky wave is remarkably stable for relatively long periods, deviations from the median amplitude must be taken into account when one considers the use of sky waves for long distance navigation.

A very considerable amount of experimental data exists on the time variations of the amplitude of the composite sky wave. However, only a small amount of data is available on the time variations of the individual sky wave modes (or hops). In the examples which follow, the distances over sea water between transmitter and receiver are given at which the median signal strength equals the median value of atmospheric noise. Table 8 gives these ranges for peak pulse radiated powers of 100 kw and 1000 kw. The asterisk(*) indicates that the corresponding signal strength for the indicated power fails to equal the median noise at any range. The examples of Table 8 are for receiver locations in the Eastern Mediterranean. The results would be substantially the same in the Bermuda area. The results shown in the example of Table 8 may be considerably different for receiver locations in either the tropics or the polar regions.

No. Hops N	Nautical Miles Winter Day	Winter Night	Summer Day	Summer Night
Gnd (0)	1350	870	1440	870
1	1870	1780	1740	1780
2	2180	2300	*	2300
3	*	*	*	*

TABLE 8a (100 kw)

No. Hops N	Nautical Miles Winter Day	Winter Night	Summer Day	Summer Night
Gnd (0)	1610	1130	1700	1130
1	2180	2040	2000	2040
2	2650	2820	1650	2820
3	*	3220	*	3220

TABLE 8b (1000 kw)

MAXIMUM DISTANCE IN NAUTICAL MILES AT WHICH LORAN-C SIGNAL-TO-NOISE RATIO IS 1-TO-1 AT 50 PERCENT SAMPLING POINT. RECEIVER LOCATION ASSUMED TO BE THE EASTERN MEDITERRANEAN.

4. Sky Wave Range

In an analysis of sky wave ranges it is necessary to consider both the maximum range, which depends upon the radiated signal power, and the minimum range which is independent of radiated signal power. For this purpose it is convenient to combine, into a single table, the minimum and maximum ranges. This has been done in Table 9 for a peak pulse radiated power of 100 kw and in Table 10 for 1000 kw. Several significant observations are immediately apparent from an examination of Table 9 and Table 10. These observations are listed in Table 11.

No. Hops N	Distances in Nautical Miles							
	Winter				Summer			
	Day		Night		Day		Night	
	Min	Max	Min	Max	Min	Max	Min	Max
Gnd (0)	0	1350	0	870	0	1440	0	870
1	870	1870	610	1780	1330	1740	610	1780
2	2180	2180	1900	2300	3200	*	1900	2300
3		*		*		*		*

TABLE 9 (100 KW)

THE ABOVE TABLE IS FOR 100 KW PEAK PULSE RADIATED POWER. THE MEANINGS OF MINIMUM (MIN) AND MAXIMUM (MAX) DISTANCES ARE THE SAME AS THOSE GIVEN IN TABLE 10.

No. Hops N	Distances in Nautical Miles							
	Winter				Summer			
	Day		Night		Day		Night	
	Min	Max	Min	Max	Min	Max	Min	Max
Gnd (0)	0	1610	0	1130	0	1700	0	1130
1	870	2180	610	2040	1330	2000	610	2040
2	2180	2650	1900	2820	3200	1650	1900	2820
3	3050	*	3200	3220	4300	*	3200	3220

TABLE 10 (1,000 KW)

The table above presents the minimum (MIN) distances from Table 7 and the maximum (MAX) distances from Table 8b.

(1) "MIN" is the minimum distance for the amplitude of the N-th hop to exceed the (N-1)-th hop by at least 10 db.

(2) "MAX" is the maximum distance for 1-to-1 signal-to-noise ratio (median values for 1,000 kw peak pulse radiated power).

(3) The receiver location is the Eastern Mediterranean.

1000 kw	100 kw
(a) The maximum ground wave range always exceeds the minimum first hop sky wave range by several hundred nautical miles.	(a) The maximum ground wave range always exceeds the minimum first hop sky wave range.
(b) The first hop and second hop ranges overlap at all time except during the daytime in summer. The maximum range of the first hop is greater than that of the second hop during the daytime in the summer.	(b) There is always an area between first hop and second hop ranges where satisfactory service is not obtained. There is no satisfactory service from the second hop in the daytime.
(c) The amplitude of the third hop is negligible in the daytime. At night the amplitude of the third hop exceeds the noise at 3200 nautical miles but does not exceed the second hop by the required 10 db. Thus, operation beyond the maximum indicated second hop range would be compromised in one of two ways: (1) by using the second hop with less than 1-1 signal-to-noise ratio, or (2) by using the third hop with greater sky wave contamination.	(c) There is no satisfactory service from the third hop.

TABLE 11

5. Sky Wave Delay

a. General

The utility of sky waves for extending the area of coverage of Loran-C systems depends upon the stability and predictability of sky wave delay. In addition, it must be possible for the user to determine unmistakably which hop the receiver is using from each of the transmitters.

The sky wave delay is defined as the time interval between arrival of the N-th hop sky wave and the ground wave. The total sky wave delay D is the difference of two parts. These are the principal part D' and the secondary part d. The principal part of the sky wave delay D' is the difference in path lengths of the N-th hop sky wave and the ground wave, expressed in microseconds. The sky wave is assumed to be reflected with no change in phase from an ionospheric reflecting layer having an apparent height, h. The principal part of the N-th hop sky wave delay D' is

$$D' = \frac{N}{C}\left[2\sqrt{h^2 + 4a\,(a+h)\,\sin^2\left(\frac{S}{4Na}\right)} - \frac{S}{N}\right] \qquad 0 \le S \le NS_{max} \qquad (16)$$

$$D' = ND'_{min} \qquad NS_{max} < S \qquad (17)$$

where

D' = principal part of N-th hop sky wave delay, microseconds

N = number of hops

S = ground wave path length, kilometers

h = apparent height of ionosphere, kilometers

a = effective earth radius, kilometers (4/3 actual radius)

C = velocity of light, kilometers per microsecond

$S_{max} \approx 2\sqrt{2ah}$, distance to radio horizon

$D'_{min} = D'$ at the distance S_{max}

The principal part D' of sky wave delay is given in Figure 40. The total sky wave delay D is

$$D = D' - d \qquad (18)$$

The secondary part d of the total sky wave delay D accounts for the phase delay (secondary factor) of the ground wave over those parts of the path which are not common to both the ground wave and sky wave ray paths. With very little error, the secondary part d can be computed as follows for paths over water:

$$d = -0.3 + 0.00208S \qquad 200\ \text{km} \leq S \leq NS_{max} \qquad (19)$$

$$d = -0.3 + 0.00208NS_{max} \qquad NS_{max} < S \qquad (20)$$

b. Identification of Sky Waves

No matter how stable and predictable sky waves may be, their practical use requires some reliable means for identification of the modes being received from each of the stations.

Theoretically, at least, the various modes can be identified by measuring their amplitudes and delays when the distance to the transmitter is known only approximately. Table 12 shows the predicted values of nighttime sky wave delays for the first four hops (with respect to the ground wave) at three different distances. Table 13 gives the delay between successive hops. It will be observed that the pattern of delay between successive hops is considerably different at the three distances. The relative amplitudes of the successive hops also have distinctive patterns at different distances. In order to use these distinctive characteristics for identification of sky wave modes, it is generally necessary to determine the following: (a) the delay between at least two modes, (b) the amplitudes of these two signal components, and (c) the approximate distance

No. Hops N	N-th Hop Sky Wave Delay (Microseconds) at Various Distances (Nautical Miles) 1400	2400	3400
1	53	53	53
2	119	108	106
3	226	171	163
4	367	255	227

TABLE 12

No. Hops (N)-(N-1)	Difference of N-th and (N-1)-th Hop Sky Wave Delay (Microseconds) at Various Distances (Nautical Miles) 1400	2400	3400
1 - 0	53	53	53
2 - 1	66	55	53
3 - 2	107	63	57
4 - 3	141	84	64

TABLE 13

to the transmitter.

The following example will help to illustrate the process (a peak pulse power of 1000 kw is assumed); assume that the receiver operator measures a delay of 55 microseconds between two successive modes. Several possibilities exist, depending upon the approximate distance to the transmitter and the signal strengths of the two modes in question. At 3400 nautical miles (3920 statute miles), the ground wave and the first hop sky wave would be undetectable, and the two observed modes would be identified as the second and third hops. If the distance to the transmitter were approximately 2400 nautical miles (2760 statute miles), the first hop sky wave would be detectable but the ground wave would not. Thus, the two modes in question would be identified as the first and second hops. Finally, if the distance between receiver and transmitter were approximately 1400 nautical miles (1610 statute miles), the two modes in question would be identified as the ground wave and the first hop sky wave.

In each of the above examples, identification should be confirmed by checking the measured signal strengths against theoretical values. Any gross error in identification could be detected in this manner. In order to extend the examples to greater ranges and to higher order modes, the average power radiated at the peak of the pulses has been assumed to be 1,000 kw.

The procedures for identification outlined above are, at present, far from fool-proof. It will be observed that the procedure calls for measurements at distances which, according to Table 10, are beyond the "Maximum" ranges for the assumed power (1,000 kw). This increases the probability of cycle identification errors which could cause errors in the identification of sky waves.

c. Stability of Sky Wave Delay

The phase and amplitude stability of the low frequency sky wave is sometimes so great that it is difficult to distinguish the sky wave from the ground wave on the basis of stability alone. At such times the N-th hop sky wave can be described as a steady component having a constant phase and approximately constant amplitude plus a component having random intensity and phase. The phase of the steady component can be associated with the reflection of the wave from a smooth ionospheric surface having a constant apparent height, h, and a reflection coefficient of constant angle, θ. The random component arises from time and space variations in the roughness of the ionosphere.

Variations in the mean value of the phase may be the result of changes in the general height of the ionosphere (as from day to night), changes in the angle, θ, of the reflection coefficient, or both. At 100 kc, most experimental investigations of sky waves have assumed that the waves are reflected with either zero or 180 degree change in phase at a sharply bounded ionosphere having an apparent height, h. Variations in sky wave delay can be described as combinations of the following types:

(a) Relatively rapid and random variations about the mean,

(b) Hour-to-hour variations,

(c) Transitions of the mean delay during sunrise and sunset periods,

(d) Day-to-day and night-to-night variations of the mean delay.

In the discussion below, unless otherwise specified, the comments apply to first hop sky waves received at distances greater than 650 nautical miles (1200 km).

The rapid and random variations of sky wave delay have a standard deviation of less than 0.1 microsecond on unusually stable nights. On more typical nights the standard deviation is about 0.25 microsecond. During the daytime, the short term stability is approximately four times as great as at night. These rapid and random variations occur about a mean value which may remain nearly constant for periods of an hour or so. However, during a period of several hours, an hour-to-hour variation in mean delay becomes apparent. During a typical night about 95 percent of the hourly means will be within 1.0 microseconds of the mean delay for that night (standard deviation of 0.5 microsecond). This estimate is based upon measurements made with the Loran-C system (see Section IV). A greater hour-to-hour deviation has been observed with continuous wave measurement techniques, possibly a result of contamination from other sky wave modes. The mean nighttime delay varies from one night to the next by as much as 2 or 3 microseconds. It is estimated that 95 percent of the nighttime mean values of sky wave delay obtained over a very large number of nights will be within 2 microseconds of the mean delay obtained on those nights (standard deviation of 1.0 microsecond).

The hour-to-hour deviations of the daytime sky wave delay are very small. Few measurements have been made over long paths in the daytime because of the high ionospheric absorption, particularly in the summer. From the data available, however, it appears that the standard deviation of sky wave delay during a typical day is about 0.25 microsecond. The day-to-day changes in mean delay are likewise small. There appears to be some relatively small variation with the seasons of the year and with latitude. There does not appear to be any simple relation between the sun's zenith angle and the daytime sky wave delay. From the limited data available, it appears that the maximum variation of daytime apparent height over a year and between lower and higher latitudes is about ± 2 km. At distances greater than

1200 km (650 nautical miles) this is equivalent to approximately ± 2 microseconds changes in sky wave delay. In order to be conservative in estimating sky wave stability assume that the seasonal and latitude variations of sky wave delay are randomly distributed from day-to-day and have a standard deviation of 1.0 microsecond.

In Loran systems, variations of sky wave delay can be measured directly if a stable time (or phase) reference is available. Frequently the ground wave is used as a reference. At other times, however, it is necessary to compare the phase of two sky waves. For example, suppose that first hop sky waves are received from a master-slave pair having a baseline length of L wavelengths. In this case, the observed standard deviation σ_{obs} is related to the standard deviations σ_a and σ_b of master and slave sky wave delays, as follows:

$$\sigma_{obs}^2 = (1-R^2)\ (\sigma_a^2 + \sigma_b^2) \tag{21}$$

In the above R is the correlation coefficient between the sky wave delays over the two independent paths (a and b) from the two sources to the receiver. The correlation for the rapid fluctuations will vary from $R = 1$ for $L = 0$ to $R \cong 0$ for $L > 40\ \lambda$. In Loran-C systems, baseline lengths are much greater than 40 wavelengths ($L \gg 40\,\lambda$). Consequently, there is no significant correlation ($R \cong 0$) between the short-term deviations of master and slave sky wave delays. This is also the case when different hops from the same transmitter are compared for short periods of time.

There appears to be a very significant correlation in the day-to-day and night-to-night deviations of two sky wave delays even when the two transmitters are separated by many hundreds of miles (or when different hops from the same transmitter are compared). The most obvious case of this sort may be observed when one compares the difference between master and slave sky wave delays obtained at night with the difference obtained in the daytime. Between nighttime and daytime the sky wave delay will change approximately 18 microseconds. Except for the relatively small difference of secondary components, d, of the sky wave delays, the sky wave correction (difference between master and slave sky wave delays) will be approximately the same at night as in the daytime. During the transition periods between daytime and nighttime conditions of the ionosphere, there are usually periods in which master and slave sky wave delays change at considerably different rates.

The time of beginning and the duration of the transitions between daytime and nighttime values of sky wave delay are very dependent upon the east-west and north-south extents of the path, the latitudes of the sending and receiving stations and the season of the year. On east-west paths of about 1200 km, the sky wave delay changes from the nighttime to the daytime values in a period of from one to two hours before ground sunrise at the path midpoint. In the afternoon the delay begins to increase near sunset but the change is more gradual, sometimes continuing to increase slowly for several hours after ground sunset at the midpoint. Although only a few measurements of correlation of sky wave delay during sunrise and sunset periods appear to be in the literature, it seems reasonable to assume that some significant correlation exists for similar paths during the hours after both ionospheric paths are in darkness. If this assumption is valid, then the time difference measured between two sky waves of the same mode would become stable after sunset much more quickly than if one signal were a ground wave and the other a sky wave.

Even after the ionosphere has taken on completely its nighttime or daytime characteristics there are hour-to-hour variations in sky wave delay which are much greater than the shorter-period random fluctuations caused by variations in roughness of the ionosphere. Likewise there are day-to-day and night-to-night changes in the mean delay. Various degrees of correlation exist between the delay of two sky waves, depending upon the degree of similarity of the ionospheric paths.

The hour-to-hour and night-to-night errors of Standard Loran time differences, when using two first hop sky waves, are about 0.3 of the errors which would occur if there were no correlation in the behavior of two points of reflection separated by about 150 to 200 miles. This corresponds to a correlation coefficient R = 0.95 in equation 21. In 2 mc sky wave synchronized Loran systems (S.S. Loran) hour-to-hour variations of apparent height of two ionospheric reflection points were found to have a correlation coefficient of about 0.7 when these reflection points were separated by 500 to 600 miles. Loran-C systems have baselines that are longer than those in Standard systems and shorter than the baselines in S.S. Loran systems. In order to be conservative in estimating the stability of Loran-C sky wave time differences, the following rules will be used for estimating correlation coefficients:

(a) for reflection points separated by 200 to 600 miles, a correlation coefficient of 0.7 is assumed for hour-to-hour deviations of apparent height. If the reflection points are separated by less than 200 miles, the hour-to-hour correlation coefficient is assumed to be 0.95.

(b) for reflection points separated by more than 600 miles, the hour-to-hour deviations are assumed to be completely uncorrelated.

(c) diurnal and seasonal variations of apparent height for any two reflection points in the first hop and second hop areas are assumed to have a correlation coefficient of 0.95.

In the foregoing discussion variations in sky wave delay have been described according to the "period" of the variations, such as, instantaneous variations, hour-to-hour variations, diurnal, seasonal and latitude variations. The same classifications may be applied to variations of time differences measured between two sky waves, that is, to the sky wave corrections. In order for sky wave working to be practical, tables or charts including sky wave corrections must be prepared and made available to navigators well in advance of their actual use. Except for very special applications it is not feasible to predict or to report additional corrections for short-time and irregular fluctuations. Thus, with the possible exception of additional corrections for seasonal and latitude variations of the daytime skywaves, the published tables or charts should include sky wave corrections for the annual mean apparent height of the ionosphere (day and night) along with a statement of the probable error of observed time differences. On this basis, the probable error will include instantaneous variations, hour-to-hour variations and diurnal (day-to-day and night-to-night) variations. Table 14 gives the estimated values of standard deviation for the time difference between various combinations

Modes	Time (Day or Night)	Instantaneous σ_i	Hour-to Hour σ_h	Diurnal σ_d
1-Hop; Gnd	Night	0.25	0.50	1.0
1-Hop; 1-Hop	Night	0.35	0.50	0.42
1-Hop; 2-Hop	Night	0.43	0.71	0.52
2-Hop; 2-Hop	Night	0.50	0.55	0.60
1-Hop; Gnd	Day	0.06	0.25	1.0
1-Hop; 1-Hop	Day	0.09	0.25	0.42
1-Hop; 2-Hop	Day	0.11	0.35	0.52
2-Hop; 2-Hop	Day	0.12	0.28	0.60

TABLE 14

ESTIMATED VALUES OF STANDARD DEVIATION IN MICROSECONDS FOR THE TIME DIFFERENCE BETWEEN TWO SKY WAVES (OR A GROUND WAVE AND FIRST HOP SKY WAVE) of ground wave and sky waves which are likely to be used in practice. Distances to the transmitter are assumed to be within the ranges (Min to Max) given in Table 10. The values of standard deviation do not include systematic errors nor errors due to sky wave contamination.

Table 15 gives the estimated values of probable error between observed sky wave corrections and the predicted mean annual sky wave corrections. In practice, there will be some error in the prediction of mean annual sky wave correction. In the case of the day time sky waves, it may prove to be feasible to publish seasonal mean sky wave corrections rather than annual corrections.

Modes	Time (Day-or-Night)	Probable Error $e = 0.6745\sqrt{\sigma_i^2 + \sigma_h^2 + \sigma_d^2}$ (microseconds)
1-Hop; Gnd	Night	0.78
1-Hop; 1-Hop	Night	0.50
1-Hop; 2-Hop	Night	0.66
2-Hop; 2-Hop	Night	0.65
1-Hop; Gnd	Day	0.67
1-Hop; 1-Hop	Day	0.34
1-Hop; 2-Hop	Day	0.43
2-Hop; 2-Hop	Day	0.45

TABLE 15

ESTIMATED VALUES OF PROBABLE ERROR
BETWEEN OBSERVED AND PREDICTED
(ANNUAL MEAN) SKY WAVE CORRECTIONS

SECTION III

TESTS IN THE GROUND WAVE SERVICE AREA

A. GENERAL

Test data of the Loran-C system have been acquired from the following sources: (1) The three transmitting stations, the two baseline extension monitors, (2) the Bermuda monitor, and (3) airborne trials of a preproduction model of an airborne Loran-C receiver.

By far, the most extensive data were accumulated from the transmitting stations and the fixed monitoring stations. These stations began regular operations in August, 1957 and continued until the master station transmitting antenna was damaged by hurricane Helene in September 1958. Data obtained during a year of operation from August 12, 1957 to August 31, 1958 have been used in this report.

In the spring and early summer of 1958 an airborne Loran-C receiver was used in experimental investigations of the long-range sky wave coverage of Loran-C. A number of airborne trials of the Loran-C receiver were conducted in the ground wave area of the system.

B. PROCEDURES AND METHODS OF ANALYSIS

1. Data Collection

Data collected at the transmitter stations, baseline monitors and Bermuda monitor consisted mainly of Esterline-Angus recordings of time differences, tabulations of visual 15-minute average time differences and narrative logs. In addition, the slave stations tabulated coding delay adjustments. The Bermuda receiver was equipped with automatic recorders for Loran-C field strength, atmospheric noise and interference.

At the end of each week, data from each site were forwarded to Sperry for preliminary examination. Sperry forwarded the data to Coast Guard Headquarters on a monthly basis. This procedure was revised in 1958 to provide for shipment of data from the sites directly to Coast Guard Headquarters.

2. Methods of Analysis

The most detailed and continuous record of operation of the triad is contained in the Esterline-Angus recordings produced at the transmitters, the baseline monitors and at the Bermuda monitor. These, together with well-kept narrative logs furnish a permanent record of the instantaneous, moment-to-moment operation of the triad. Analysis of instantaneous deviations and examination of simultaneous occurrences observed throughout the system requires inspection of these recordings. To display one week's output of recordings, however, requires an area of 504 square feet (12 ft. x 42 ft.).

Relatively long-term variations can be examined by re-plotting certain selected characteristics of the original data on a compressed time scale. The particular characteristics to be preserved and the optimum amount of time-compression depend upon the objectives of the analysis. Several such reductions of original data have been employed.

Fifteen-minute average time differences were plotted at Coast Guard Headquarters for most of the cycle data obtained from January 1958 to August 1958. These plots are useful in the examination of hour-to-hour and day-to-day stability and certain diurnal effects. One month's operation can be displayed on a strip about 25 feet long with a convenient time scale.

Plots of daily mean time differences are useful for examination of seasonal or other long-term effects. Plots have been prepared for the average time differences recorded at all stations in the eight-hour periods from 0800 to 1600 for a full year of system operation.

C. TEST RESULTS

1. General

This sub-paragraph gives the results observed at the transmitters and the fixed monitors and observations of several trials of a pre-production model of an airborne Loran-C receiver in the ground wave area of the East Coast system.

2. System Calibration

The East Coast Loran-C system was calibrated by Sperry during June, July and August 1957. A detailed description of the calibration procedure is given in Reference 6. On the basis of measurements made during the calibration period, Sperry computed the baseline transmission times and the corresponding values required for coding delays. The time difference readings at the two baseline extension monitors corresponding to the computed values of coding delay were recorded for reference. The baseline extension monitors directed the slaves to hold these reference readings constant from September 4, 1957 to September 19, 1957. During this period, the average indicated values of time difference at the baseline monitors, at Bermuda and at the master station were determined. These values are referred to as "calibration reference" values because they were obtained immediately after system calibration. The calibration reference time differences are given on the left-hand side of Figures 6,7 and 8.

3. System Synchronization and Monitoring

Except for periods of special tests, the system has been operated with coding delays held constant at the calibration reference values. The master synchronizer automatically monitors both slaves. Variations in time differences measured at the master may indicate changes in coding delay or changes in baseline transmission time, or both. When the system operates with baseline extension monitors, they have been used for accurate checks of slave coding delay. Standard operating procedure, in this case, is for the baseline extension monitor to notify the slave of any significant variations in coding delay. The slave then examines the time difference recorded by its own standby timer which serves as a monitor. If there is any substantial disagreement between slave and the baseline monitor, the slave may consult the master, or Bermuda, or both. When the system operates without baseline extension monitors, the slave monitors its own coding delay with assistance from the master and Bermuda. Overall monitoring of the system is coordinated by the Master.

The Bermuda monitor, being well out in the service area, can serve as an overall system monitor. Time differences recorded by the Bermuda monitor are particularly useful for examination of overall system synchronization, stability and reliability. Figure 2 is an example of time-difference recordings made at the Bermuda monitor. During the 12-hours shown in Figure 2, the triad provided Loran-C service 96.8 percent of the time. The only interruption occurred at 1605 EST. Normal service was resumed at 1628 EST. This interruption was caused by breakdown of a capacitor in the master transmitter. The system operated without the West Palm Beach monitor. The Cape Cod monitor secured at 1630 EST. In the 12-hour period only one coding delay adjustment was made. The master observed that the MY cycle time-difference had increased gradually during the afternoon. At 1930 EST the increase amounted to 0.1 microsecond. By 2230 EST the mean MY time-difference measured at the master had increased 0.2 microsecond above the afternoon value. At 2232 the master directed the Y-slave to reduce its coding delay by 0.2 microsecond. A very high degree of correlation is evident between the Bermuda Y-cycle (lower trace, Figure 2) and the master Y-cycle chart (not shown). The Y coding delay adjustment of -0.2 microsecond at 2232 EST can be seen clearly on the Bermuda Y-cycle recording.

The continuity of Loran-C service in the Bermuda area was equal to or greater than 95 percent on 32 percent of the days between February 3, 1958 and August 28, 1958. On 50 percent of the days in this period, the Bermuda monitor received usable Loran-C data about 87 percent of the time. Table 16 gives the percent of days on which the usable Bermuda data exceeded the indicated percent.

Percent of Usable Bermuda Data Equal to or Greater than:	On Percent of Days
100	5.6
97	20
95	32
90	40
85	55
80	61
62	82
56	90
38	95

TABLE 16

An analysis of the causes for interruption of Loran-C service has been made. The period from June 2, 1958 to July 31, 1958 was selected for this analysis. In this period, the triad operated a total of 1352 hours. Of this total, 1264 hours were scheduled on a 24-hour per day basis from June 2 to July 25. During the 1352-hour period, 362 interruptions of synchronization were recorded in the master station log. Table 17 summarized these according to cause of failure, the number of occurrences of each type and the percent of total failures of each type.

More than one-half the failures were caused by inadequate supporting facilities, such as over-loaded transmitter power supply, inadequate communications and primary power failure. Approximately 30 percent of the failures were caused by frequency divider malfunctions (including Phase Code errors). The principles of frequency division

Cause of Failure	Number Occurrences	Percent of Total Occurrences
Transmitter Power Supply	64	17.7
Phase Code Errors	55	15.2
Divider Jumps	55	15.2
Unexplained Jumps	45	12.4
Inadequate Communications	33	9.1
Commerical Power Failure	23	6.4
Operator Errors	20	5.5
Component Failure	18	5.0
400 Cycle Generator Faults	11	3.0
Inadequate Commercial Power	7	1.9
Oscillator Drift	7	1.9
Atmospherics	7	1.9
High Ambient Temperature	6	1.7
All others	11	3.1
TOTALS	362	100

TABLE 17

are widely used in Standard Loran with an exceptionally high degree of reliability. Thus, these faults appear to be extraneous to the ultimate attainable reliability of Loran-C. The only faults which appear to be uniquely associated with Loran-C were caused by atmospheric noise. Less than two percent of the failures were caused by atmospherics.

4. Time Difference Measurements

a. General

The precision of time difference measurements at fixed locations, such as at the transmitters and baseline monitors, can be increased by averaging the continuous readings for a few minutes. Likewise, certain requirements for high precision position fixing or surveying of fixed geographical areas permit the averaging of continuous time difference readings obtained over periods of minutes or even hours. There are other applications, however, which require stability of the continuous time difference measurements. The stability of time difference measurement in the U.S. East Coast Loran-C system has been examined for three different amounts of averaging. These are: (1) instantaneous or continuous measurement, (2) 15-minute averages, and (3) eight-hour average values.

b. Instantaneous (Continuous) Time Differences

An example of continuous envelope and cycle time difference recordings at Bermuda is given in Figure 2. The following comments refer to the cycle time differences.

The relatively fast fluctuations of the cycle time differences have a peak-to-peak amplitude of about 0.2 to 0.3 microsecond during the daytime. The amplitude of these fluctuations begins to increase at about the time of surface sunset. Within an hour after surface sunset, the cycle time difference recordings assumed their nighttime characteristics. The fluctuations of the X-cycle recordings are greater than those of the Y-cycle at night. In the daytime the difference is not large.

Recordings of cycle time difference for a full year have been examined. No regular seasonal effects were found except for the obvious variations in length of the days and nights. There is a considerable day-to-day and night-to-night variation in the amplitude of the cycle time difference fluctuations.

The period of the relatively rapid fluctuations is determined by the time constants of the filter and servo circuits of the receiver. Abrupt changes in the mean may occur when a coding delay adjustment is made at the slave transmitter. Relatively slow variations in the mean cycle time difference occur during periods of several hours and from day-to-day. The amplitude fluctuations becomes randomly distributed within a period of an hour or two. The standard deviation or RMS deviation from the mean is a convenient measure of the fluctuations. Recordings of cycle time differences from all stations for all seasons of the year have been examined. About 90 percent of the recordings have standard deviations between the lower and higher values given in Table 18.

Receiver Location	Rate	Standard Deviation-Microseconds Day	Night
Bermuda	X	.04-.09	.07-.20
	Y	.03-.07	.06-.11
Cape Cod	X	.04-.06	.06-.10
	Y	.02-.05	.03-.05
West Palm Beach	X	.02-.03	.02-.03
	Y	.05-.08	.06-.11
Master	X	.01-.04	.02-.04
	Y	.02-.05	.02-.05

TABLE 18

TYPICAL VALUE OF STANDARD DEVIATION
OF CYCLE TIME DIFFERENCE RECORDINGS
(Continuous Recordings-No Smoothing)

c. 15-Minute and 8-Hour Average Time Differences

Examples of 15-minute average time-difference plots are given in Figures 3,4 and 5. Examples of eight-hour average plots are given in Figures 6,7 and 8. The 15-minute average plots are useful for examination of hour-to-hour and day-to-day variations. When annotated to show coding delay adjustment, equipment malfunctions and other significant occurrences, these plots are useful for overall analysis of the system.

Deviations of the 15-minute average time differences tend to become randomly distributed in a period of about eight hours. In a period of several days, deviations of the 15-minute average values are completely random except for a very gradual variation in the long-term mean. Examination of much more than a week's plot of 15-minute averages becomes very inconvenient. Examination of the very long-term trend of data can be supplemented by plots of daily average readings over periods of many months. Figures 6,7 and 8 are such plots. These plots show the average time differences recorded in the eight-hour periods 0800 to 1600 from August 12, 1957 to August 28, 1958. The hours 0800 to 1600 EST were used for the following reasons: (1) this is the period of lowest atmospheric noise and so permits more accurate investigation of seasonal variations of propagation velocity, (2) the nighttime hours 2000 to 0400 EST were investigated separately for several months to discover diurnal effect, if any. There was no evidence of regular day-to-night changes in mean eight-hour time difference. The nighttime averages were discontinued after seven months.

It is convenient to identify the eight-hour periods by numbers rather than by calendar dates. The calendar date corresponding to each operating period is given in Table 19.

Standard deviation of the 15-minute averages from the eight-hour mean were computed for each daytime operating period from February 3, 1958 to May 29, 1958. These were computed for both rates (X and Y), for both master times (standby and operating), and for the Ground Monitor

TABLE 19

OPERATING PERIOD AND DATES FOR
THE PERIODS 1 THROUGH 274, AUGUST 12, 1957
THROUGH AUGUST 28, 1958

Period No.	Date	Period No.	Date	Period No.	Date
1	Aug. 12	41	Oct. 15	81	Jan. 15
2	14	42	16	82	16
3	15	43	17	83	17
4	16	44	18	84	20
5	17	45	19	85	21
6	19	46	21	86	22
7	20	47	22	87	23
8	21	48	23	88	24
9	22	49	24	89	27
10	23	50	Nov. 1	90	28
11	26	51	4	91	29
12	27	52	5	92	30
13	28	53	6	93	31
14	29	54	7	94	Feb. 3
15	30	55	8	95	4
16	Sept. 4	56	12	96	5
17	5	57	13	97	6
18	6	58	14	98	7
19	7	59	15	99	10
20	9	60	18	100	11
21	10	61	19	101	12
22	12	62	20	102	13
23	13	63	21	103	14
24	14	64	22	104	15
25	15	65	Dec. 9	105	16
26	16	66	10	106	17
27	17	67	11	107	18
28	18	68	12	108	19
29	19	69	13	109	20
30	20	70	16	110	25
31	23	71	17	111	26
32	30	72	18	112	27
33	Oct. 1	73	19	113	28
34	3	74	20	114	Mar. 1
35	4	75	30	115	2
36	8	76	Jan. 2	116	3
37	9	77	3	117	4
38	10	78	10	118	5
39	11	79	13	119	6
40	14	80	14	120	7

Continued -

Continuation of TABLE 19

Period No.	Date	Period No.	Date	Period No.	Date
121	Mar. 8	161	Apr. 18	201	June 9
122	9	162	22	202	10
123	10	163	23	203	11
124	11	164	24	204	12
125	12	165	25	205	13
126	13	166	26	206	14
127	14	167	28	207	15
128	15	168	29	208	16
129	16	169	30	209	17
130	17	170	May 1	210	18
131	18	171	2	211	19
132	19	172	5	212	20
133	20	173	6	213	21
134	21	174	7	214	22
135	22	175	8	215	23
136	23	176	9	216	24
137	24	177	10	217	25
138	25	178	11	218	26
139	26	179	12	219	27
140	27	180	13	220	28
141	28	181	14	221	29
142	29	182	15	222	30
143	30	183	16	223	July 1
144	31	184	19	224	2
145	Apr. 1	185	20	225	3
146	2	186	21	226	4
147	3	187	22	227	5
148	4	188	23	228	6
149	5	189	25	229	7
150	6	190	26	230	8
151	7	191	27	231	9
152	8	192	28	232	10
153	9	193	29	233	11
154	10	194	June 2	234	12
155	11	195	3	235	13
156	12	196	4	236	14
157	13	197	5	237	15
158	14	198	6	238	16
159	15	199	7	239	17
160	16	200	8	240	18

Continued -

Continuation of TABLE 19

Period No.	Date
241	July 19
242	20
243	21
244	22
245	23
246	24
247	29
248	30
249	31
250	Aug. 1
251	2
252	3
253	4
254	5
255	6
256	7
257	8
258	9
259	10
260	11
261	12
262	13
263	14
264	15
265	19
266	20
267	21
268	22
269	23
270	24
271	25
272	26
273	27
274	28

Receivers at Bermuda, Cape Cod and West Palm Beach. The values of standard deviation obtained on the indicated number of days have been averaged. The results are summarized in Table 20.

Receiver Location	Standard Deviation Microseconds		Number of Days Averaged	
	X	Y	X	Y
Bermuda	.036±.014	.040±.019	91	91
Master Timer #1	.032	.039	52	69
Master Timer #6	.037	.040	55	78
Cape Cod	.098	.039	71	73
West Palm Beach	.030	.060	69	66

TABLE 20

STANDARD DEVIATION OF 15-MINUTE AVERAGES
FROM THE 8-HOUR DAYTIME MEAN TIME DIFFERENCES
(Average of All Days - February 3-May 29, 1958)

The (±) signs in Table 20 indicate the range of values obtained on 50 percent of the days at Bermuda.

The eight-hour average time differences for each daytime operating period between August 12, 1957 to August 28, 1958 have been averaged to obtain a mean value for the year. The mean value for the year and the standard deviation of the eight-hour averages from the mean are given in Table 21 for the Bermuda monitor. Data obtained on the Y-rate before September 4, 1957 are not included in Table 21.

Rate	Time Difference (microseconds)	Standard Deviation (microseconds)	Total Number 8-hour Periods
X	15,888.94	0.116	238
Y	33,091.95	0.131	229

TABLE 21

MEAN VALUE OF BERMUDA 8-HOUR TIME DIFFERENCE
AND STANDARD DEVIATION FROM THE MEAN

5. Position Fixes

a. Bermuda Fixes

The long-term stability of the Loran-C system is indicated in Figure 9. Each dot represents the intersection of an X and a Y line of position obtained from eight-hour average time difference readings of the Bermuda monitor. The mean values (in microseconds) are shown. The X and Y time differences associated with each point may be determined by measuring the perpendicular distance from the point to each of the mean lines and comparing these distances to the microsecond scales. Distances are indicated by the "Distance in Feet Scale." The true north direction is indicated by the arrow.

Figure 9 shows that 50 percent of the fixes obtained from daytime eight-hour averages at Bermuda during a year fall within a circle of 260 foot radius.

Figure 10 is a plot of the Bermuda fixes obtained by averaging the indicated time differences for one-month periods. The X and Y lines of position obtained during the calibration period (Sept. 4 - Sept. 19, 1957) are shown. (These are very slightly different from the year-mean lines of Figure 9.) The maximum departure of a month's mean indicated position from the position indicated in the calibration period was 440 feet (January and February, 1958).

Figure 11 shows the Bermuda fixes obtained from 15-minute average time difference readings during a period of 36.5 hours. The period is large enough for the 15-minute readings to become normally distributed. The circle of radius 105 feet contains 50 percent of the fixes.

b. <u>Fixes From Aircraft</u>

In the spring and summer of 1958 a number of flight trials of a Loran-C receiver were undertaken. The primary purpose of the trials was to determine the suitability of the receiver for Loran-C propagation tests. The receiver was operated during several long over-water missions. On these flights, the plane's position was determined by Standard Loran. Accuracy of the Loran-C envelope time difference was checked by the Standard Loran measurements. Checks of the Loran-C cycle measurements, however, required a more accurate determination of the plane's position. Flight paths were selected to go over ground check points which had been surveyed previously. Several passes were made over each of three ground check points. On each pass, the operators locked the time difference dials on the Loran-C receiver at the instant the aircraft passed over the ground check point. This procedure for obtaining Loran-C readings eliminated any tendency for the operator to make a mental computation of the "average" reading. Visual fixes of the aircraft position relative to the ground check points were obtained with a vertically stabilized drift sight. The average altitude of the aircraft was 1300 feet and the average ground speed was 120 knots. The accuracy of aircraft position relative to the ground check points is estimated to be less than 10 feet.

Figures 12, 13 and 14 show the results of three tests of airborne Loran-C fixes in the vicinity of the Little Bahama Banks, B.W.I. In each figure, a point marked "tabulated position" corresponds to the ground check point. The positions indicated by Loran-C measurements are shown by crosses enclosed in circles. (The indicated Loran-C time differences were corrected for land along the paths before plotting.)

The results of the tests are summarized in Table 22 and Table 23.

Fix No.	Deviation of Fix From Mean Indicated Position (feet) Bassett Cove	Little Sale Cay	Walker Cay
1	100	-	82
2	-	675	46
3	420	690	200
4	195	55	270
5	1235	480	-
6	420	470	34
7	-		-
8	1040		
9	225		
10	390		
Average:	503	474	126

TABLE 22

Distance and Bearing From Tabulated to Mean Measured Position

	Bassett Cove	Little Sale Cay	Walker Cay
Distance	405 ft.	430 ft.	126 ft.
Bearing	337°	341°	328°

TABLE 23

6. Accuracy of Envelope Match

Envelope and cycle time difference recordings from the Loran-C system have been examined to determine the ability of the receivers to measure envelope time differences with sufficient accuracy to make the cycle time difference unambiguous. An example will illustrate the meaning of "cycle ambiguity" and "envelope-to-cycle discrepancy." Suppose that the envelope time difference were 15,888 microseconds and the cycle time difference was 8.1 microseconds. The ultimate precision of measurement comes from the cycle measurement. Thus, the envelope measurement would be refined by the addition of 0.10 microsecond obtained from the cycle measurement, and the "composite" time difference reading would be 15,888.10 microseconds. The discrepancy between envelope and cycle readings is called "the envelope-to-cycle discrepancy." In this example, the discrepancy is -0.1 microsecond. If for some reason the envelope reading had been 15,883, the discrepancy would be either +4.9 microsecond or -5.1 microsecond. There would be considerable doubt about the composite reading. The composite value could be either 15,888.1 or 15,878.1. To avoid this ambiguity, it is necessary for the envelope measurement to be accurate to within about ± 4 microseconds. An accuracy of ± 1 or ± 2 microseconds gives more confidence that no cycle identification error has been made.

Typical fluctuations of the indicated envelope time difference are shown for the X envelope in Figure 2. (The Y envelope recorder was out of order during the period shown in Figure 2.) During the daytime hours the average X envelope reading was 15,887 microseconds. The average X cycle was about 9.1 microseconds. Thus the average discrepancy was -2.1 microseconds.

During the daytime the discrepancy at Bermuda is less than 2 microseconds more than 90 percent of the time.

The discrepancy is only slightly higher on the Y pair at nighttime than during the daytime. The fluctuations of X envelope increase sharply, however, soon after sunset. On many consecutive nights the X discrepancy may be less than 4 microseconds for 90 percent of the time, regardless of season of the year. However, on other nights there were several hours during which the X discrepancy exceeded 5 microseconds for more than 10 percent of each hour.

Figure 36 is a plot of X envelope-to-cycle discrepancy for two periods of one week each, one in the winter and one in the summer. Figure 37 shows plots for one week in the spring and one week in the fall. During the two weeks illustrated in Figure 36, the X envelope-to-cycle discrepancy for 90 percent of each hour was less than

4 microseconds for 164 hours out of a total of 167 hours, or for 98.2 percent of the hours. During the two weeks illustrated in Figure 37, the discrepancy for 90 percent of each hour was less than 4 microseconds for 74.6 percent of the hours.

7. <u>Instrumental Stability of The Monitors</u>

Long-term stability of the East Coast triad has been obtained from the use of multiple monitoring facilities which should not be required in an operational system and which may not be available in future Loran-C systems. For example, the East Coast triad has depended upon assistance from one or both of the slave baseline extension monitors or the Bermuda monitor for control of coding delay adjustments. Theoretically, no location is better for monitoring slave coding delay than at the slave station. Practically, however, a great deal of care and good engineering practice is required in order to obtain stable time difference measurements in the immediate vicinity of one of the transmitters involved in the measurement. This applies to the master as well as to the slaves. It should be pointed out that satisfactory monitoring at the slaves and at the master does not require absolute accuracy but does require stability; if time difference measurements are stable and dependable, the question of accuracy can be taken care of during initial system calibration.

Instrumental stability of the monitors at the master and slaves was examined throughout the first year of system operation. Some of the results of this analysis are given below.

Stability of time difference measurements made at the slave can be examined by comparing these measurements with corresponding measurements made at the baseline extension monitor. Comparisons of this type can be found in Figures 3 through 8. In these Figures, time differences are represented by the letter "T". The first subscript identifies the station pair (T_x for MX time differences and T_y for MY time differences). The second subscript identifies the receiver location; for example, the symbol T_{yy} refers to the MY time difference (first subscript) measured at the Y slave station (second subscript). The baseline extension monitor locations are identified as X' (West Palm Beach) and Y' (Cape Cod).

Figures 3, 4 and 5 give plots of 15-minute average time differences measured at all stations during a 48-hour period. In Figure 4, the plot of T_{yy} shows that measurements of Y time difference at the Y slave (Martha's Vineyard) were very unstable. Each slave uses a standby transmitter synchronizer (timer) as a receiver to monitor its own coding delay and to monitor the opposite slave. Time differences measured at the Y baseline monitor, at

Bermuda, and at the master (Figure 4) show that many of the apparent variations in Y coding delay indicated by the standby (monitor) timer at the Y slave were not real. Monitoring at the X slave was more stable during this 48-hour period (Figure 3).

Long term variations in time differences recorded at the transmitters can be seen in Figures 6, 7 and 8. It will be observed that very little correlation exists between long term variations of time differences recorded at the slaves and those recorded at the corresponding baseline monitor.

An estimate of the stability of the master monitors can be obtained by comparing time differences indicated by the two master timers (operating and standby timers). The two master timers may agree (or differ by a small constant) for periods of several days (Figures 3 and 4). The long term stability is not so great, however. Figure 7 shows that there was very little correlation between the eight-hour average time differences obtained from the two master timers during the first three months of 1958. Correlation between the two master timers increased considerably during the next five months.

During the first five months of system operation (August-December 1957) several methods were investigated for improving the stability of monitoring at the transmitters.

Particular attention was given to three arrangements of the monitoring (receiving) antennas. The notes across the top border of Figures 6 and 7 show the antenna arrangements that were used for monitoring at the transmitters. Before operating period 39 (October 11, 1957), the monitoring antennas were 90 foot masts located approximately 1500 feet from the transmitting antennas. This arrangement was unsatisfactory because of the difficulty of controlling leakage of the local signal into the 1500 foot transmission line which connected the monitor receiver to the 90 foot receiving antenna.

The problems of the 1500 foot transmission line were eliminated by using a short whip receiving antenna located only a short distance from the monitor receiver (operating periods 39 through 55). The monitor receiver, a part of the transmitter synchronizer (timer), was located in the transmitter building beneath the top-loading elements of the 625 foot transmitting antenna. It was believed that a more stable sample of the local signal could be obtained by sampling the current at the base of the transmitting antenna. The whip antenna was replaced by an inductive pick-up loop located near the base feed line of the transmitting antenna. Of the three methods, the inductive pick-up loop was found to be the most stable. The loop method was used for monitoring at the master station after operating period 77

(January 3, 1958). The slave station adopted the loop method shortly thereafter.

One of the most difficult problems of monitoring time differences at one of the transmitters is to obtain phase-stable samples of the local signal. The phase of the local signal voltage at the receiver input is determined by the relative amplitude of electric and magnetic components of the local field coupled into the receiver. Ability of a slave to monitor its own coding delay can be checked by comparing time difference measured at the slave with those obtained at the slave baseline extension monitor. Variations of time differences measured at the master, however, may be caused by (a) variations in baseline transmission time, (b) variations in slave coding delay, (c) variations in the phase of the local (master) signal supplied to the master monitor receiver, or (d) errors within the receiver itself. The variations (c) and (d) above may be considered together as "instrumental", in which case, the receiver's antenna arrangement is considered to be a part of the receiver. If there were no instrumental errors, variations in round trip baseline transmission time would appear directly in the master-slave time difference measured at the master (after allowance for variations in coding delay variations). Conversely, if the baseline transmission time and coding delay were constant, variations in master-slave time difference measured at the master would be caused by instrumental variations only.

A test for instrumental variations of the monitors has been developed and is given in equation 22.

$$(T_{YM} - T_{XM}) - (T_{YX} - T_{XY}) = K \tag{22}$$

Equation 22 is independent of the coding delay of either slave and is independent of transmission times between stations. Variations in K (referred to as the K factor) are caused only by instrumental variations. Certain equal (or equal and opposite) instrumental variations do not cause variations in K. For example, variation in the apparent phase of the master signal would cause equal changes in T_{YM} and T_{XM} (Y and X time differences measured at the master station).

Another useful test for instrumental variations is given in equation 23:

$$(T_{YM} - T_{XM}) - (T_{YX}' - T_{XY}') = K' \tag{23}$$

Equation 23 uses time differences T_{YX}' and T_{XY}' measured at the baseline extension monitors rather than T_{YX} and T_{XY}.

Measurements at the baseline extension monitors are usually more stable than those at the slaves. Use of measurements made at the baseline monitors is justified because both signal sources (master and the distant slave) are a great distance from the receiver compared to the distance between the slave and its baseline monitor.

Plots of the K factors (K and K') are shown in Figures 32 and 33. A constant (10 microseconds) was added to each plot in order to avoid negative numbers. Figure 32 shows the plots which were computed from eight-hour mean daytime values of time differences. Figure 33 shows plots of the K factors computed from 15-minute average time differences.

In the top trace of Figure 32, approximately 95 percent of the eight-hour average K factors for the period January through August, 1958 are within 0.5 microsecond of the mean (standard deviation of 0.25 microsecond). The K factors computed from 15-minute average time differences have a standard deviation of about 0.15 microsecond for the 48-hour period shown in the top trace of Figure 33.

Two reasons for the relatively large deviations of the K factors are as follows: (a) operators of the slave stations have monitored the opposite slave in order to detect gross errors in synchronization and have not been greatly concerned with cycle time difference accuracy; (b) operating and standby times do not agree precisely. Time differences used to compute the K factors were obtained from the master operating timer and the slave standby timers. Many of the large deviations in the eight-hour average K factors can be traced to exchanges of timers.

Examination of instrumental stability of the monitors suggested two further investigations, the results of which are shown in Figures 34 and 35. Between operating periods 88 and 144, the standby timer at the X slave (Jupiter) indicated that the eight-hour average X coding delay had increased gradually by about 0.2 microseconds. During the same period, the X baseline extension monitor (West Palm Beach) observed no such long term drift (see Figure 6). No satisfactory explanation for the gradual departure of time differences indicated by the two monitors could be found. An attempt was made to determine which of the two monitors (Jupiter or West Palm Beach) gave the more stable indication of X coding delay. The question was not answered conclusively; however, a remarkable correlation was found between the X time difference indicated by the X slave (T_{XX}) and by the Bermuda monitor (T_{XB}). Plots of eight-hour average values of T_{XX} and T_{XB} for operating periods 88 through 144 (January 24 through March 31, 1958) are given in Figure 34. The exceptionally high correlation is obvious.

The use of eight-hour averages for examination of long-term stability becomes complicated, or even misleading, if the stations change timers (monitors) during the eight-hour periods. (This did not happen at the X slave during the periods shown in Figure 34). The possibility of using shorter periods within the day was investigated. Figure 35 compares eight-hour and one-hour average time differences obtained at the Bermuda monitor for a period of about two and one-half months. Notice that the two scales have been offset by 0.2 microsecond so that the two curves can be identified separately. The one-hour averages were obtained between 1300 and 1400 EST. Figure 35 shows that one-hour and eight-hour averages at Bermuda were very highly correlated throughout the entire period. This indicates high daytime stability of the Bermuda monitor and of system synchronization.

SECTION IV
INVESTIGATIONS OF SKY WAVE COVERAGE

A. INTRODUCTION

The feasibility of using sky waves for greatly extending the range of Loran-C coverage was investigated in the spring and summer of 1958. An aircraft of the U.S. Coast Guard was equipped with a Loran-C receiver and was prepared for flights to probe the extent of the ground wave and the first and second hop sky waves. Two principal flights (and supporting flights) were planned. The first flight, in March and April, covered the area from Bermuda to Puerto Rico, Trinidad, the northern coast of South America (Belem, Brazil) and the northeast coast of South America (Natal, Brazil). The second flights, in June and July, covered the area from Newfoundland, Iceland, Western Europe, the Mediterranean, the Azores and Bermuda.

B. PREDICTIONS

Prior to making the trips, predictions were prepared for each of 18 locations included in the flight plan. The prediction sheets included the following information:

(1) Survey data prepared by the Hydrographic Office of the U.S. Navy including the following: name of location; latitude and longitude of a prominent landmark near the aircraft runway (called the "Control Point"); distance and

bearing angle from the control point to the three Loran-C transmitters; a description of the great circle path from each transmitter to the control point giving a land-water breakdown; a statement of survey accuracy relative to the U.S. datum.

(2) Ground wave time difference for the control point and gradients of the lines-of-position.

(3) Ground wave and sky wave field strengths and sky wave delay (first four hops).

(4) Atmospheric noise by four-hour time blocks.

The exact parking position of the aircraft could not be known in advance of arrival at each air field. However, the prediction sheets provided step-by-step instructions for rapid computation of time difference offset corrections to account for the final offset of the aircraft from the control point. Ground wave time differences of the control point included secondary ground wave corrections for the actual paths. Conductivity of the land near the transmitters had been measured during system calibration. Estimated values of conductivity were used for other land areas along the paths.

Ground wave transmission times were computed for all of the landing points on the flight plan even though many of these points were well beyond the range of the ground wave. Transmission times were computed on the basis of all-water paths and then re-computed for the actual paths. Sky wave delays were computed with reference to a fictitious ground wave having an all water path. When both ground wave and sky waves could be received, the sky wave delay relative to the actual ground wave could be measured. Beyond the range of the ground wave, it was convenient to reference all sky wave delays to the fictitious all-water path ground wave. This procedure aided the identification of sky wave hops by measuring the difference of delay between successive hops.

C. INSTRUMENTATION AND CALIBRATION

The aircraft used for the second evaluation flight (June 15 - July 10, 1958) is shown in Figure 15. The aircraft, a U.S. Coast Guard Type R5D is shown at the U.S. Coast Guard Air Station, Argentia, Newfoundland, prior to take off for Keflavik, Iceland. Seven of the antennas available for the Loran-C receiver and other equipments can be seen in Figure 15. Three long-wire antennas ran from the forward fuselage to the vertical stabilizer of the tail assembly. Four short whip antennas, two on top and two below the midship section, are shown. In addition, two trailing-wire antennas were available.

An interior view of the aircraft is shown in Figure 16. In the foreground is the Loran-C flight test bench. To the left of center in the background, the Standard Loran test bench can be seen. To the right of center in the background, the low-frequency monitoring bench can be seen. A close-up view of the low-frequency monitoring bench is given in Figure 17.

Loran-C time difference measurements were recorded with the four Esterline-Angus recorders shown in the lower left of Figure 16. The other equipments below the bench are special test equipment. The three units of the Loran-C receiver and two test oscilloscopes are shown on the top of the test bench. Field strength measurements of the Loran-C signals were made with the Loran-C receiver. The field strengths of other signals between 70 and 130 kc were measured at the low-frequency monitoring bench using either of the two AN/SRR-11 radio receivers.

The Loran-C receiver was calibrated for use as a measuring set for Loran-C signal strengths. First, the receiver was calibrated as a voltmeter to measure the voltage at its own antenna input terminals. Next, a URM-6 field strength measuring set was used to measure the field strength in the immediate vicinity of the aircraft of several continuous wave signals near 100 kc. Finally, the URM-6 was used as a voltmeter to measure the voltage produced by these same signals across the antenna input terminals of the Loran-C receiver. Thus, the URM-6 was used to measure the effective height of the receiving antenna, including all loading and mismatch factors. As a final check on calibration, the field strengths of the Loran-C signals at Bermuda were measured. The indicated field strengths were within ± 3 db of the computed values.

There was initially some doubt about the directional pattern of the receiving antennas, particularly regarding the phase. In order to check the phase pattern, the heading of the aircraft was varied continuously through one full turn (360°) on the runway. The test indicated that the antenna patterns were circular.

The AN/SRR-11 low-frequency radio receivers and their receiving antennas were calibrated with the URM-6 field strength set so that they could be used to measure the field strength of other signals and atmospheric noise from 70 to 130 kc.

D. ITINERARY AND TEST PROCEDURES

Flight operations were conducted in two periods. Evaluation flight No. 1 extended from March 12 to April 9, 1958. Evaluation flight No. 2 extended from June 9 to July 10, 1958. The dates and approximate times of arrival and departure are given in Table 24.

Availability of the aircraft and other considerations required that the extended range evaluation flights be undertaken before the final design of the Loran-C receiver had been completed and tested. Preliminary flight trials of the Loran-C receiver were conducted near the U.S. East Coast prior to the principal flights No. 1 and No. 2. The purpose

Location	Arrival Date (1958)	Arrival Time (EST)	Departure Date (1958)	Departure Time (EST)
<u>Flight No. 1</u>				
Preliminary Flight Trials	March 12		March 21	1630
Bermuda, B.W.I.	March 21	2019	March 26	1615
San Juan, P.R.	March 26	2151	March 30	1746
Piarco, Trinidad	March 30	2127	April 1	2203
Belem, Brazil	April 2	0620	April 3	2229
Natal, Brazil	April 4	0400	April 7	0004
Piarco, Trinidad	April 7	1050	April 8	0700
San Juan, P.R.	April 8	1000	April 8	1150
Elizabeth City	April 8	2017	April 9	0830
<u>Flight No. 2</u>				
Preliminary Flight Trials	June 9		June 16	0855
Argentia, Nfld.	June 16	1700	June 18	1628
Keflavik, Iceland	June 19	0141	June 20	1942
Prestwick, Scotland	June 20	2350	June 22	1500
Wiesbaden, Germany	June 22	1937	June 25	
Rhodes, Greece	June 25		June 26	
Ankara, Turkey	June 26		June 27	
Rhodes, Greece	June 28		June 30	
Tripoli, Lybia	July 1		July 2	
Port Lyautey, Morocco	July 2		July 4	
Lagens, Azores	July 5	0050	July 7	0336
Bermuda, B.W.I.	July 7	1615	July 9	0715
Nassau, B.W.I.	July 9	1154	July 9	1245
Eleuthera, B.W.I.	July 9	1330	July 9	1545
Nassau, B.W.I.	July 9	2230	July 10	0900
Elizabeth City, CGAS	July 10	1530	July 10	1830
Washington, D.C.	July 10	1945		

TABLE 24

ITINERARY OF FLIGHTS NO. 1 AND NO. 2

of the preliminary flights was to examine the characteristics of the receiver under known conditions in the ground wave area. The preliminary trials in March 1958 indicated that the receiver occasionally made errors of one or more whole cycles in the measurement of envelope time difference. However, the cycle time difference measurements were quite reliable and accurate. It was decided that the receiver could be used for propagation studies but that no effort should be made to evaluate the potential performance of the receiver itself. In the two-month period between evaluation flights No. 1 and No. 2, the design and construction of the receiver was completed. Preliminary flight trials in June 1958 indicated that the envelope circuit difficulty had been eliminated and that the receiver was ready for trials as a navigation aid as well as for further propagation studies.

Continuous recordings were made of X and Y envelope and cycle time differences. Instantaneous readings of time differences indicated by the receiver dials were recorded every 10 or 15 minutes. The chart recordings were calibrated at least once each hour.

Field strength measurements of three Loran signals were made every 15 to 30 minutes. These measurements were limited to the particular ground wave or sky wave modes that the receiver was recording at the time. It was felt that more useful information could be obtained from uninterrupted time difference recordings than from additional field strength readings. The Loran-C signals (and noise) at the output of the RF amplifier were displayed on an oscilloscope which had been included in the test-bench setup. Photographs of the Loran-C signals were made frequently.

Continuous recordings of atmospheric noise and continuous-wave interference, derived from the noise and CW detector in the receiver, were made. The noise and CW recordings were of little value, however, because of unreliable calibration. Reliable measurements of atmospheric noise and field strength of other low-frequency signals were obtained once each hour with the AN/SRR-11 receivers.

On the long over-water runs, Standard Loran readings were taken at the same instants that Loran-C readings were made. Two manual tracking Standard receivers were used so that readings on two rates could be made simultaneously.

E. TEST RESULTS

1. Extent of the Ground Wave Area

Flight plans were arranged to probe the extent of the ground wave area in the daytime and at night. The ground wave could be tracked continuously far beyond the charted Loran-C area. This made it difficult to obtain direct comparisons of Loran-C and Standard readings. The accuracy and stability of Loran-C measurement near the fringe of the ground wave area could be checked by making continuous time difference recordings for several hours at certain of the previously surveyed ground check points. The maximum useful range of the ground wave was usually some distance between the available ground check points. Fairly reliable estimates of this maximum useful range were obtained by observing the operation of the Loran-C receiver on out-bound and in-bound flights. As expected, the ground wave signals could be tracked, once they were acquired, to a distance somewhat greater than the maximum distance for acquisition of the signals. Thus, one real test for maximum range is to determine the distance at which the operator is able to acquire signals for satisfactory operation of the receiver. On two separate in-bound flights, both in daytime, the operators were able to acquire ground wave signals at about 1500 nautical miles from the most distant transmitter. Acquisition was possible only when signals could be seen on the test oscilloscope. The ground wave signals were completely invisible in the noise. However, the first hop sky wave signals, being several times as great, could be seen. The receiver was synchronized on the visible first hop sky waves. Then the sampling gates were moved manually to coincide with the invisible ground wave. Synchronization with all three ground wave signals was acquired in this manner. Thus, the sky wave signals were found to have some practical value even to ground wave operation; that is, the sky wave, being of greater amplitude at great distances, served as fairly accurate markers and showed where the sampling gates should be positioned in order to find the ground wave.

Two means were available and were used by the operator to determine that the receiver was synchronized with ground waves. Field strength measurements indicated immediately that the visible signals had several times the field strength that the ground waves could possibly have within several hundred miles of the estimated aircraft position. The field strength of the lesser signal checked reasonably well with the predicted value for a ground wave at that distance. As an additional check, the delay between the visible sky wave signal and the invisible ground wave signal was measured. The measured delay confirmed that the invisible signal was a ground wave and that the visible signal was the first hop sky wave.

2. <u>Extent of the Sky Wave Area</u>

First hop sky wave signals were received at Piarco, Trinidad day and night, a distance of 1906 nautical miles from the most distant transmitter (Y slave). Daytime first hop signals were acquired on an in-bound flight from Brazil to Trinidad at a distance of 2300 nautical miles. Daytime second hop signals could not be detected at any range. At night, however, the second hop signals were received with good signal strength at Natal, Brazil, 3435 nautical miles from the Y slave. At this range, both the third and fourth hop waves had even greater amplitude than the second. The receiver operated on the third hop waves for several hours with surprising stability.

As expected, the number of hours during which stable nighttime sky waves were received was limited by the illumination of the ionosphere by the sun's rays. In general, the nighttime sky wave signals were acquired only after the entire ionospheric path had been in darkness for one or two hours. On long east-west paths (the Azores and Port Lyautey), the entire path had been in darkness for two to five hours, respectively, before signals were acquired at nighttime. In all cases, the signal strength dropped quickly after surface sunrise at the receiver.

Photographs of the Loran-C signals at the output of the receiver RF amplifier are shown in Figures 18, 19, 20 and 21.

3. Time Difference Measurements

Instantaneous time difference measurements, made at intervals of 10 to 15 minutes, were plotted throughout the course of the flights. The continuous recordings were analyzed later and compared with the plots of instantaneous readings. It was found that plots of the instantaneous time difference readings gave an accurate picture of the long-term variations. The continuous recordings gave a better indication of short-term fluctuations. Examples of plots of the instantaneous time difference readings are given in Figures 22 and 23. Examples of the continuous recordings are given in Figures 24, 25, 26, 27 and 28.

Table 24 summarizes the instantaneous time difference measurements. It is interesting to notice that the sky waves for periods of several hours have nearly the stability that ground waves have at the fringe of the ground wave area.

The range of 95 percent of the first hop sky wave time differences was almost always less than ±0.75 microsecond from the mean for periods of several hours (standard deviation less than 0.375 microsecond). The second and third hop sky waves had nearly the same short-term stability as the first hop but had a greater variation within a period of several hours. For periods of four hours or more, 95 percent of the second and third hop time differences were within ±1.5 microseconds of the four-hour mean (standard) deviation of 0.75 microsecond.

4. Envelope-to-Cycle Discrepancy

The indicated cycle time difference seldom deviated from the predicted value by more than 1.0 microseconds. However, the envelope reading occasionally differed

TABLE 24

TIME-DIFFERENCE MEASUREMENTS
(INSTANTANEOUS READINGS)

Receiver Location	No. Hops	Dist. in Nautical Miles	Xmtr.	Mean* TD Error (Meas.-Pred.)	Range* of 95% of TD Readings	No. of Readings	Time of Readings (EST)	Date (1958)	Uncertainty of Recv. Location (U sec)
Bermuda	G	665	M-Y	+ 0.5	± 0.45	16	1700-2330	3/22	± 0.42
"	"	665	"	+ 0.45	± 0.35	10	0600-1115	3/23	± 0.42
"	"	665	"	+ 0.35	± 0.35	17	1730-2200	3/24	± 0.42
"	"	665	"	+ 0.5	± 0.4	16	0030-0430	3/25	± 0.42
"	"	665	"	+ 0.5	± 0.35	39	1400-0230	3/25,26	± 0.42
"	"	665	"	+ 0.3	± 0.1	11	0615-0900	3/26	± 0.42
"	"	856	M-X	- 0.1	± 0.4	16	1700-2330	3/22	± 0.26
"	"	856	"	+ 0.4	± 0.4	16	1730-2200	3/24	± 0.26
"	"	856	"	+ 0.4	± 0.5	12	0015-0330	3/25	± 0.26
"	"	856	"	+ 0.5	± 0.55	32	1400-2345	3/25	± 0.26
"	"	856	"	+ 0.15	± 0.4	12	0600-0900	3/26	± 0.26
Puerto Rico	"	1129	M-X	+ 0.2	± 0.65	8	1800-1945	3/29	± 0.11
"	"	1129	"	+ 0.4	± 0.6	12	1215-1645	3/30	± 0.11
Newfound-land	"	1340	M-Y	+ 0.2	± 1.4	13	1600-1915	6/17	± 0
"	"	1340	"	- 0.25	± 1.0	15	0845-1200	6/18	± 0

* Microseconds

Continued -

TABLE 24

TIME DIFFERENCE MEASUREMENTS (INSTANTANEOUS READINGS)

Receiver Location	No. Hops	Dist. in Nautical Miles	Xmtr.	Mean* TD Error (Meas.-Pred.)	Range* of 95% of TD Readings	No. of Readings	Time of Readings (EST)	Date (1958)	Uncertainty of Recv. Location (U sec)
Newfoundland	1	1340	M-Y	- 0.3	± 0.8	20	2030-0030	6/17,18	0
"	1	1730	M-X	+ 0.1	± 0.9	29	1945-0145	6/17,18	0
Puerto Rico	1	1129	M-X	+ 0.75	± 1.2	34	2000-0500	3/29,30	± 0.11
"	1	1390	M-Y	- 0.85	± 0.1	10	0545-0800	3/29	± 0.12
"	1	1390	M-Y	0	± 0.45	39	2000-0430	3/29,30	± 0.12
Trinidad	1	1445	M-X	- 0.9	± 0.5	15	1130-1500	3/31	± 0.25
"	1	1445	M-X	- 0.28	± 0.72	36	2000-0500	3/31 4/1	± 0.25
"	1	1906	M-Y	- 0.5	± 0.7	16	1130-1500	3/31	± 0.29
"	1	1906	M-Y	- 0.2	± 0.8	32	2000-0430	3/31 4/1	± 0.29
"	1	1906	M-Y	+ 0.2	± 0.7	11	1930-2145	4/1	± 0.29
"	1	1445	M-X	- 0.9	± 0.8	14	1215-1615	4/7	± 0.25

* Microseconds

Continued -

TABLE 24

TIME-DIFFERENCE MEASUREMENTS
(INSTANTANEOUS READINGS)

Receiver Location	No. Hops	Dist. in Nautical Miles	Xmtr.	Mean* TD Error (Meas.-Pred.)	Range* of 95% of TD Readings	No. of Readings	Time of Readings (EST)	Date (1958)	Uncertainty of Recv. Location (U sec)
Belem, Brazil	2	2692	M-X	+ 0.5	± 1.6	28	2130-0430	4/2,3	± 1.03
"	2	2692	M-X	- 0.2	± 0.3	11	0130-0400	4/3	± 1.03
"	2	2830	M-Y	+ 5.0	± 1.0	29	2130-0430	4/2,3	± 1.32
Natal, Brazil	3	3402	M-X	+ 2.9	± 1.2	19	2115-0215	4/5,6	± 0.89
"	3	3435	M-Y	- 1.45	± 0.7	10	0054-0330	4/6	± 1.16

* Microseconds

from the cycle reading by 5 microseconds or more. There were many periods of several hours each, however, when the envelope-to-cycle discrepancy was much less than 5 microseconds. During these periods it was assumed that the receiver was functioning properly. At other times, it was not possible to determine definitely whether the envelope errors were the fault of the receiver or were caused by dispersion of the sky waves. In most cases, it could be determined, with only a small uncertainty, that the envelope errors were caused by malfunctioning of the receiver.

Figures 22 and 23 show plots of the envelope-to-cycle discrepancy recorded at Piarco, Trinidad when all three signals were being received by the first hop sky wave. Figure 22 shows that the X discrepancy was less than ± 3 microseconds throughout the nighttime (9 hours). During the daytime, the X discrepancy was somewhat more variable. The Y discrepancy in the daytime varied between 10 and 15 microseconds. This could be caused by the lower signal to noise ratio for the Y signal or malfunctioning of the receiver.

5. Sky Wave Delay

Additional information regarding the stability of sky waves was obtained from measurements of sky wave delay. Sky wave delay could be measured directly at locations within ground wave range of both the master and one slave. At other locations, such as Trinidad, only one station (the

X slave) was within ground wave range. In this case, the sky wave delay could be determined by operating the receiver on the master sky wave and the X ground wave. The indicated MX time difference would be lower than the value predicted for ground wave reception of both stations. A correction, called the sky wave correction, could be applied to the indicated time difference to obtain the equivalent all-ground wave time difference. The magnitude of the sky wave correction, in this example, is the delay of the master sky wave with reference to the master ground wave.

At the more remote receiving locations, such as Brazil, the ground wave could not be received from any of the Loran-C stations. However useful information is contained in the tabulations of sky wave corrections measured at these receiving locations.

Table 25 gives the sky wave corrections measured at distances from 614 to 3435 nautical miles. In each case the sky wave correction is the predicted ground wave time difference minus the time difference indicated by the receiver.

6. Sky Wave Field Strength Measurements

A summary of 258 measurements of Loran-C sky wave field strength at distances from 856 to 3435 nautical miles (984 to 3944 statute miles) is given in Table 26. Field strengths are given in decibels below the field at

TABLE 25

SUMMARY OF MEASURED SKYWAVE CORRECTIONS

Receiver Location	Xmtr. and No. of Hops		Distance Nautical Mi.		Skywave Correction U sec	Date (1958)	Time (EST)
Bermuda	M-G	X-1	665	856	- 37.2	3/23	0820
"	M-G	X-1	665	856	- 37.4	3/23	0845
"	M-G	X-1	665	856	- 37.2	3/23	0900
"	M-G	X-1	665	856	- 59.4	3/24	2124
"	M-G	X-1	665	856	- 59.4	3/24	2125
"	M-G	X-1	665	856	- 58.8	3/25	0106
"	M-G	X-1	665	856	- 59.0	3/25	0115
"	M-G	X-1	665	856	- 60.2	3/25	0222
"	M-G	X-1	665	856	- 60.6	3/25	0235
"	M-G	X-1	665	856	- 61.2	3/25	0400
"	M-G	X-1	665	856	- 59.0	3/25	2351
"	M-G	X-1	665	856	- 59.2	3/25	2353
"	M-G	X-1	665	856	- 59.2	3/26	0000
"	M-G	X-1	665	856	- 58.8	3/26	0006
"	M-1	Y-G	665	614	+ 51.3	3/26	0530
"	M-1	Y-G	665	614	+ 51.5	3/26	0545
Puerto Rico	M-1	X-G	1129	928	+ 37.5	3/29	0605
"	M-1	X-G	1129	928	+ 37.1	3/29	0615
"	M-1	X-G	1129	928	+ 37.2	3/29	0630
"	M-1	X-G	1129	928	+ 37.3	3/29	0645
"	M-1	X-G	1129	928	+ 37.2	3/29	0700
"	M-G	Y-1	1129	1391	- 39.5	3/30	1615
"	M-G	Y-1	1129	1391	- 40.3	3/30	1625

Continued -

TABLE 25

SUMMARY OF MEASURED SKYWAVE CORRECTIONS

Receiver Location	Xmtr. and No. of Hops		Distance Nautical Mi.		Skywave Correction U sec	Date (1958)	Time (EST)
Puerto Rico	M-G	Y-1	1129	1391	- 39.1	3/30	1640
Newfoundland	M-G	X-1	1340	1730	- 38.7	6/18	0847
"	M-G	X-1	1340	1730	- 39.1	6/18	0857
"	M-G	X-1	1340	1730	- 38.7	6/18	0907
"	M-G	X-1	1340	1730	- 38.4	6/18	0930
"	M-G	X-1	1340	1730	- 39.1	6/18	0955
"	M-G	X-1	1340	1730	- 38.6	6/18	1000
"	M-G	X-1	1340	1730	- 38.6	6/18	1005
"	M-G	X-1	1340	1730	- 39.4	6/18	1019
"	M-G	X-1	1340	1730	- 37.3	6/18	1030
"	M-G	X-1	1340	1730	- 37.3	6/18	1045
"	M-G	X-1	1340	1730	- 38.2	6/18	1100
"	M-G	X-1	1340	1730	- 39.2	6/18	1112
"	M-G	X-1	1340	1730	- 38.4	6/18	1120
"	M-G	X-1	1340	1730	- 38.8	6/18	1150
Trinidad	M-1	X-G	1673	1445	+ 57.2	3/30	2245
"	M-1	Y-2	1673	1906	- 64.4	3/30	2245
"	M-1	Y-2	1673	1906	- 65.1	3/31	0000
Natal, Brazil	M-3	Y-2	3402	3435	+ 61.3	4/5	2142
"	M-3	Y-2	3402	3435	+ 60.8	4/5	2148
"	M-3	Y-2	3402	3435	+ 59.8	4/5	2220
"	M-3	Y-2	3402	3435	+ 59.6	4/5	2231
"	M-3	Y-2	3402	3435	+ 59.4	4/5	2245

Continued -

TABLE 25

SUMMARY OF MEASURED SKYWAVE CORRECTIONS

Receiver Location	Xmtr. and No. of Hops		Distance Nautical Mi.		Skywave Correction U sec	Date (1958)	Time (EST)
Natal, Brazil	M-3	Y-2	3402	3435	+ 58.2	4/5	2300
"	M-3	Y-2	3402	3435	+ 59.0	4/5	2322
"	M-3	Y-2	3402	3435	+ 56.8	4/5	2349
"	M-3	Y-2	3402	3435	+ 56.8	4/6	0000
"	M-3	Y-2	3402	3435	+ 55.0	4/6	0025
"	M-3	Y-2	3402	3435	+ 55.8	4/6	0033
"	M-3	X-2	3402	3264	+ 57.6	4/6	0230
"	M-3	X-2	3402	3264	+ 58.1	4/6	0237
"	M-3	X-2	3402	3264	+ 57.1	4/6	0245
"	M-3	X-2	3402	3264	+ 57.5	4/6	0300
"	M-3	X-2	3402	3264	+ 57.2	4/6	0315
"	M-3	X-2	3402	3264	+ 60.9	4/6	0330
"	M-2	Y-3	3402	3435	- 61.6	4/6	2155

Receiver Location	No. Hops	Dist. St. Mi.	Median Field in db Below Field at 1-mile		No. of Measurements	Time of Measurements (EST)	Date (1958)	Xmtr.
			Measured	Predicted				
Bermuda	1	984	56±0	60	2	2130-2137	3/24	X
Puerto Rico	1	1070	61±3	61	5	0140-0500	3/29	X
"	1	1070	59±6	61	14	2145-0430	3/29,30	X
"	1	1300	60±2	63	5	0140-0500	3/29	M
"	1	1300	57±2	63	14	2145-0430	3/29,30	M
"	1	1598	73±3	67	5	0140-0500	3/29	Y
"	1	1598	57±5	67	14	2145-0430	3/29,30	Y
Trinidad	1	1656	69±3	69	7	2345-0420	3/30,31	X
"	1	1656	91±8	89	15	1130-1500	3/31	X
"	1	1656	71±2	69	12	2200-0430	3/31 4/1	X
"	1	1920	73±3	74	8	2245-0420	3/30,31	M
"	1	1920	89±3	97	15	1130-1500	3/31	M
"	1	1920	79±6	74	12	2245-0430	3/31 4/1	M
"	1	2196	89±3	83	7	2245-0420	3/30,31	Y
"	1	2196	108±5	106	15	1130-1500	3/31	Y

TABLE 26

SKY WAVE FIELD STRENGTHS

CONTINUED

Receiver Location	No. Hops	Dist. St. Mi.	Median Field in db Below Field at 1-mile		No. of Measurements	Time of Measurements (EST)	Date (1958)	Xmtr.
			Measured	Predicted				
Trinidad	1	2196	89±5	83	12	2245-0430	3/31 4/1	Y
Belem, Brazil	2	2864	81±5	81	14	2130-0400	4/2,3	X
"	2	3094	83±4	85	14	2130-0400	4/2,3	M
"	2	3254	81±6	88	10	2130-0300	4/2,3	Y
Natal, Brazil	2	3749	98±4	100	4	0230-0345	4/6	X
"	2	3749	91±3	100	6	2245-0015	4/6,7	X
"	2	3910	89±3	104	6	2245-0015	4/6,7	M
"	2	3944	97±5	105	7	2015-0015	4/5,6	Y
"	2	3944	93±2	105	6	2245-0015	4/6,7	Y
"	3	3749	71±2	88	10	2015-0200	4/5,6	X
"	3	3910	83±6	90	13	2130-0315	4/5,6	M
"	3	3944	85±2	91	5	0045-0246	4/5,6	Y

TABLE 26

SKY WAVE FIELD STRENGTHS

one mile. The radiated power is assumed to be 100 kilowatts at the peak of the pulse. The predicted nighttime field strengths were obtained from the curves of Figure 29. The predicted daytime field strengths were obtained from the curves of Figure 31 (for the summer season) because the ionospheric path from the U.S. East Coast to Trinidad in March and April is more nearly characterized by the summer than by the winter ionospheric reflection coefficient. The plus-minus signs indicate the range in decibels of 80 percent of the measured field strengths. Mean measurements in 19 of the 28 periods were within ± 6 db of the predicted values. The measured field strengths were greater than the predicted values in 17 periods and less than the predicted values in 7 periods.

7. Other Signals From 70 to 130 KC

Synchronous detection, synchronous filtering and other techniques make the Loran-C receiver insensitive to non-synchronous interference, up to a certain point. Figure 39 shows that non-synchronous interference causes deviations of the cycle time difference of the Loran-C receiver to increase abruptly when the interfering signal strength exceeds about ten times the Loran-C signal strength. When a very large number of signals are present simultaneously, it can be assumed that their disturbing effect will approach that of random noise. The effect of random noise on deviation of Loran-C cycle time difference measurements is shown in Figure 38.

In order to estimate the effects of other radio services on existing and future Loran-C operations, other signals between 70 and 130 kc were monitored during evaluation flights No. 1 and No. 2.

Interference to Loran-C reception was negligible in the Caribbean and in South America (Flight No. 1). Table 27 shows the field strength of signals observed from 70 to 130 kc during Flight No. 1.

Considerably greater activity in the vicinity of 100 kc was observed in the North Atlantic, Europe and the Mediterranean during Flight No. 2. Table 28 shows the root-sum-square (RSS) value of all signals observed in a particular frequency range during the indicated four-hour local standard time block. A dash indicates that no measurements were obtained. Local transmitting stations near Keflavik, Iceland and Port Lyautey, Morocco were shut down for short periods so that measurements on other signals could be made. The local station signals are shown above the values recorded when the local station was off the air.

TABLE 27

FIELD STRENGTH OF OTHER SIGNALS OBSERVED FROM 70 TO 130 KC

Composite (Root-Sum-Square) Values

Receiver Location	Time (EST)	Date (1958)	Incident Field: Atmos. Noise 30 kc BW RMS UV/M	Incident Field: Other Signals RSS UV/M	Total Equivalent Incident Field (Attenuated by RF Bandpass) RSS UV/M
Puerto Rico	1145	3/27	31	2910	1454
"	0000	3/29	175	331	266
"	0735	3/29	25	143	105
"	1000	3/29	25	252	118
"	1905	3/29	175	509	328
"	2205	3/29	175	595	400
"	2205	3/29	175	595	311
"	2330	3/29	175	289	253
"	0330	3/30	175	377	324
"	1745	3/30	192	263	196
Trinidad	0225	3/31	246	289	274
"	0400	3/31	246	336	288
"	0500	3/31	246	256	250
"	0600	3/31	246	248	161
"	1907	3/31	175	179	116
"	0035	4/1	175	280	216
"	0310	4/1	246	384	297
"	0400	4/1	246	322	246
"	1200	4/1	49	56	36
Belem, Brazil	2000	4/1	273	277	179
"	2200	4/3	273	274	179
Natal, Brazil	1935	4/5	273	353	187
"	2050	4/5	273	324	206
"	2150	4/5	273	314	180

TABLE 28

ANALYSIS OF RADIO SIGNALS OBSERVED IN THE VICINITY OF 100 KC

Receiver
Location - Floyd Bennett Field, New York

Date 13-16 June 1958

Typical Root-Sum-Square Value of Incident Field Strength (E) in UV/Meter and Maximum No. of Significant Signals (N) Observed at Any One Time Within the Indicated Time Block and Frequency Range

Time Block LST	70-75 kc E	N	75-80 kc E	N	80-85 kc E	N	85-110 kc E	N	110-115 kc E	N	115-120 kc E	N	120-125 kc E	N	125-130 kc E	N
00-04	1410	1	-	-	185	1	2145	2	710	2	545	2	1590	1	256	1
04-08	700	1	-	-	240	1	960	2	1560	1	274	1	1600	1	672	2
08-12	285	2	-	-	-	-	178	1	-	-	200	2	137	1	189	3
12-16	-	-	-	-	-	-	-	-	-	-	-	-	-	-	-	-
16-20	-	-	-	-	-	-	-	-	-	-	-	-	-	-	-	-
20-24	1400	1	-	-	375	1	1173	1	3190	1	252	3	1782	1	193	3

Continued -

TABLE 28

ANALYSIS OF RADIO SIGNALS OBSERVED IN THE VICINITY OF 100 KC

Receiver
Location - Argentia, NFLD

Date 16-18 June 1958

Typical Root-Sum-Square Value of Incident Field Strength (E) in UV/Meter and Maximum No. of Significant Signals (N) Observed at Any One Time Within the Indicated Time Block and Frequency Range

Time Block LST	70-75 kc		75-80 kc		80-85 kc		85-110 kc		110-115 kc		115-120 kc		120-125 kc		125-130 kc	
	E	N	E	N	E	N	E	N	E	N	E	N	E	N	E	N
00-04	6820	2	57	1	1240	2	4719	4	623	3	586	2	742	2	508	1
04-08	4360	2	-	-	546	2	1300	2	623	3	370	2	300	2	507	2
08-12	1650	2	-	-	546	2	988	1	623	1	168	1	150	1	508	1
12-16	2740	2	-	-	966	2	1505	2	712	1	660	2	300	1	507	1
16-20	3500	3	29	3	1732	3	1420	4	676	1	372	2	192	1	508	1
20-24	7000	3	242	2	1670	2	3360	2	783	3	737	2	671	2	934	1

Continued -

TABLE 28

ANALYSIS OF RADIO SIGNALS
OBSERVED IN THE VICINITY OF 100 KC

Receiver
Location - Keflavick, Iceland

Date 19-20 June 1958

Typical Root-Sum-Square Value of Incident Field Strength (E) in UV/Meter and Maximum No. of Significant Signals (N) Observed at Any One Time Within the Indicated Time Block and Frequency Range

Time Block LST	70-75 kc E	70-75 kc N	75-80 kc E	75-80 kc N	80-85 kc E	80-85 kc N	85-110 kc E	85-110 kc N	110-115 kc E	110-115 kc N	115-120 kc E	115-120 kc N	120-125 kc E	120-125 kc N	125-130 kc E	125-130 kc N
00-04	610	2	94	2	143	2	170	4	66	1	104	2	77	2	-	-
04-08	255	1	101	2	111	2	60	4	79	2	12	1	56	1	68,000 / 0	1 / 0
08-12	280	2	195	1	382	3	265,000 / 1,428	1 / 9	125	3	175	1	157	2	62,000 / 7,350	1 / 1
12-16	-	-	-	-	-	-	259,000 / 0	1 / 0	-	-	-	-	-	-	-	-
16-20	178	2	87	1	117	1	260,000 / 218	1 / 10	86	2	23	1	85	1	79,000 / 0	1 / 0
20-24	666	3	315	2	14,504 / 465	1 / 2	211,000 / 3760	1 / 6	386	2	-	-	83	1	16,000 / 290	1 / 1

Continued -

TABLE 28

ANALYSIS OF RADIO SIGNALS OBSERVED IN THE VICINITY OF 100 KC

Receiver
Location - Prestwick, Scotland

Date 21-22 June 1958

Typical Root-Sum-Square Value of Incident Field Strength (E) in UV/Meter and Maximum No. of Significant Signals (N) Observed at Any One Time Within the Indicated Time Block and Frequency Range

Time Block LST	70-75 kc		75-80 kc		80-85 kc		85-110 kc		110-115 kc		115-120 kc		120-125 kc		125-130 kc	
	E	N	E	N	E	N	E	N	E	N	E	N	E	N	E	N
00-04	-	-	-	-	1325	1	1235	7	870	3	504	1	1732	1	-	-
04-08	1428	1	950	2	1723	2	1500	4	1424	1	-	-	4026	1	290	1
08-12	2858	1	1869	2	1885	2	1290	8	1380	1	455	1	4026	1	508	1
12-16	3175	1	2770	2	2332	1	1400	6	1602	1	-	-	5032	1	5,440	2
16-20	2645	3	1869	2	1723	2	1660	5	1540	2	174	1	4294	1	10,556	1
20-24	1810	1	575	1	928	1	1095	5	222	1	-	-	-	-	-	-

Continued -

TABLE 28

ANALYSIS OF RADIO SIGNALS
OBSERVED IN THE VICINITY OF 100 KC

Receiver
Location - Weisbaden, Germany

Date 23-24 June 1958

Typical Root-Sum-Square Value of Incident Field Strength (E) in UV/Meter and Maximum No. of Significant Signals (N) Observed at Any One Time Within the Indicated Time Block and Frequency Range

Time Block LST	70-75 kc E	70-75 kc N	75-80 kc E	75-80 kc N	80-85 kc E	80-85 kc N	85-110 kc E	85-110 kc N	110-115 kc E	110-115 kc N	115-120 kc E	115-120 kc N	120-125 kc E	120-125 kc N	125-130 kc E	125-130 kc N
00-04	1070	2	307	2	306	3	34,850	5	2,270	1	570	1	137	1	716	2
04-08	992	1	850	1	-	-	42,300	7	73,075	2	-	-	107	1	637	1
08-12	1048	1	21735	2	1560	2	65,700	5	36,260	1	22,750	1	47,400	1	-	-
12-16	1535	2	20125	1	1350	2	44,800	8	41,446	1	38,675	1	37,800	1	495	1
16-20	1520	2	12650	1	1530	2	70,900	9	56,248	1	51,350	1	59,250	1	425	1
20-24	754	1	7784	1	41870	1	13,650	8	15,540	1	13,650	1	975	1	1450	3

Continued -

TABLE 28

ANALYSIS OF RADIO SIGNALS
OBSERVED IN THE VICINITY OF 100 KC

Receiver
Location - **Rhodes, Greece**

Date 25-26 June 1958

Typical Root-Sum-Square Value of Incident Field Strength (E) in UV/Meter and Maximum No. of Significant Signals (N) observed at any one time within the indicated time block and frequency range.

Time Block LST	70-75 kc		75-80 kc		80-85 kc		85-110 kc		110-115 kc		115-120 kc		120-125 kc		125-130 kc	
	E	N	E	N	E	N	E	N	E	N	E	N	E	N	E	N
00-04	1226	2	374	1	547	2	1043	5	796	2	83	2	61	1	301	3
04-08	133	3	86	1	98	2	170	5	570	2	78	2	61	1	100	2
08-12	577	2	116	1	88	2	535	5	1177	2	139	2	92	1	-	-
12-16	-	-	98	1	75	1	1574	4	70	1	46	1	45	1	-	-
16-20	424	2	-	-	91	2	238	4	48	1	59	2	55	1	-	-
20-24	686	2	155	1	443	2	2014	5	1360	2	392	2	240	1	85	1

Continued -

TABLE 28

ANALYSIS OF RADIO SIGNALS OBSERVED IN THE VICINITY OF 100 KC

Receiver
Location - Ankara, Turkey

Date 26-28 June 1958

Typical Root-Sum-Square Value of Incident Field Strength (E) in UV/Meter and Maximum No. of Significant Signals (N) Observed at Any One Time Within The Indicated Time Block and Frequency Range

Time Block LST	70-75 kc		75-80 kc		80-85 kc		85-110 kc		110-115 kc		115-120 kc		120-125 kc		125-130 kc	
	E	N	E	N	E	N	E	N	E	N	E	N	E	N	E	N
00-04	186	1	96	2	247	1	405	5	191	2	105	1	54	1	128	1
04-08	80	2	39	1	46	1	275	3	107	1	-	-	27	1	-	-
08-12	-	-	-	-	-	-	394	1	-	-	-	-	-	-	-	-
12-16	302	2	77	1	-	-	318	2	73	1	127	4	126	5	33	1
16-20	162	1	88	2	-	-	126	5	46	1	212	5	202	5	65	2
20-24	42	1	87	2	-	-	339	7	263	5	600	10	610	10	142	10

Continued -

TABLE 28

ANALYSIS OF RADIO SIGNALS
OBSERVED IN THE VICINITY OF 100 KC

Receiver
Location - Tripoli, Lybia

Date 1-2 July 1958

Typical Root-Sum-Square Value of Incident Field Strength (E) in UV/Meter and Maximum No. of Significant Signals (N) Observed at Any One Time Within the Indicated Time Block and Frequency Range

Time Block LST	70-75 kc		75-80 kc		80-85 kc		85-110 kc		110-115 kc		115-120 kc		120-125 kc		125-130 kc	
	E	N	E	N	E	N	E	N	E	N	E	N	E	N	E	N
00-04	150	2	85	1	91	1	400	6	189	1	110	1	49	1	383	2
04-08	120	2	100	2	55	1	145	3	294	2	95	2	162	1	280	2
08-12	425	2	151	2	174	2	930	4	260	2	600	1	187	2	504	1
12-16	112	1	173	1	159	1	269	2	277	2	184	1	275	4	184	1
16-20	200	1	173	1	133	1	264	3	183	1	205	1	270	1	252	2
20-24	289	1	-	-	312	2	404	3	-	-	-	-	-	-	-	-

Continued -

TABLE 28

ANALYSIS OF RADIO SIGNALS
OBSERVED IN THE VICINITY OF 100 KC

Receiver
Location - Port Lyautey, Morocco

Date 3-4 July 1958

Typical Root-Sum-Square Value of Incident Field Strength (E) in UV/Meter and Maximum No. of Significant Signals (N) Observed at Any One Time Within the Indicated Time Block and Frequency Range

Time Block LST	70-75 kc		75-80 kc		80-85 kc		85-110 kc		110-115 kc		115-120 kc		120-125 kc		125-130 kc	
	E	N	E	N	E	N	E	N	E	N	E	N	E	N	E	N
00-04	478	2	124	1	211	1	730	4	1,898	1	-	-	92	1	174	1
04-08	212	2	-	-	222	1	248	5	$\frac{140,620}{4830}$	$\frac{1}{1}$	-	-	-	-	-	-
08-12	138	2	173	2	239	2	88	1	$\frac{27,412}{0}$	$\frac{1}{0}$	33	1	-	-	-	-
12-16	112	2	172	1	280	2	605	7	$\frac{95,392}{21}$	$\frac{1}{1}$	81	1	57	1	-	-
16-20	190	2	75	1	162	2	351	3	$\frac{230,724}{0}$	$\frac{1}{0}$	15	1	15	1	924	1
20-24	197	1	124	1	670	2	861	5	$\frac{256,360}{318}$	$\frac{1}{2}$	-	-	168	1	161	1

Continued -

TABLE 28

ANALYSIS OF RADIO SIGNALS
OBSERVED IN THE VICINITY OF 100 KC

Receiver
Location - Lajens, Azores

Date 5-6 July 1958

Typical Root-Sum-Square Value of Incident Field Strength (E) in UV/Meter and Maximum No. of Significant Signals (N) Observed at Any One Time Within the Indicated Time Block and Frequency Range

Time Block LST	70-75 kc		75-80 kc		80-85 kc		85-110 kc		110-115 kc		115-120 kc		120-125 kc		125-130 kc	
	E	N	E	N	E	N	E	N	E	N	E	N	E	N	E	N
00-04	340	2	190	1	133	1	410	5	2250	1	183	1	81	1	156	1
04-08	257	2	-	-	456	1	559	3	175	1	-	-	-	-	-	-
08-12	200	2	56	1	120	2	178	7	292	1	-	-	-	-	250	1
12-16	230	2	60	1	73	2	152	4	292	1	-	-	-	-	-	-
16-20	242	1	-	-	135	2	247	5	510	1	-	-	40	1	-	-
20-24	342	3	159	1	250	2	686	6	1930	1	-	-	68	1	125	1

Continued -

TABLE 28

ANALYSIS OF RADIO SIGNALS
OBSERVED IN THE VICINITY OF 100 KC

Receiver
Location - Bermuda, B.W.I.

Date 8 July, 1958

Typical Root-Sum-Square Value of Incident Field Strength (E) in UV/Meter and Maximum No. of Significant Signals (N) Observed at Any One Time Within the Indicated Time Block and Frequency Range

Time Block LST	70-75 kc		75-80 kc		80-85 kc		85-110 kc		110-115 kc		115-120 kc		120-125 kc		125-130 kc	
	E	N	E	N	E	N	E	N	E	N	E	N	E	N	E	N
00-04	1460	2	164	1	171	1	1295	4	260	1	255	2	571	2	197	1
04-08	1010	2	-	-	-	-	500	2	-	-	60	1	240	1	50	1
08-12	770	1	-	-	15	1	374	2	140	1	160	1	149	2	40	1
12-16	759	2	-	-	117	2	405	2	-	-	-	-	246	2	21	1
16-20	-	-	-	-	-	-	-	-	-	-	-	-	-	-	-	-
20-24	2650	2	-	-	220	2	2130	4	236	1	586	2	359	2	169	1

SECTION V
CONCLUSIONS

A. INTRODUCTION

The potential capability of Loran-C systems to provide highly accurate and reliable position fixing information over very great areas has been demonstrated. The maximum range depends upon the signal-to-noise ratio at the receiver. It is feasible to obtain reliable position fixes with signal-to-noise ratios as low as 1-to-1. For Loran-C systems of 1000 kw peak radiated power it is feasible to obtain reliable position fixes with a probable error of 0.1 to 0.2 microseconds on over-water paths of about 1700 nautical miles in the daytime and about 1200 nautical miles at night in receiving areas such as the Eastern Mediterranean Sea, Bermuda and the Mid-Pacific. Maximum ranges will be less in high noise areas of the world.

The possibility of greatly extending the radionavigation service area by the use of sky waves seems promising but has not been explored completely. Preliminary tests and theoretical considerations indicate that a system having a radiated power of 1000 kw would have a sky wave range of about 2800 nautical miles at night, 2600 nautical miles on winter days and about 2000 nautical miles on summer days.

Sky wave fixes would have a probable error of about 1 to 1.5 microseconds.

Full potential accuracy and reliability were not expected from the U.S. East Coast system because of the temporary and experimental nature of the installations and operating procedures; also it was known in advance that some reduction in accuracy and reliability would be caused by other radio services presently operating in the 90-110 kc band. These disadvantages were overcome almost entirely for periods long enough and frequent enough to permit a conclusive analysis of the potential capabilities of Loran-C systems.

The Loran-C evaluation has led to the following conclusions:

(1) The feasibility of unambiguous cycle matching for ground waves with signal-to-noise ratios as low as 1-to-1 has been demonstrated.

(2) Cycle matching has been accomplished successfully for sky waves in limited tests. Experimental and theoretical results are most encouraging. They indicate that Loran-C sky waves are useful for general purpose radionavigation.

(3) Stability and accuracy of a Loran-C system are greatest when a service area monitor directs coding delay adjustments once or twice each day.

(4) With the assistance of a service area monitor, fixes at the extreme limits of the ground wave area have a probable

error of less than 0.1 microsecond plus a seasonal error of about 0.1 microsecond for paths predominantly over water. Seasonal variations of propagation velocity are several times greater over land than over water.

(5) Fixes obtained from sky waves have a probable error of 1 to 1.5 microseconds.

(6) A certain minimum radiated power is required to supply continuous Loran-C coverage between the areas of the ground wave and the first hop, first hop and second hop areas, etc.

(7) Continuity of service between the ground wave and first hop areas requires a peak radiated power of about 100 kw.

(8) Continuity of service into the second hop area requires a peak radiated power of about 1000 kw; however, second hop operation during the daytime in the summer will be unsatisfactory or impossible.

(9) Loran-C pulse emissions can be confined within the band 90-110 kc and do not cause harmful interference to other services operating outside the band.

(10) Interference to Loran-C from other radio services operating outside the band 90-110 kc is not harmful.

(11) Other radio services operating within the band 90-110 kc may, under certain circumstances, limit the range, accuracy and reliability of Loran-C service.

B. ACCURACY OF ENVELOPE MATCH

The Bermuda fixed monitor has demonstrated the feasibility of making envelope time difference measurements with an accuracy of ± 4 microseconds at least 96 percent of the time when signal-to-noise ratio is at least 1-to-1 at the sampling point. Larger envelope errors may have been caused by other signals in the 90-110 kc band. At night the root-sum-square (RSS) amplitude of other signals between 88 kc and 110 kc in the Bermuda area is 20 db to 26 db greater than the Loran-C signal from the X slave. Two of the principal interfering signals (88 kc and 105 kc) can be suppressed with notch filters. The remaining interference, together with atmospheric noise, make envelope measurements very critical on the X rate at Bermuda during the nighttime hours. Even under these difficult conditions, however, envelope time difference measurements have been made at Bermuda over periods of months with an accuracy of ± 4 microseconds at least 96 percent of the nighttime hours.

C. MAXIMUM RANGE

1. Atmospheric Noise

Maximum range is determined by the signal-to-noise ratio required at the receiver for the grade of service which is desired. The level of atmospheric noise varies over extremely wide limits from one area of the world to the next and from one time of day and one season to the next. In high-noise areas of the earth it is not uncommon to observe differences of 20 to 30 db in the noise level between two receiving points separated by one or two thousand miles. Thus, it is impossible to state a "maximum range" of Loran-C service unless some particular area of the world is specified.

In order to give some specific examples of Loran-C ranges, several simplifying assumptions have been made. These are as follows:

(1) The examples of maximum range are for receiving locations in the general area of the Eastern Mediterranean Sea. These apply also to the general areas of the Mid-Atlantic (Bermuda) and the Mid-Pacific (Hawaii).

(2) "Daytime" ranges are for the hours 0800-1200. In general, these are the hours of lowest daytime noise. Highest daytime atmospheric noise usually occurs during the late afternoon. Thus, "daytime" maximum ranges are probably too great.

Specific examples of maximum ranges are given in order to give the reader some idea of the very great areas over which Loran-C service may be obtained in many areas of the earth. Maximum ranges are much less in high noise areas.

2. Minimum Radiated Power

The optimum signal power is, generally, the minimum power required for the desired service. Useful sky wave signals exist at some distances beyond the maximum ground wave range. "Minimum" power is defined as the minimum radiated power required to extend the ground wave range to the distance at which satisfactory first hop sky wave service can be obtained. If service from second hop sky waves is desired, the radiated power should be sufficient to cause some overlap of first hop and second hop ranges.

The minimum radiated power for first hop sky wave service is about 100 kw (at pulse peak). The minimum radiated power for second hop service is 1000 kw.

3. Ground Wave Range Over Water

The maximum ground wave range for 100 kw radiated power is about 1400 nautical miles in the daytime and about 900 to 1000 nautical miles at night. A 10-to-1 increase in radiated power (1000 kw) increases the ground wave range another 260 nautical miles. These are the maximum ranges for a 1-to-1 signal-to-noise ratio when the atmospheric noise at the receiver is approximately the same as in the area of the Eastern Mediterranean Sea. The results in the vicinity of Bermuda would be substantially the same.

4. Sky Wave Range Over Water

For 100 kw radiated power, the maximum first hop sky wave range is approximately 1800 nautical miles; the second hop range extends to 2300 nautical miles at night but is negligible in the daytime.

For 1000 kw radiated, the maximum first hop sky wave range is about 2100 nautical miles; the second hop range extends to about 2800 nautical miles at night, 2600 nautical miles on winter days and about 2000 nautical miles on summer days. The third hop range extends to 3200 nautical miles at night but is contaminated by the second hop.

5. Range Over Land

The maximum ground wave or sky wave range over land paths of average conductivity (0.005 mho/meter) is about 200 miles less than over an all water path.

D. ACCURACY OF LINES OF POSITION

1. Ground Wave Accuracy

The probable error of instantaneous MX time differences measured at the Bermuda monitor from August 12, 1957 to August 28, 1958 was approximately 0.09 microsecond in the daytime and about 0.13 microsecond at night. During periods of a month or more, however, the mean time difference monitored at Bermuda departed from the yearly mean (and from the system calibration value) by 0.2 microsecond. The mean 8-hour time difference occasionally changed 0.1 microsecond from one day to the next and occasionally changed 0.3 microsecond in a period of four or five days. The day-to-day variations appear to be systematic variations and could be reduced greatly with one or two daily corrections of coding delay on advice of the Bermuda monitor. If coding delays were adjusted for fixed lines of position at

Bermuda, without regard to seasonal variations in velocity of propagation, seasonal variations of time difference would be less than ± 0.1 microsecond throughout the entire ground wave service area. Seasonal variations of time difference would be a minimum at locations about equi-distant from master and slave and would increase gradually to about 0.1 microsecond near the transmitters and along the baseline extensions.

From the demonstrated performance of the U.S. East Coast System and from theoretical considerations, it is concluded that it is feasible to obtain position fixes at the extreme limits of the ground wave area with a probable error on each line-up-position of less than 0.1 microsecond plus a seasonal error of 0.1 microsecond or less.

2. Sky Wave Accuracy

From the limited and inadequate experimental and theoretical data available it appears that cycle identification can be obtained from sky waves. The probable error of cycle time difference obtained from sky waves is 1 to 1.5 microseconds. Most of the error comes from contamination of the desired sky wave hop by the next lower hop. This type of contamination can be reduced by reducing the length of the Loran-C pulse.

E. STABILITY OF THE MONITORS

In the U.S. East Coast system, master station and slave station monitors do not have sufficient long-term stability to control the system for long periods with full potential accuracy. Short term stability of master and X slave monitors is excellent; monitoring at the Y slave is less stable. The master station can control the system without outside assistance for one or two days. After a few days, assistance from outside the triad is required. The area monitor at Bermuda can observe long term errors in system timing. With one or two daily adjustments of coding delays on advice of the Bermuda monitor, the system can be synchronized with extremely high accuracy.

SECTION VI

RECOMMENDATIONS

A. INTRODUCTION

The capability of the U.S. East Coast Loran-C system to satisfy certain special purpose requirements for highly accurate position fixing over very great areas has been demonstrated. It is recommended that Loran-C systems be created in other areas of the world to satisfy similar special purpose requirements. Considerable progress has been made in this direction. Other Loran-C systems are already in operation or are in advanced stages of planning.

System performance requirements for hydrographic and aeronautical surveying are quite different from the requirements of general purpose long-distance radionavigation. The Loran-C system can satisfy the needs of both the surveyor and the navigator. Accuracy of the system has been conclusively demonstrated. Reliability can be as great as that of any other radionavigation system, but it has not been demonstrated adequately.

It is recommended that Loran-C systems be operated in a manner to encourage their use for general purpose long-distance radionavigation by all potential users. Implementation of this recommendation requires the following minimum actions:

(1) Loran-C tables and charts should be published and made available to all potential users.

(2) Loran-C systems should operate continuously with as nearly 100 percent reliability of transmission as possible.

(3) Investigations of range, accuracy and reliability of Loran-C should be continued as new and improved systems are established. Results of these investigations should be brought to the attention of the general public, particularly to all potential users.

The recommendations which follow are intended to point out specific areas in which some effort is required in order to realize the general recommendation above.

B. SUPPORTING FACILITIES

Nearly one-half of all synchronization failures in the U.S. East Coast system can be traced to inadequate supporting facilities, such as unreliable commercial power, lack of emergency power, and inadequate standby transmitters.

It is recommended that the Loran-C transmitting stations be supplied with emergency and standby facilities at least equivalent to those provided for Standard Loran stations.

C. SYSTEM CONTROL - MONITORING

No satisfactory method has been developed for detecting more or less permanent (though small) errors in synchronization except by relying on time difference measurements made outside of the Loran-C system. Two methods for minimizing these errors are recommended:

(1) Method 1: Dual Monitors at the Transmitters

At least two monitor receivers should operate simultaneously at each transmitter until the use of duplicate monitors is proven unnecessary. Every reasonable effort should be made for pairs of receivers to operate independently of each other so that more or less permanent changes would not occur at the same time in the indications of both receivers. By the use of good engineering practices, such as improved grounding, bonding and shielding, indications from the two receivers should become perfectly correlated. Dual monitors would then be unnecessary. Artificial means for obtaining correlated readings, such as, using the same antenna for both receivers, should be avoided.

(2) Method 2: Service Area Monitoring

In many cases, apparent changes in time differences observed at the transmitters are not real and are not observed far from the transmitters. Real changes in time interval between emission of master and slave pulses can be observed by a monitor receiver located well out in the ground wave service area. If the paths from master and slave to the area monitor are predominantly over water and have even approximately the same length, long-term variations in ground wave propagation velocity over the two paths are highly correlated.

It is recommended that coding delay adjustments be made once or twice daily, on advice of the area monitor, to hold long-term average lines-of-position constant at the area monitor. It is further recommended that two monitor receivers be operated independently of each other at the area monitor.

D. ADDITIONAL RESEARCH AND DEVELOPMENT

1. Investigation of Sky Waves

Investigations of Loran-C sky waves to date indicate that they are useful for long-range radionavigation. However, many questions of vital importance to the future of Loran-C have not been answered satisfactorily. Some of these questions are the following:

(1) How reliable is the cycle matching technique when using sky waves?
(2) Can sky waves be identified reliably? How is it done?
(3) How stable are sky wave delays and sky wave corrections? How accurately can they be predicted?

It is recommended that the U.S. Coast Guard conduct investigations to determine the usefulness of Loran-C sky waves for long-range radionavigation. An adequate investigation would require about one year for completion and would involve a minimum of effort and expense. It is recommended that Loran-C receivers be installed at several Coast Guard stations located at appropriate distances for monitoring first-, second-, and third-hop sky waves. The intermediate areas would be monitored periodically by mobile monitors. The fixed monitors would obtain data concerning sky wave stability. The mobile monitors would examine the practical problems associated with identification of sky waves and their utility for radionavigation.

2. Investigation of Over-Land Paths

Propagation velocity of the low-frequency ground wave depends upon the conductivity of the earth's surface. When the paths from the transmitters to the receiver are entirely over sea water, Loran-C time differences can be predicted accurately with very little difficulty. When the paths lie wholly, or in part, over land an additional correction for the effect of the land must be made. The transmitters of the U.S. East Coast system are located near the water with very little land along the paths toward the sea. Time difference corrections range from zero to a few tenths of a microsecond on the Atlantic side of the triad. Over the mainland, however, corrections as great as two or three microseconds must be applied to time difference measurements.

It is not always possible to locate the transmitters so that the paths to the primary service area lie entirely over sea water. In certain proposed Loran-C systems, for example, large land masses lie along one or more of the paths to many parts of the over-water service areas. Time difference measurements in these areas may differ by as much as one or two microseconds from values tabulated for over-water paths.

Corrections for the effects of land are being prepared in the form of charts for Loran-C service areas which lie predominantly at sea. It is recommended that the feasibility of preparing similar correction charts for overland areas of all Loran-C systems be investigated.

3. Transmitters and Antennas

The reliability of Loran-C service could be increased greatly by increasing peak radiated power to about 1000 kw. This is about the minimum radiated power for satisfactory service from the second-hop sky wave. It is recommended that the problems associated with generation and radiation of 1000 kw low-frequency pulses be examined. Generation of the required power is only a part of the problem. Development of efficient antenna systems for radiation of low-frequency pulses offers the greatest opportunity for increasing Loran-C radiated power. A fundamental investigation and analysis of the transient behavior of pulse transmission, coupling and radiating elements is needed and is recommended.

Additional investigation of Loran-C pulse duration is required before full use can be made of sky waves.

Present practice is to elongate the crest and the trailing edge of the pulse in order to increase the power radiated within the 90-110 kc band. This practice increases the contamination of sky waves by lower modes. Other methods for increasing in-band radiation can be found which do not interfere with sky wave working. It is recommended that methods be investigated for reducing the contamination of sky waves caused by lower modes. Reducing the duration of the pulse is only one of several possible methods.

SECTION VII

BIBLIOGRAPHY AND REFERENCES

A very large number of references were examined during the course of this investigation. The works which are cited specifically in this report are given below as References 1 through 6. Several additional references which are particularly pertinent, but not specifically cited in this report, are given in the bibliography below. A short note follows a few of the references to indicate the particular subjects of interest.

A. REFERENCES

1. J. R. Johler, W. J. Kellar, and L. C. Walters, "Phase of the Low Radio-Frequency Ground Wave," NBS Circular 573, July 1956.

2. B. R. Bean and J. D. Horn, "On the World Wide Variations of Radio Refractivity as Derived from Standard Weather Observations," NBS Report 5083, June 1957.

3. G. Millington, "Ground-Wave Propagation Over an Inhomogeneous Smooth Earth," Proc. I.E.E., Part III, Vol. 96, P. 53, January 1949.

4. G. Millington, "Ground-Wave Propagation Over an Inhomogeneous Smooth Earth Part 2. Experimental Evidence and Practical Implications," Proc. I.E.E., Part III, Vol. 97, P. 209, July 1950.

5. B. G. Pressey, G. E. Ashwell, and C. S. Fowler, "The Measurement of the Phase Velocity of Ground-Wave Propagation at Low Frequencies Over a Land Path," Proc. I.E.E., Part III, Vol. 100, P. 73, March 1953.

6. Sperry Gyroscope Company, "Calibration of Loran-C East Coast Chain," Report No. 4223.8500, October 1957.

B. BIBLIOGRAPHY

7. B. R. Bean, L. P. Riggs, and J. D. Horn, "A Study of the Three Dimensional Distribution of the Radio Refractive Index," NBS Report 6042, February 1959.

(An analysis of radio refractivity in the region of an intense cold front.)

8. Department of the Navy, Bureau of Ordnance, "Preliminary Handbook of Instructions Loran-C Transmitter Synchronizer," Vol. 1 and Vol. 2, OP2534, March 1958.

(Refers to the modified Cytac experimental transmitter synchronizers.)

9. Department of the Navy, Bureau of Ordnance, "Preliminary Handbook of Instructions Loran-C Ground Monitor Receiver," Vol. 1 and Vol. 2, OP2537, March 1958.

(Refers to the modified Cytac experimental ground monitors receiver.)

10. Department of the Navy, Bureau of Ordnance, and Treasury Department, U. S. Coast Guard, "Technical Manual for Loran "C" Receiver AN/SPN-28 (XZ-1)," OP2642, CG-273-45, August 1958.

(A light-weight receiver-indicator; the first receiver developed for Loran-C, not modified from Cytac equipment.)

11. Department of State, "Telecommunication Convention Final Protocol and Radio Regulations," (Atlantic City Convention, 1947), U.S. Department of State Publication 3509, 1950.

12. W. T. Dickinson, "Sky Wave Delay at 100 Kilocycles," Jansky & Bailey, Inc. Report to the U.S. Coast Guard, June 1959.

13. R. H. Doherty, "Pulse Sky Wave Phenomena Observed at 100 kc," NBS Report 6CB103, February 1957. (Confidential)

(Reports on sky wave operation of a Cytac receiver aboard the U.S. Coast Guard Ship Androscoggin in Central and South America in the Spring of 1956.)

14. W. P. Frantz, W. N. Dean, and R. L. Frank, "A Precision Multi-Purpose Radio Navigation System," 1957 I.R.E. Convention Record, Part 8, P. 79.

(One of the few unclassified references on the navigation portion of the Cytac system.)

15. International Radio Consultative Committee (C.C.I.R.) "Revision of Atmospheric Radio Noise Data," Report No. 65, International Telecommunication Union, Geneva, 1957.

16. R. F. Linfield, R. H. Doherty, and G. Hefley, "Evaluation of the Propagation Aspects of the Cytac System," NBS Report 4CB101 (Confidential), March 1957.

(Deviations of the phase of the 100 kc ground wave over large inhomogeneous land paths, Eastern U.S., are reported.)

17. K. A. Norton, "Transmission Loss in Radio Propagation: II," NBS Report 5092, July 1957.

(Figure 21, p. 34, gives median transmission loss over sea water at 100 kc. Table I-1, of Appendix I gives estimates of the variance of phase of low-frequency sky waves.)

18. Radiation Laboratory, M.I.T., "Loran" McGraw-Hill Book Company, New York, 1948.

(Contains an extensive bibliography on Loran before 1948. Gives history of L.F. Loran prior to 1948, experimental results.)

19. Sperry Gyroscope Company, "Final Engineering Report Cytac Long Range Tactical Bombing System," Report No. 5223-1307-14, March 1956. (SECRET).

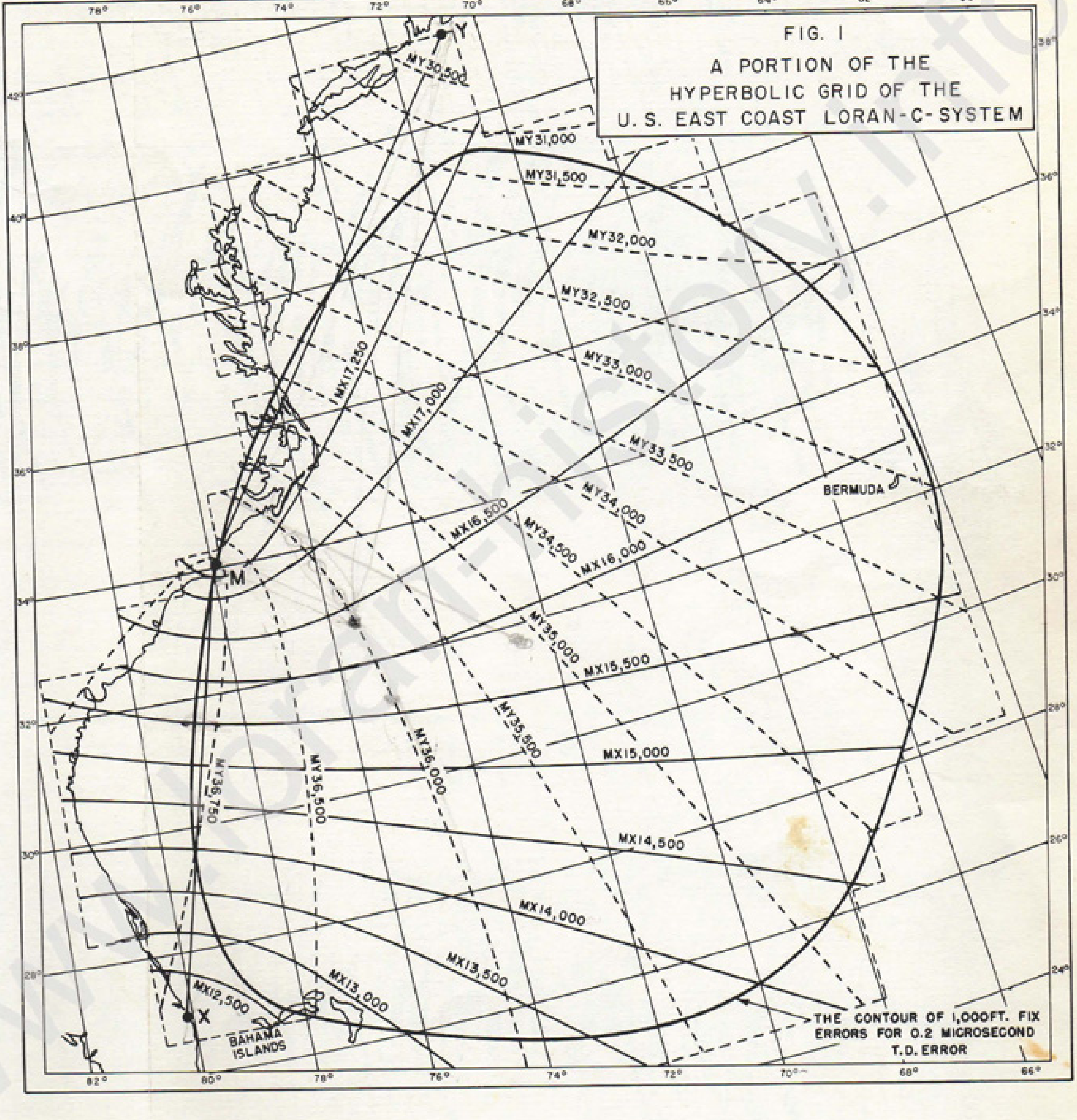
FIG. I
A PORTION OF THE
HYPERBOLIC GRID OF THE
U. S. EAST COAST LORAN-C-SYSTEM
MY30,500
MY31,000
MY31,500
MY32,000
MY32,500
MY33,000
MY33,500
MY34,000
MY34,500
MY35,000
MY35,500
MY36,000
MY36,500
MY36,750
MX17,250
MX17,000
MX16,500
MX16,000
MX15,500
MX15,000
MX14,500
MX14,000
MX13,500
MX13,000
MX12,500
BERMUDA
BAHAMA ISLANDS
M
X
Y
THE CONTOUR OF 1,000FT. FIX ERRORS FOR 0.2 MICROSECOND T.D. ERROR

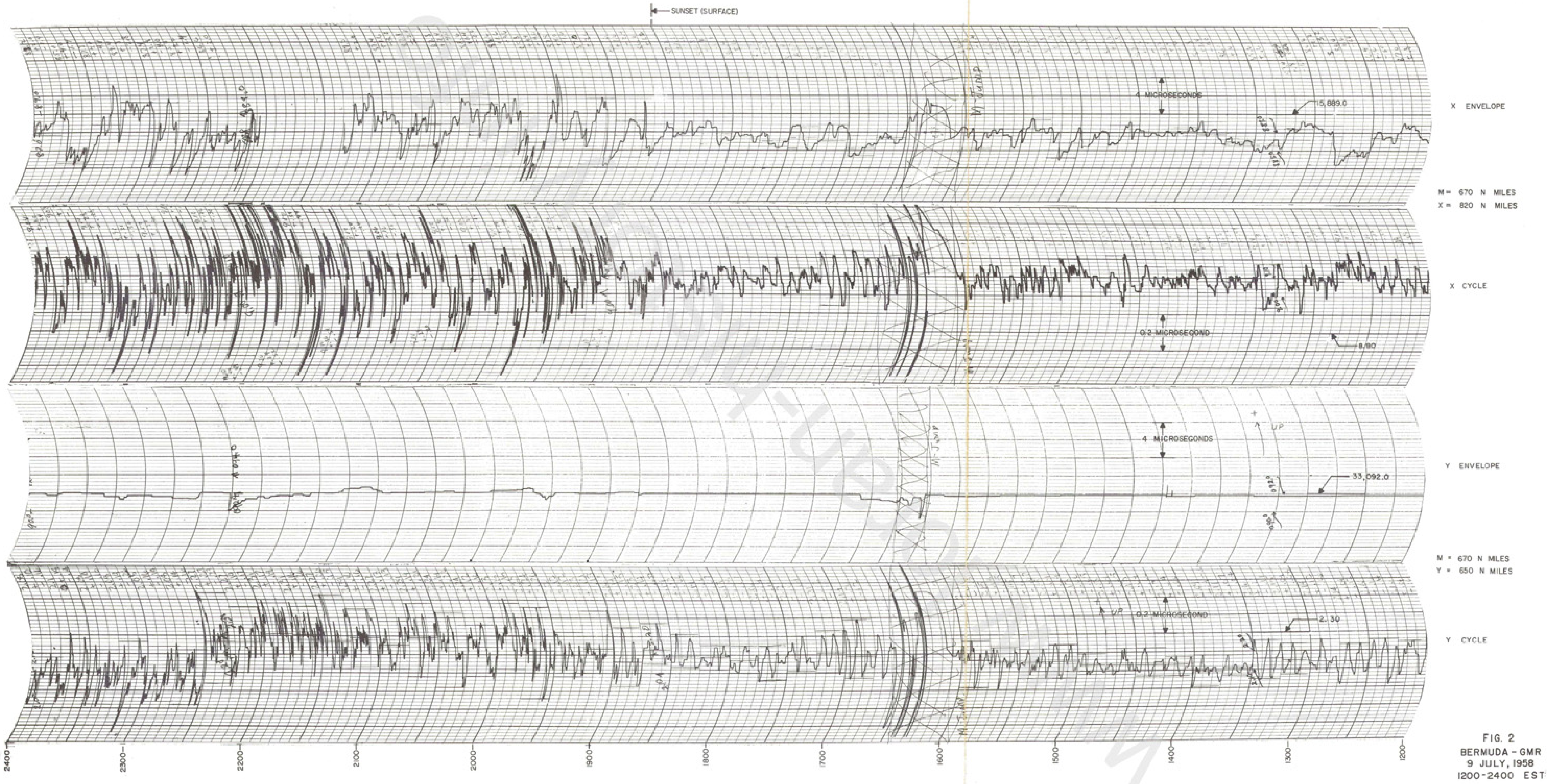

FIG. 2
BERMUDA - GMR
9 JULY, 1958
1200-2400 EST

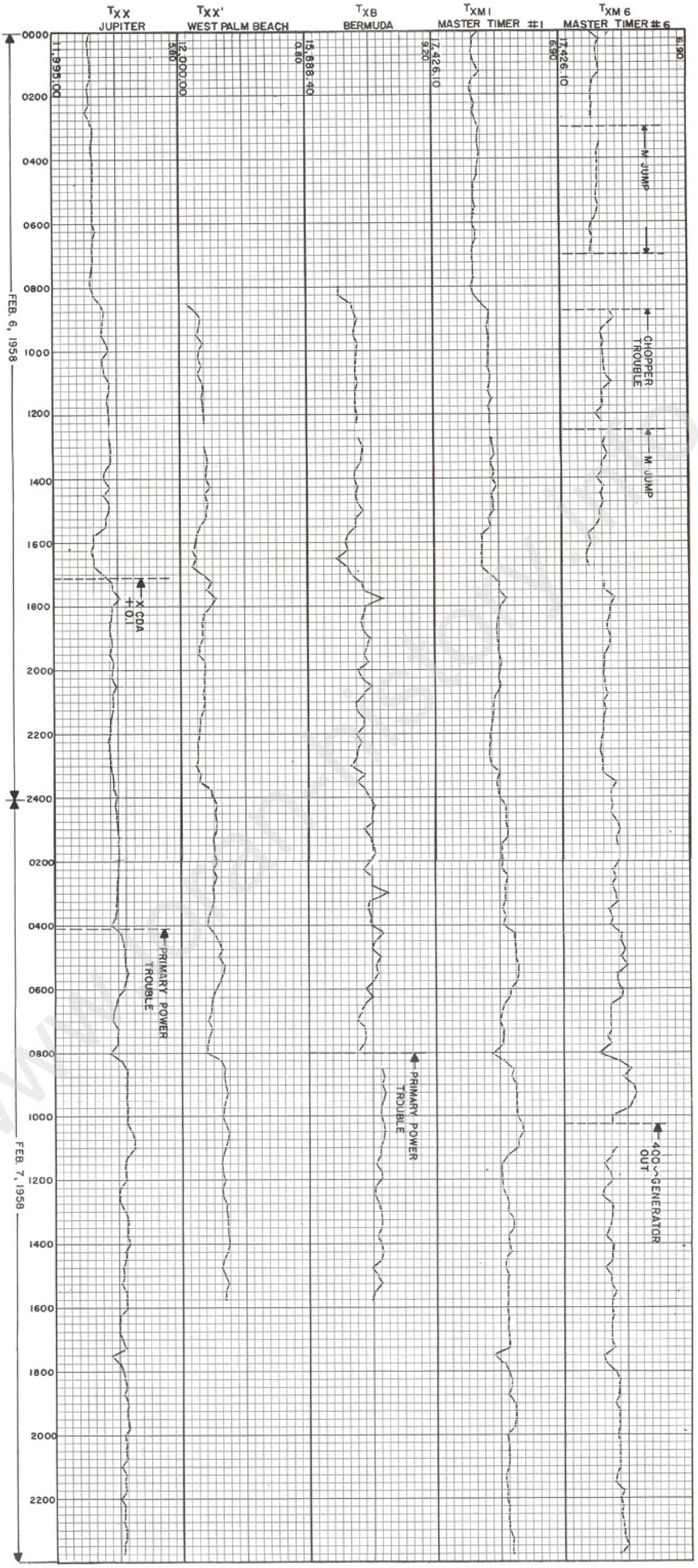

FIG. 3

15 MINUTE AVERAGE
X TIME DIFFERENCE
FOR FEB. 6, 7, 1958

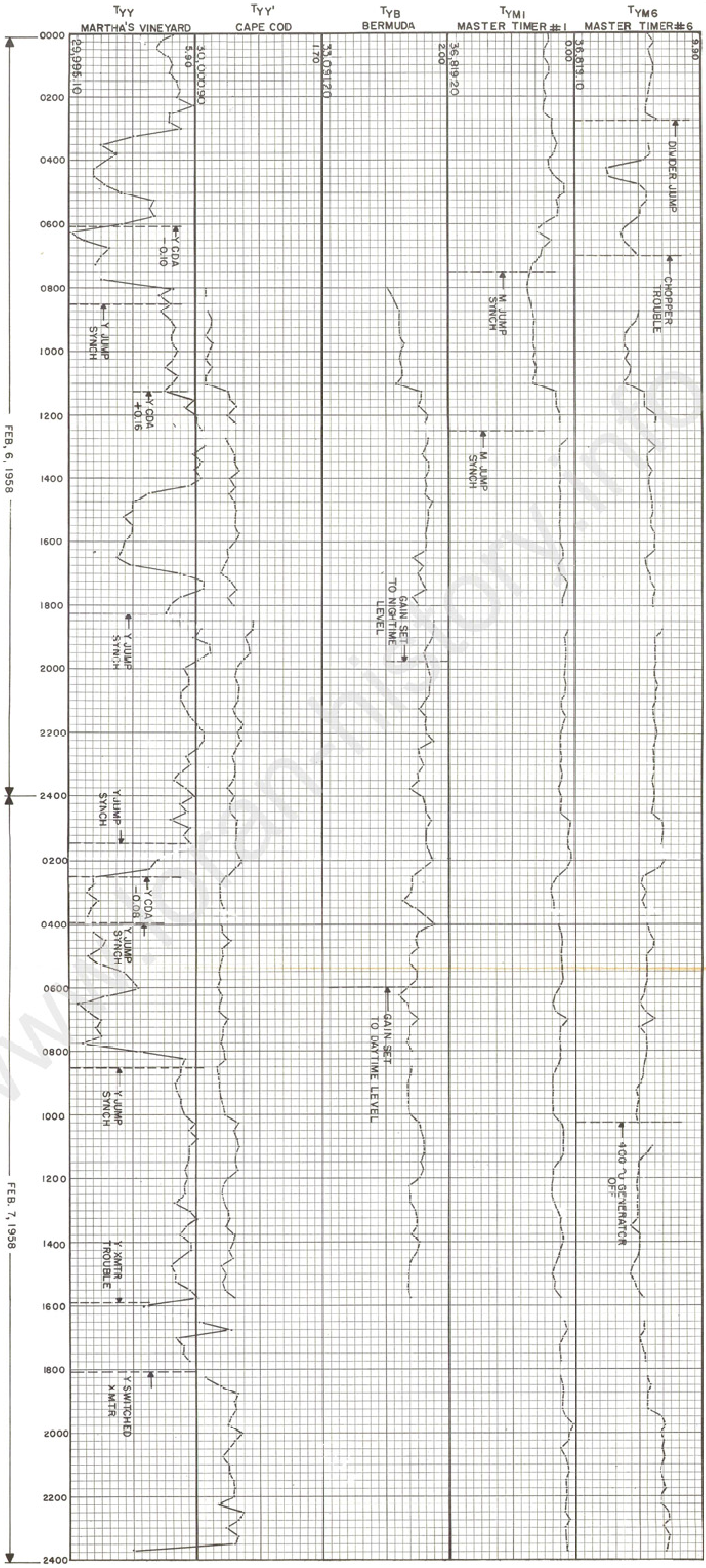

FIG. 4
15 MINUTE AVERAGE
Y TIME DIFFERENCE
FEB. 6,7, 1958

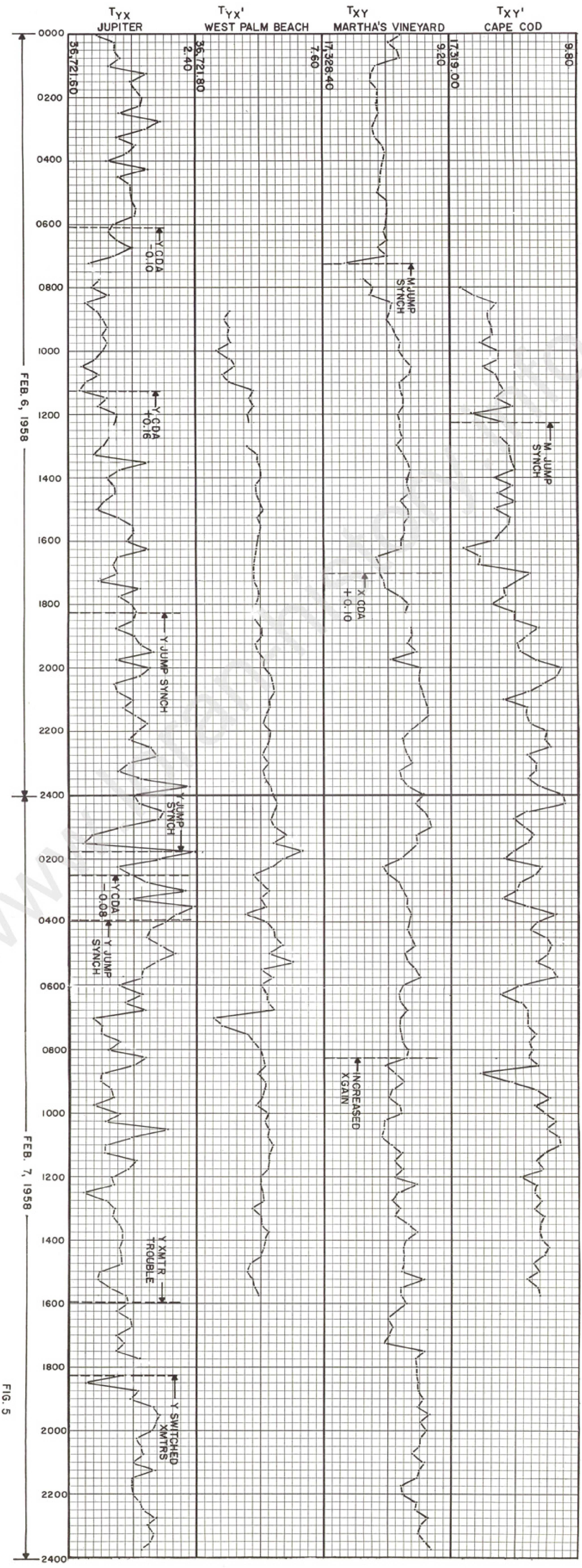

FIG. 5
15 MINUTE AVERAGE TIME DIFFERENCE
FOR FEB. 6, 7, 1958
(MONITORING ACROSS THE TRIAD)

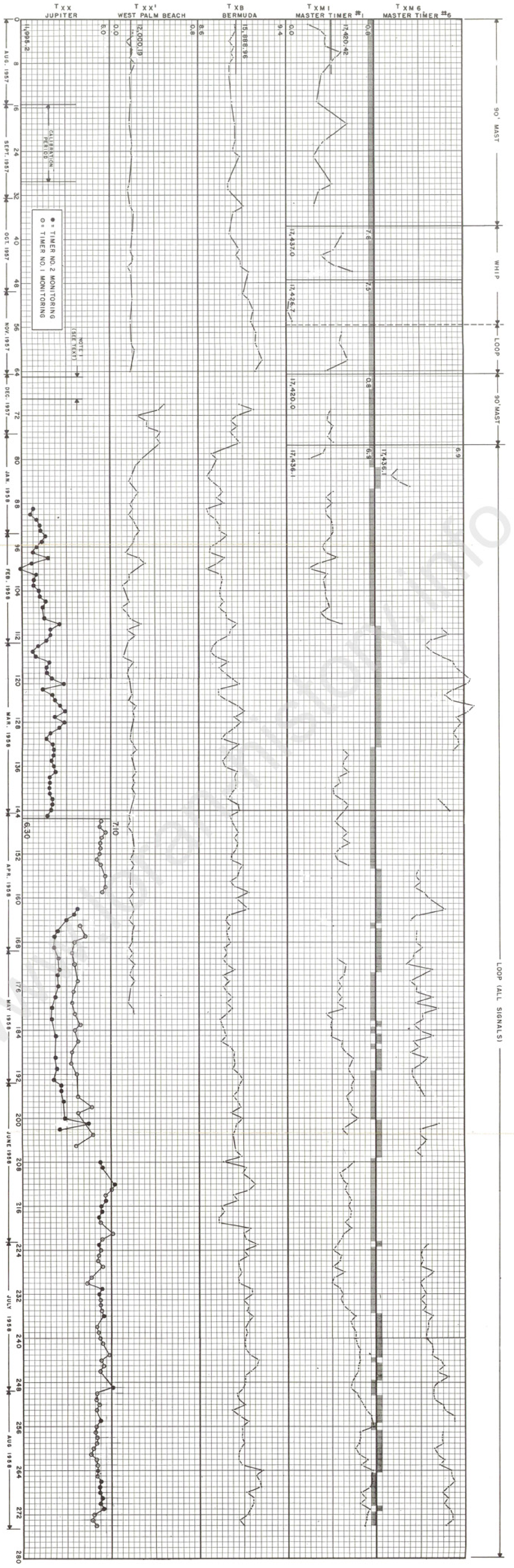

FIG. 6
8-HOUR AVERAGE X TIME DIFFERENCE
BY OPERATING PERIODS

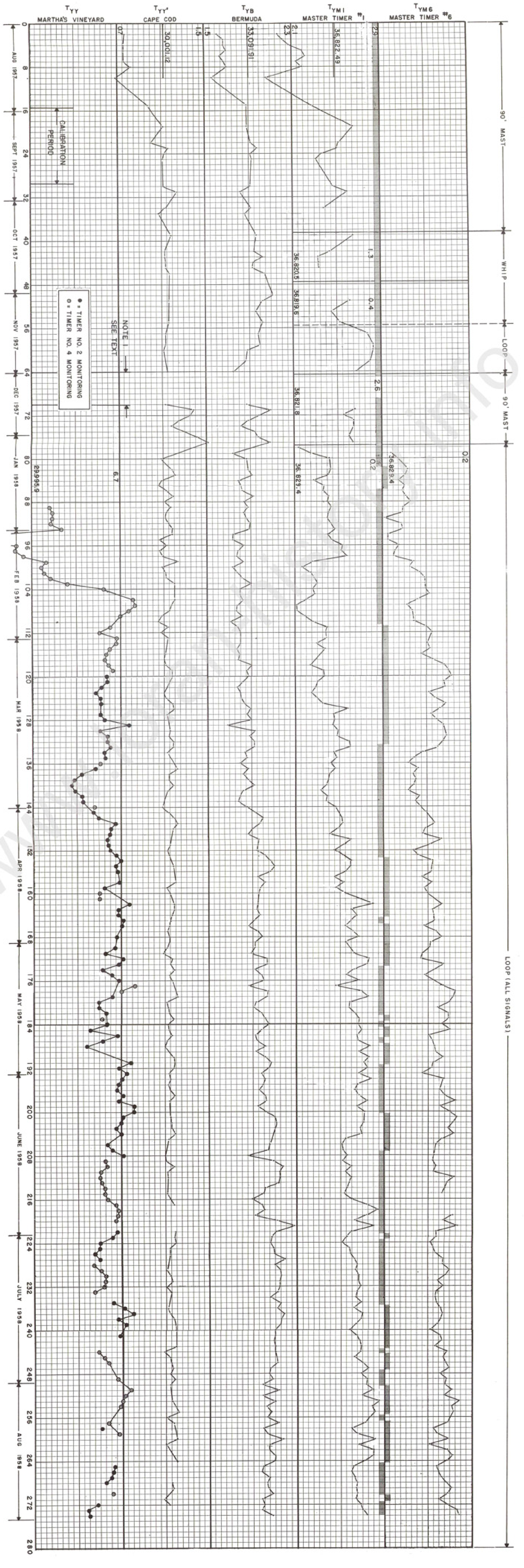

FIG 7
8-HOUR AVERAGE Y TIME DIFFERENCE
BY OPERATING PERIODS

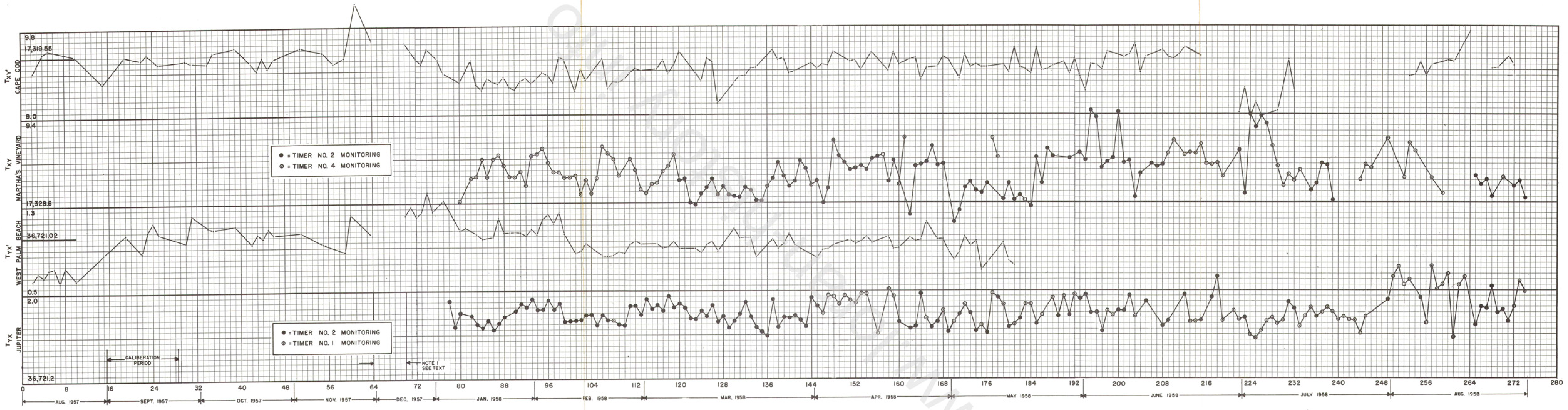

FIG. 8
8-HOUR AVERAGE TIME DIFFERENCE
BY OPERATING PERIOD
(MONITORING ACROSS THE TRIAD)

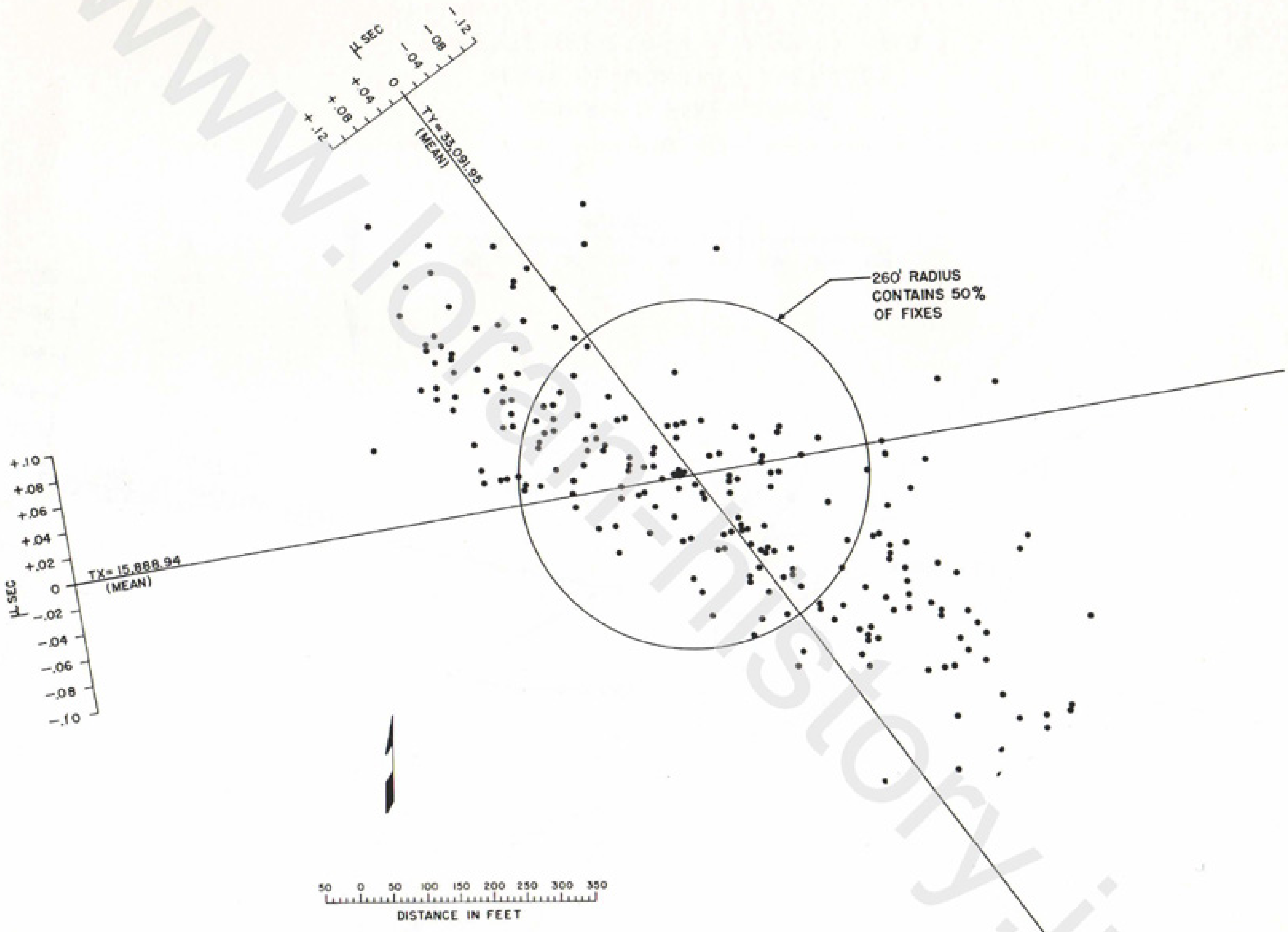

FIG. 9
LORAN-C FIXES USING
8 HOUR DAYTIME AVERAGE TIME
DIFFERENCES AT BERMUDA
SEPTEMBER 1, 1957—AUGUST 28, 1958

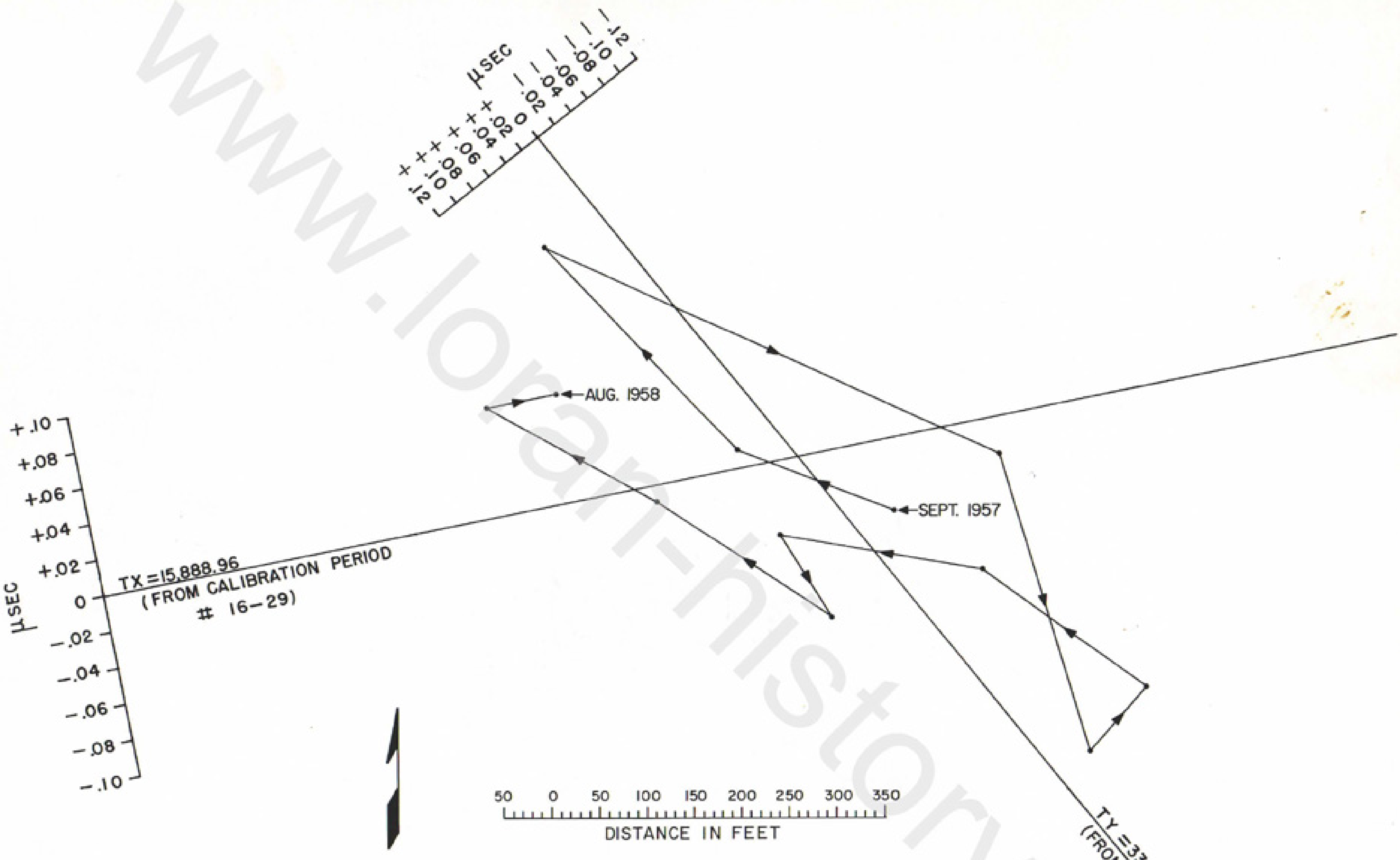

FIG. 10
LORAN-C FIXES USING
BERMUDA MONTHLY AVERAGES
SEPTEMBER 1957 – AUGUST 1958

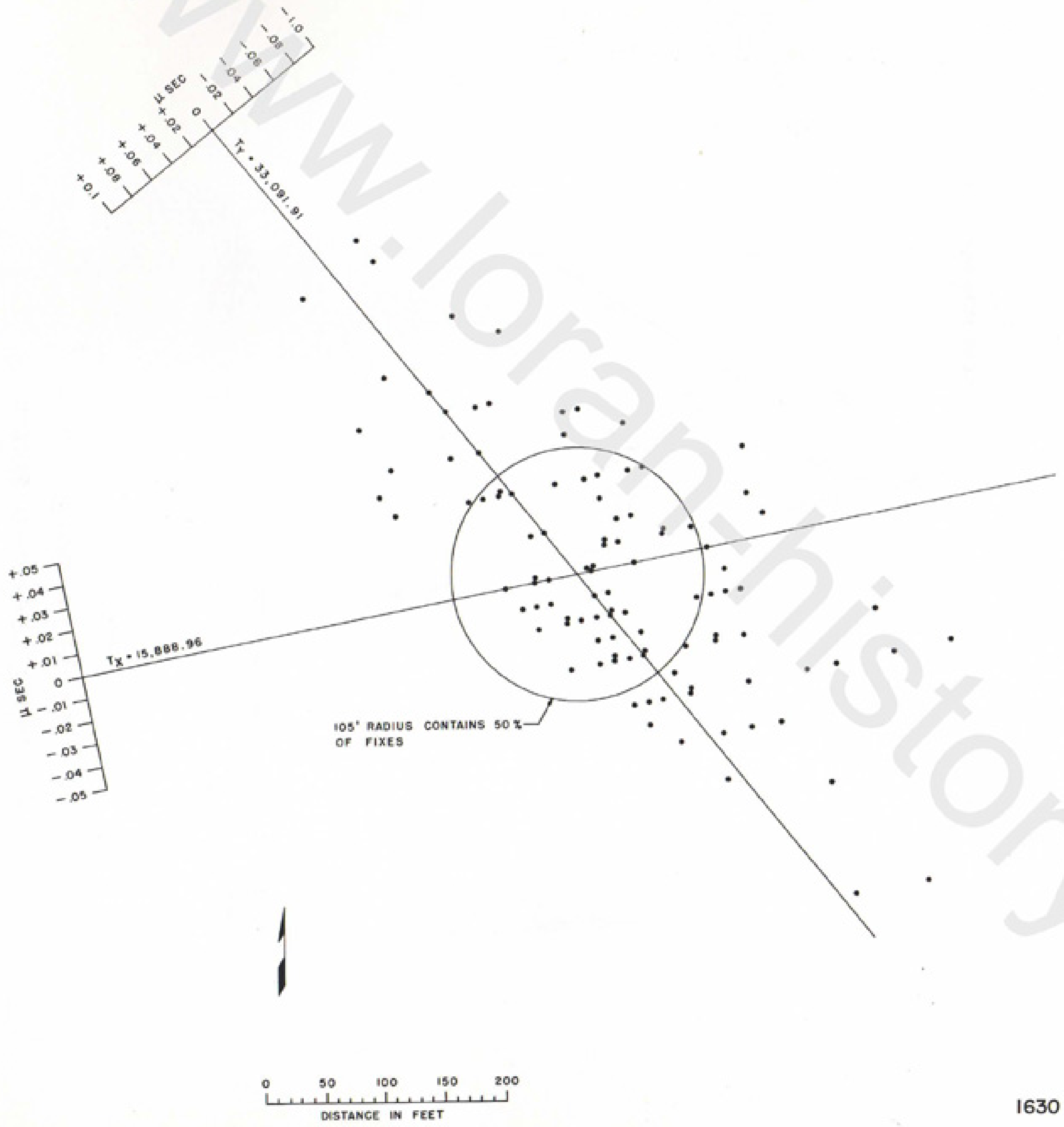

FIG. 11
LORAN–C FIXES
USING 15 MINUTE AVERAGE
TIME DIFFERENCES AT BERMUDA
1630 SEPTEMBER 4–0700 SEPTEMBER 6, 1957

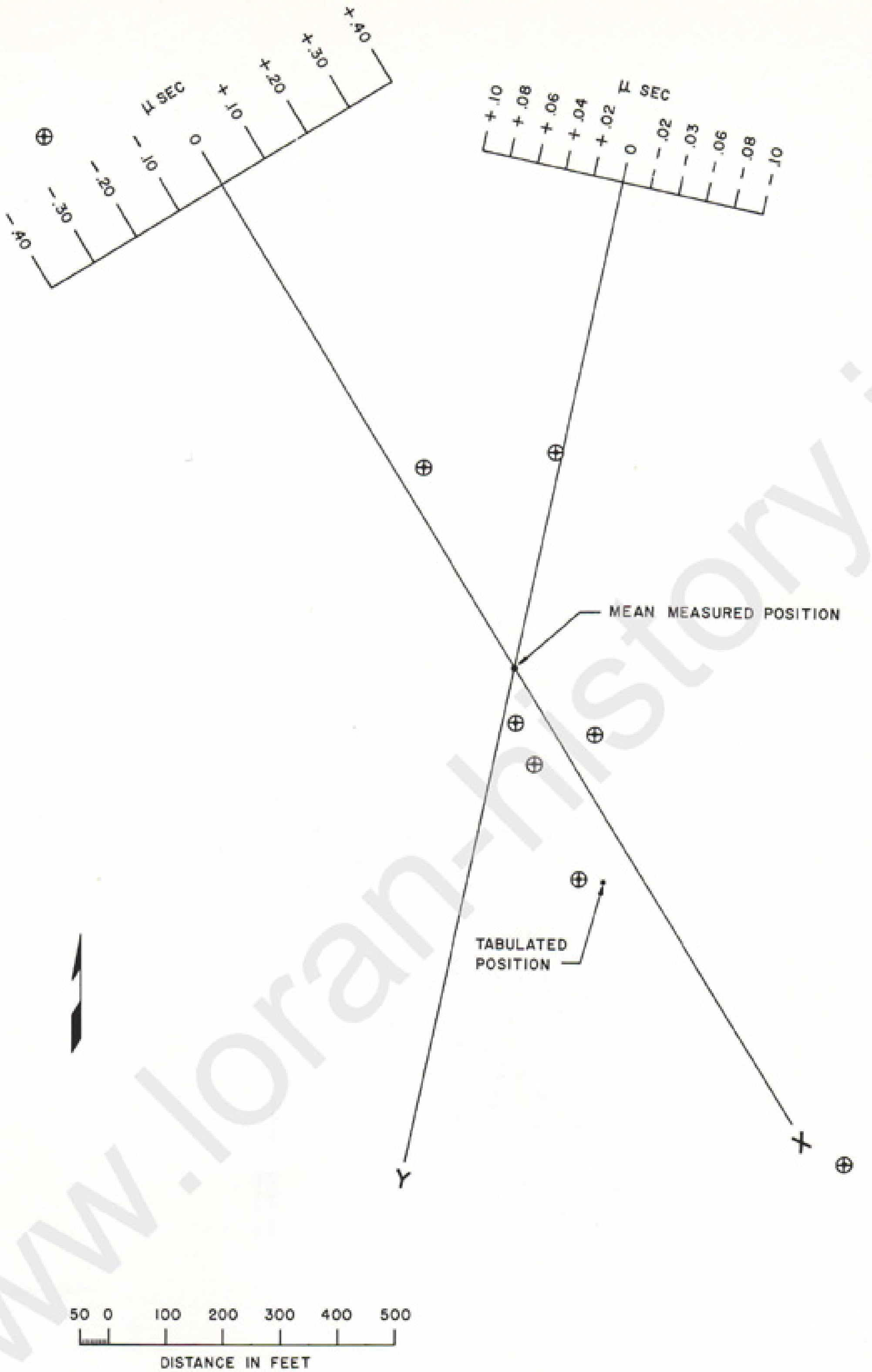

FIG. 12

BASSETT COVE
AIRBORNE LORAN—C FIXES
JULY 9, 1958

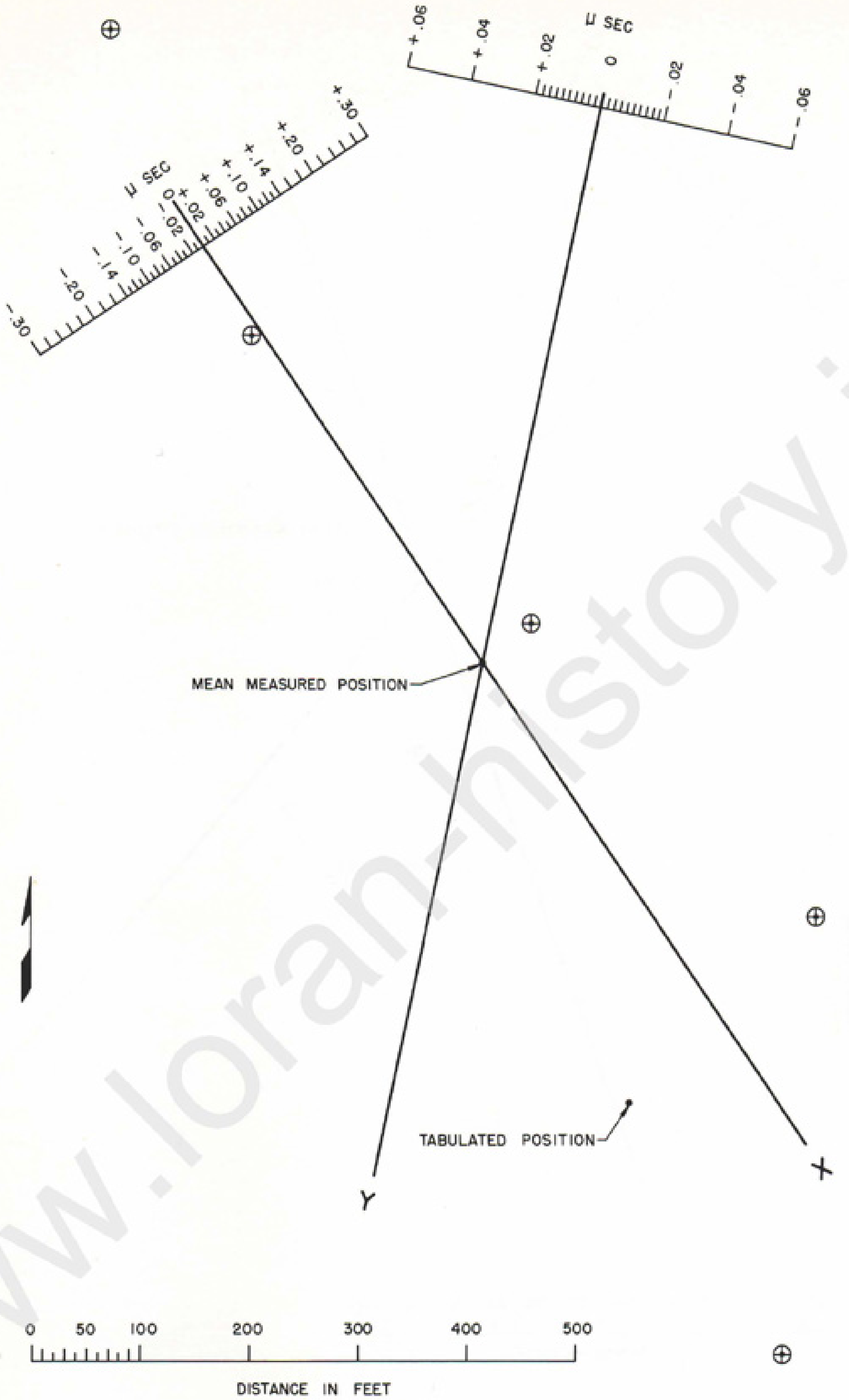

FIG. 13
LITTLE SALE CAY
AIRBORNE LORAN-C FIXES
JULY 9, 1958

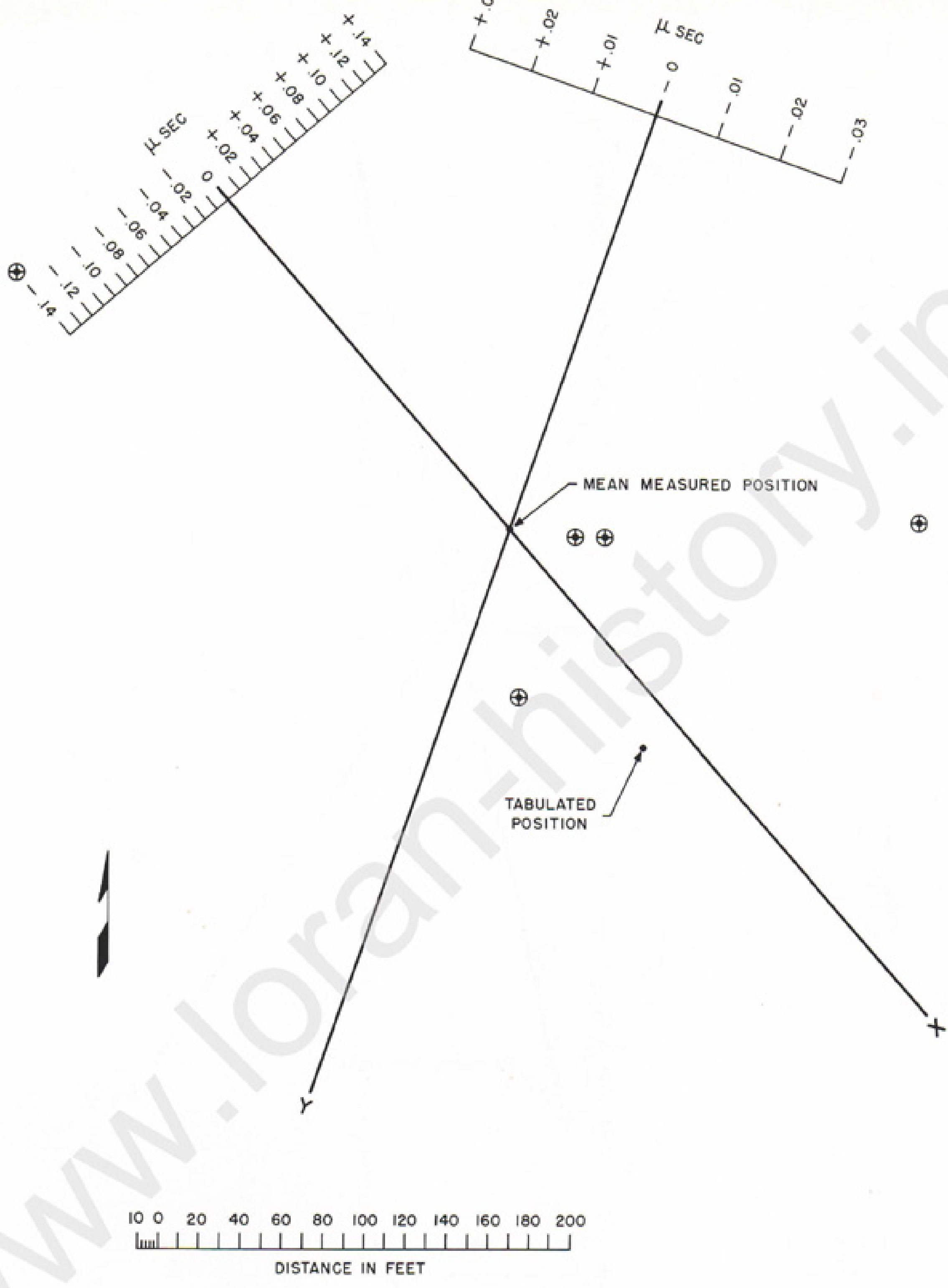

FIG. 14
WALKER CAY
AIRBORNE LORAN-C FIXES
JULY 9, 1958

OFFICIAL U.S. COAST GUARD PHOTOGRAPH

FIG. 15

U.S. COAST GUARD AIRCRAFT
R5D 72486
LORAN-C EVALUATION FLIGHT NO. 2

OFFICIAL U.S. COAST GUARD PHOTOGRAPH

FIG. 15

U.S. COAST GUARD AIRCRAFT
R5D 72486
LORAN-C EVALUATION FLIGHT NO. 2

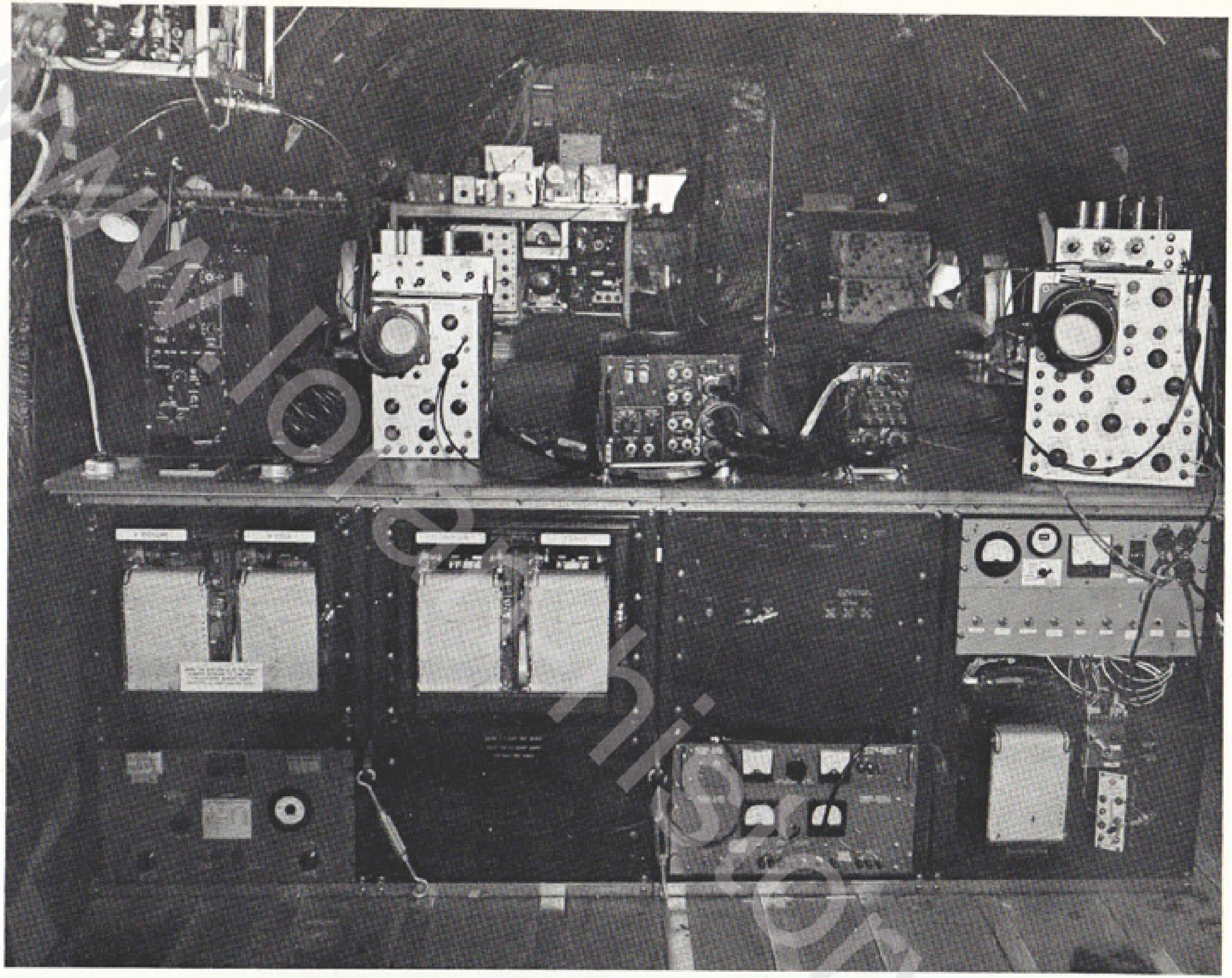

OFFICIAL U.S. COAST GUARD PHOTOGRAPH

FIG. 16

LORAN—C FLIGHT TEST BENCH

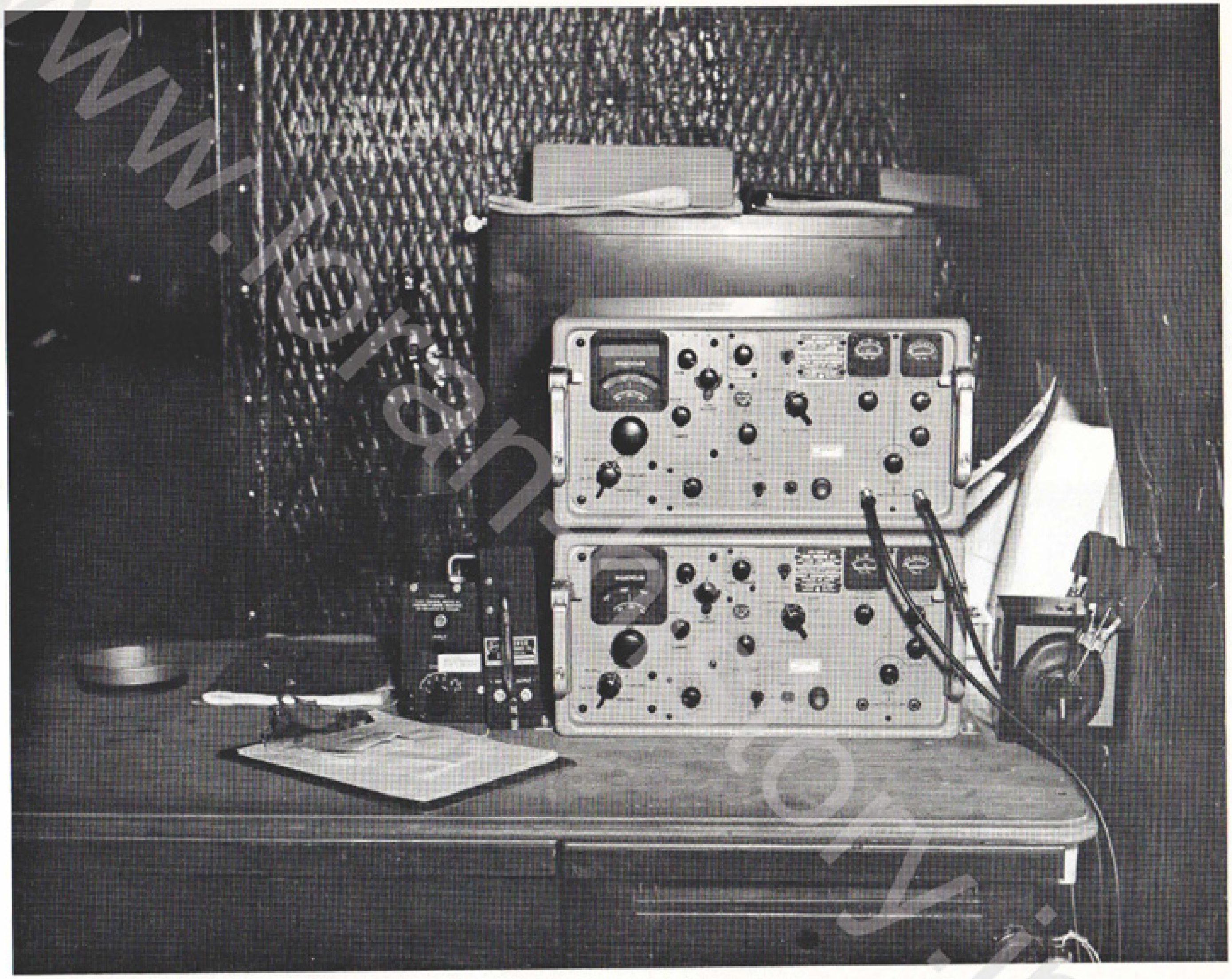

OFFICIAL U.S. COAST GUARD PHOTOGRAPH

FIG. 17

LOW-FREQUENCY MONITORING BENCH

DISTANCE IN
NAUTICAL MILES

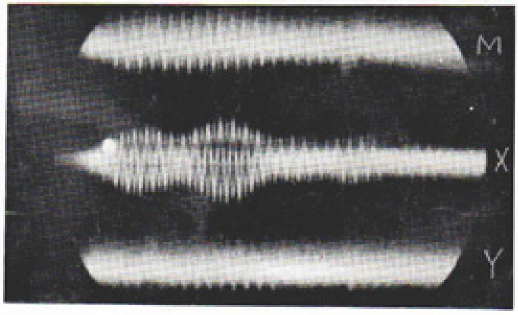

M	1673
X	1445
Y	1906

PIARCO, TRINIDAD
2300 EST MARCH 31, 1958

EXPANDED VIEW OF
MULTI-HOP SKY WAVES
FROM X SLAVE

PIARCO, TRINIDAD
2300 EST MARCH 31, 1958

FIG. 18

	DISTANCE IN NAUTICAL MILES
M	2692
X	2494
Y	2830

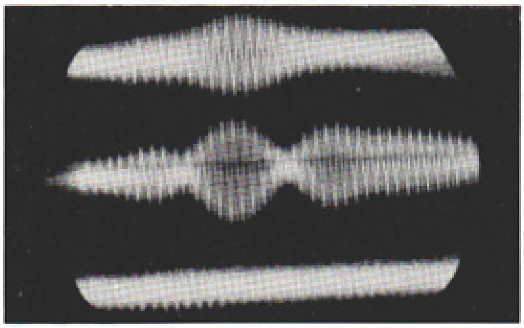

BELEM, BRAZIL
0355 EST APRIL 3, 1958

M	3402
X	3264
Y	3435

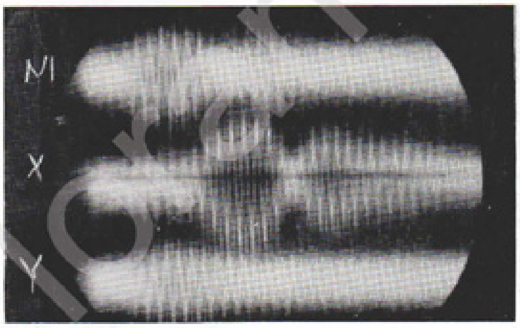

NATAL, BRAZIL
0242 EST APRIL 6, 1958

FIG. 19

DISTANCE IN NAUTICAL MILES

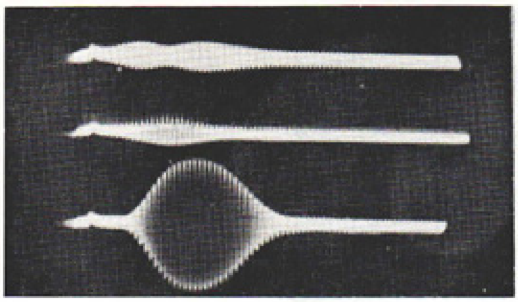

M	1341
X	1731
Y	806

ARGENTIA, NEWFOUNDLAND
0050 EST JUNE 18, 1958

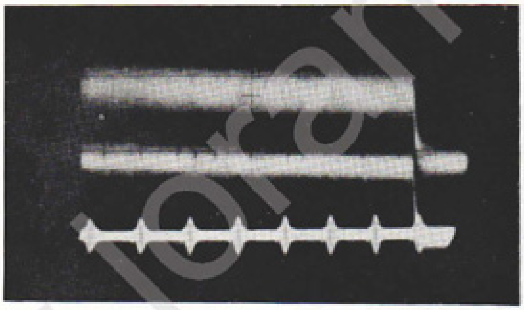

M	2691
X	3115
Y	2142

KEFLAVIK, ICELAND
2015 EST JUNE 19, 1958

FIG. 20

	DISTANCE IN NAUTICAL MILES
M	2446
X	2731
Y	2000

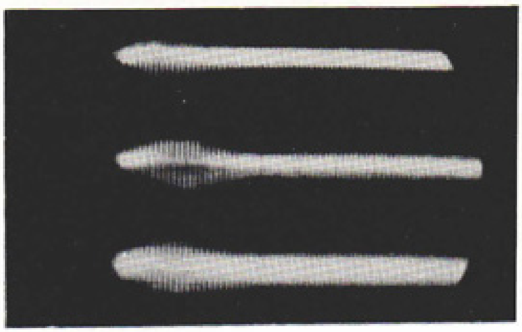

LAGENS, AZORES
0120 EST JULY 5, 1958

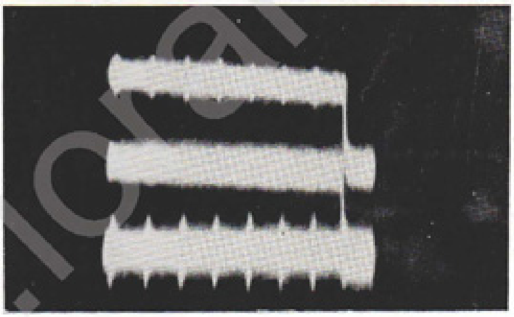

M
X
Y

SLOW SWEEP VIEW SHOWING COMPLETE PULSE GROUP — (8 PULSES)

LAGENS, AZORES
0120 EST JULY 5, 1958

FIG. 21

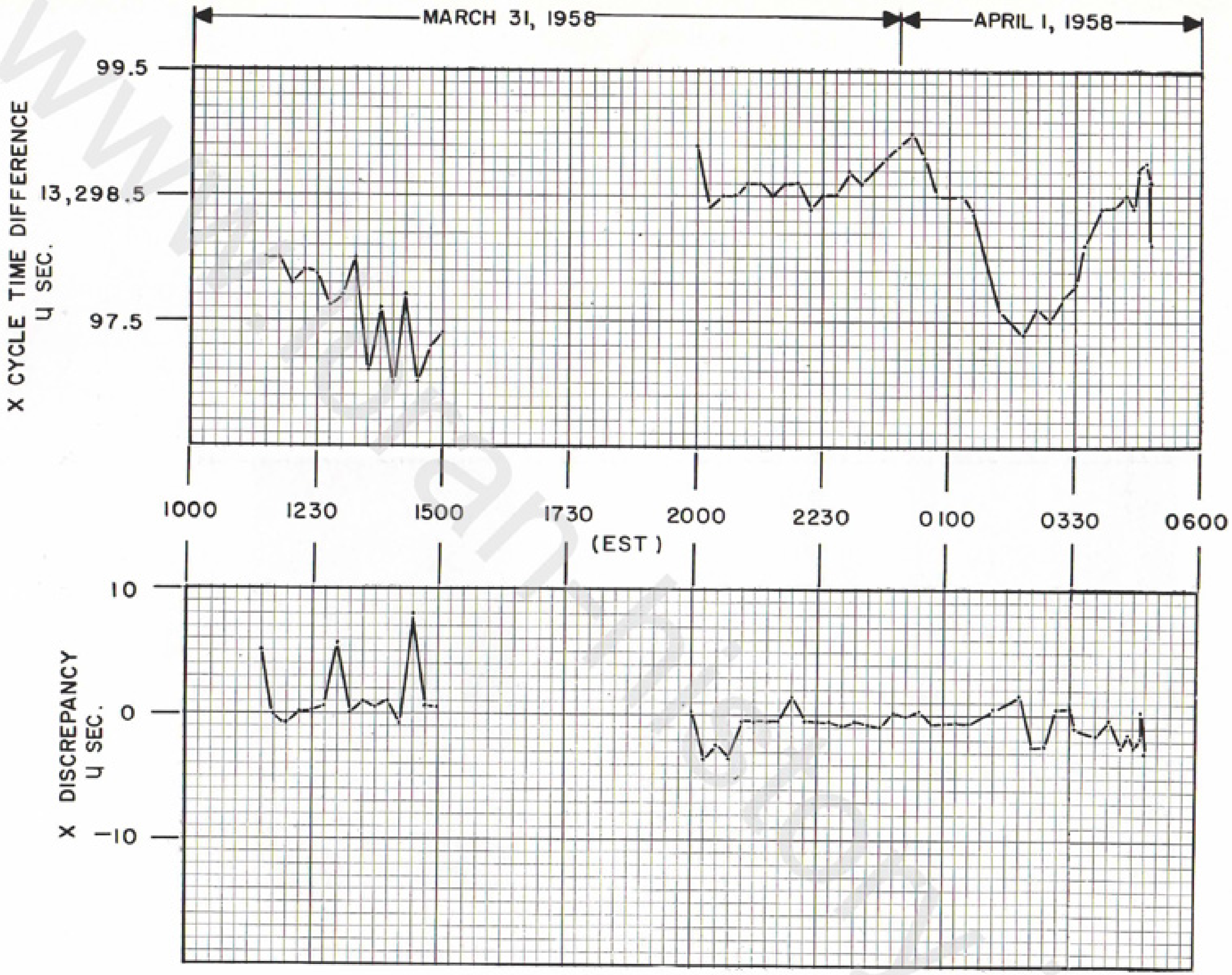

FIG. 22

X CYCLE TIME DIFFERENCE AND DISCREPANCY
PIARCO TRINIDAD
MARCH 31,—APRIL 1, 1958

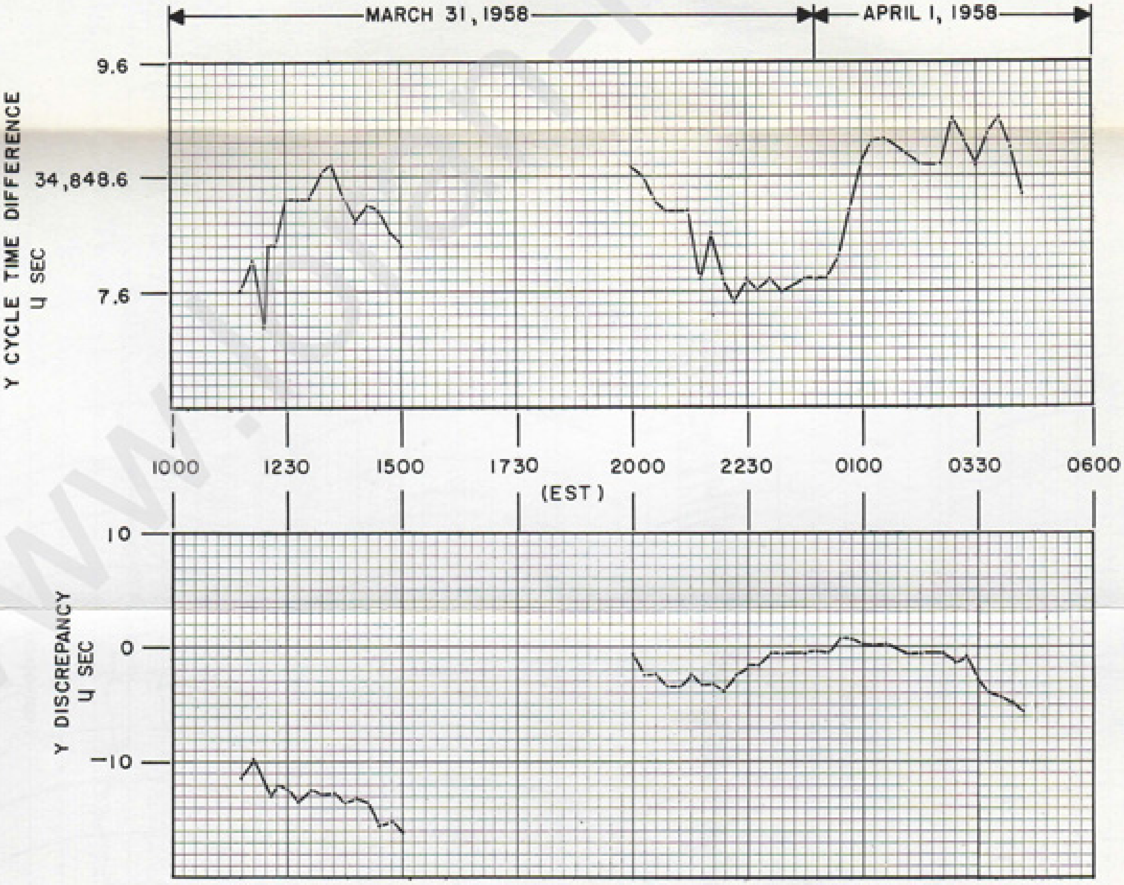

FIG. 23

Y CYCLE TIME DIFFERENCE AND DISCREPANCY
PIARCO TRINIDAD
MARCH 31, —APRIL 1, 1958

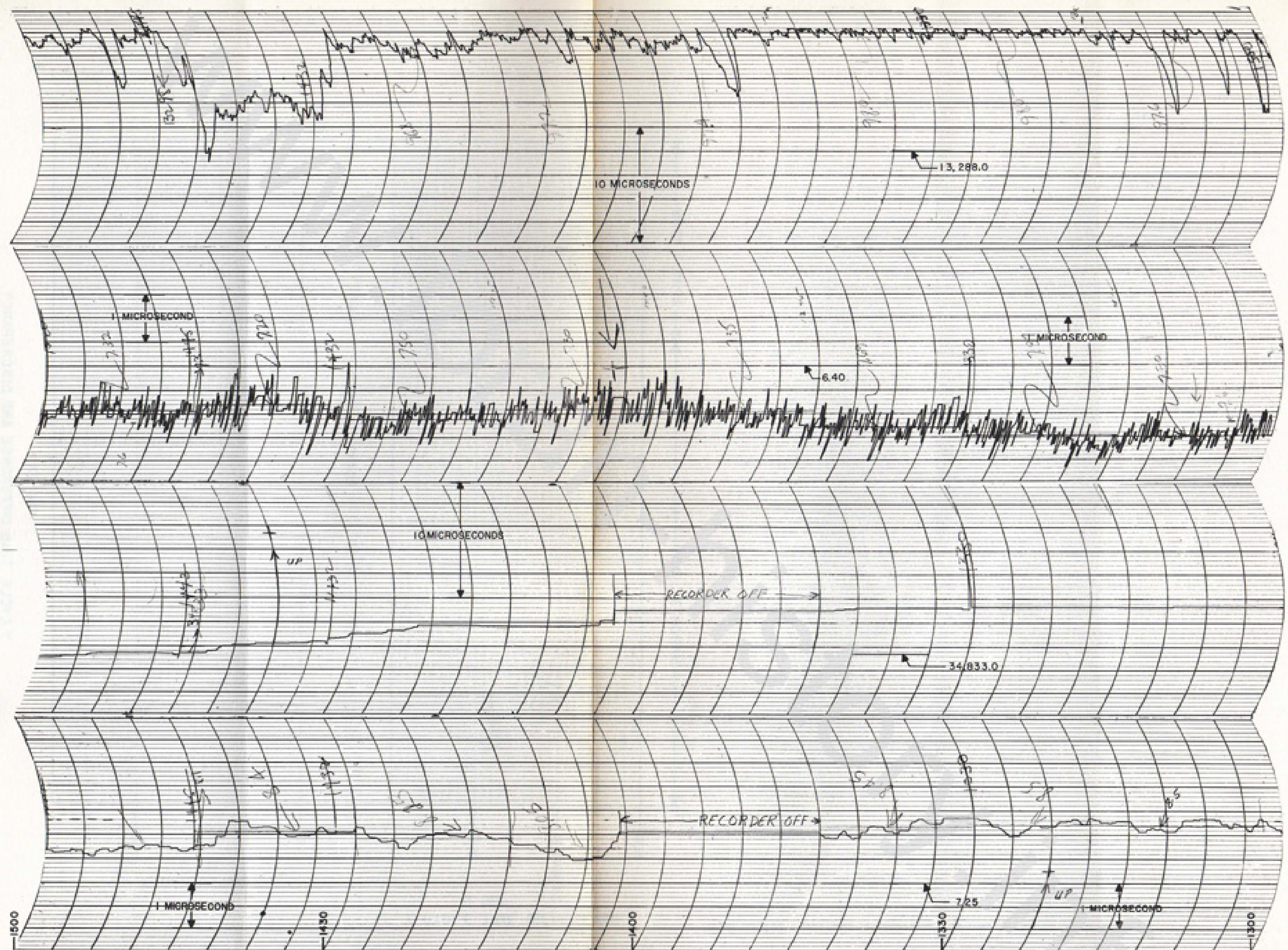

1673 N.M. TO M
1906 N.M TO Y
1442 N.M. TO X

FIG. 24
PIARCO TRINIDAD
31 MARCH, 1958
1300-1500 EST
1 HOP

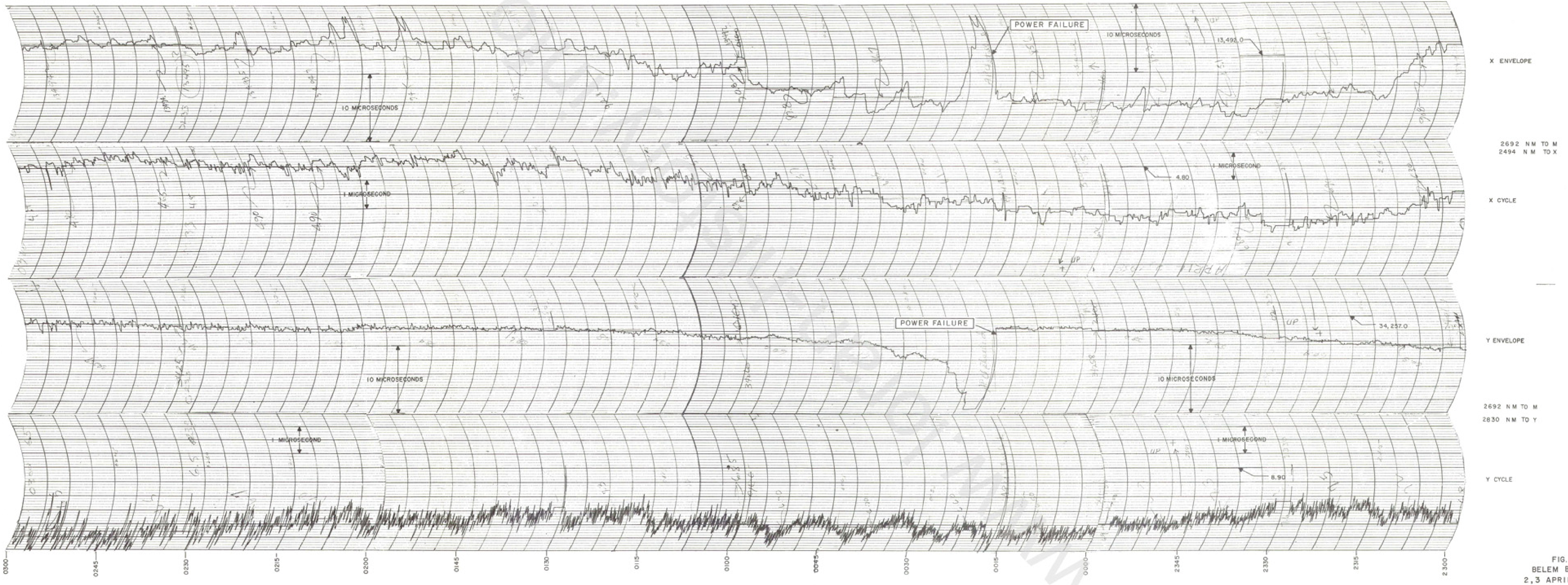

FIG. 25
BELEM BRAZIL
2,3 APRIL, 1958
2300-0300 EST
2 HOP

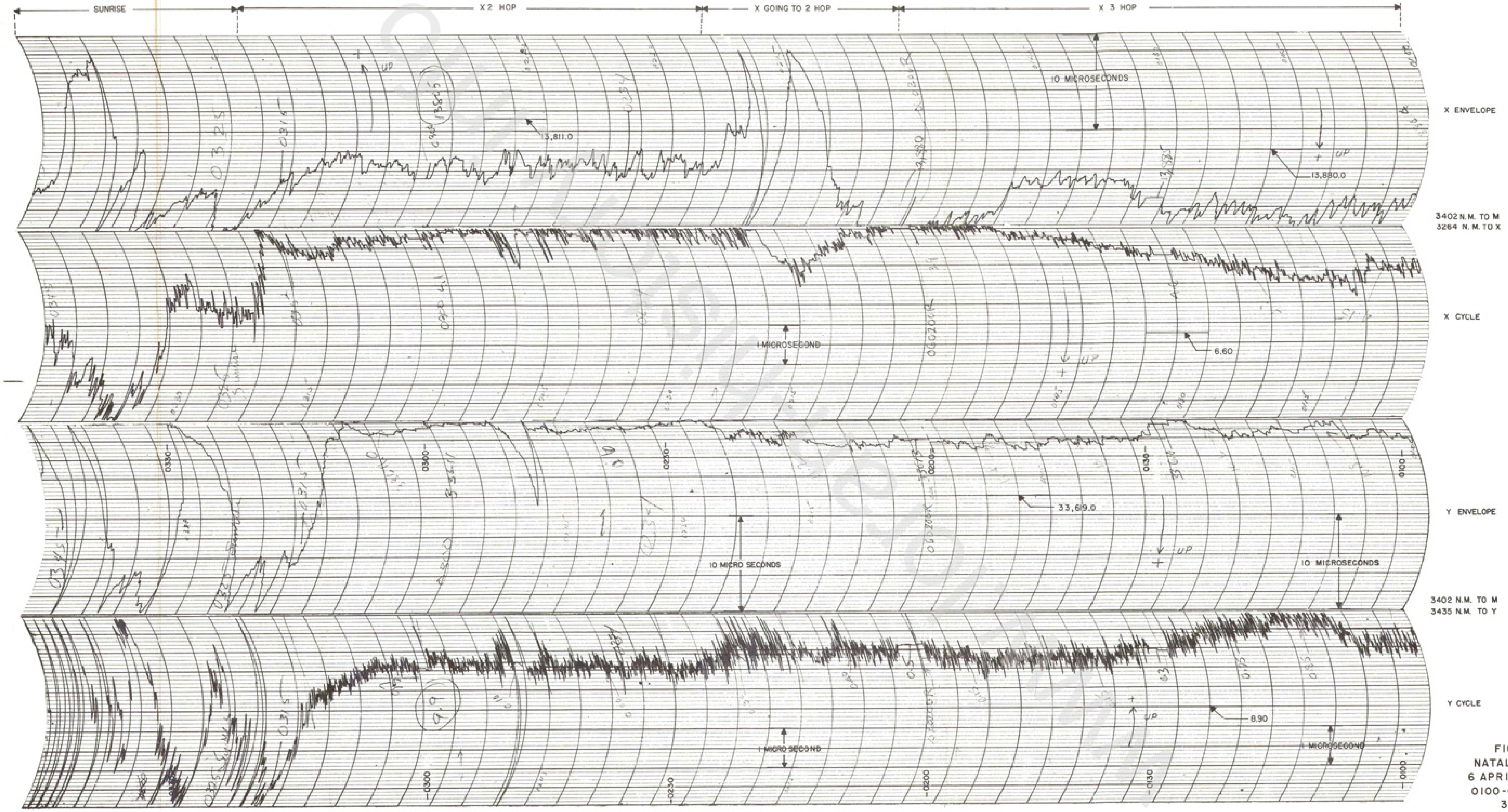

FIG. 26
NATAL BRAZIL
6 APRIL, 1958
0100-0345 EST
3 HOP

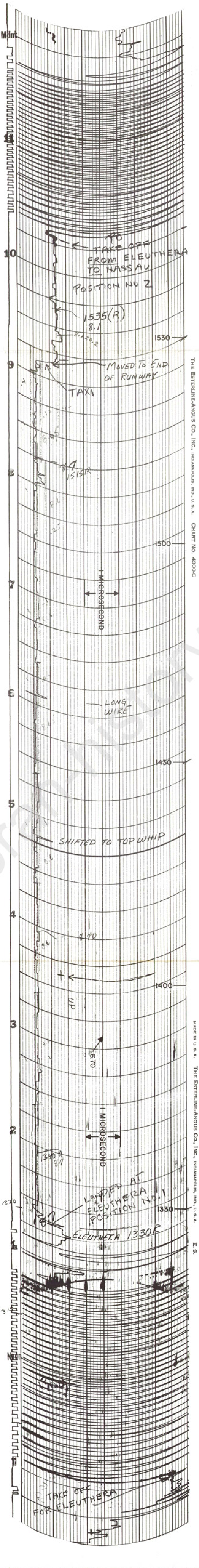

531 NM TO M
227 NM TO X

FIG. 27
ELEUTHERA B.W.I.
9 JULY 1958
1245 - 1545 EST
X CYCLE
GROUND WAVE

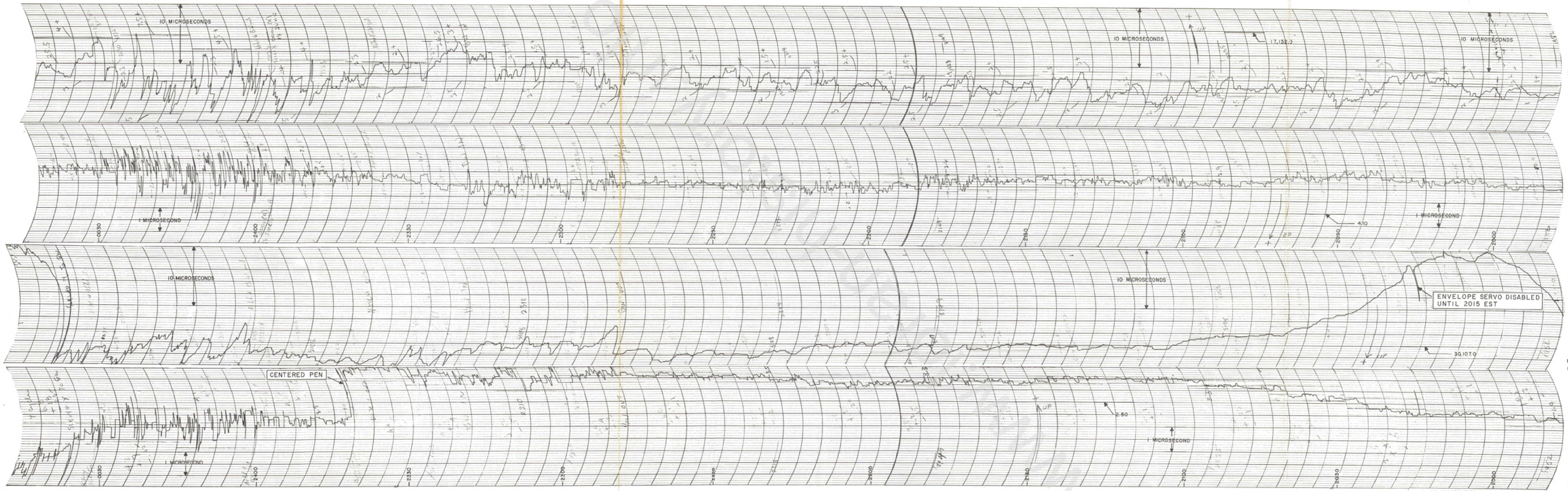

FIG. 28
ARGENTIA NEWFOUNDLAND
17, 18 JUNE, 1958
2000-0045 EST
1 HOP

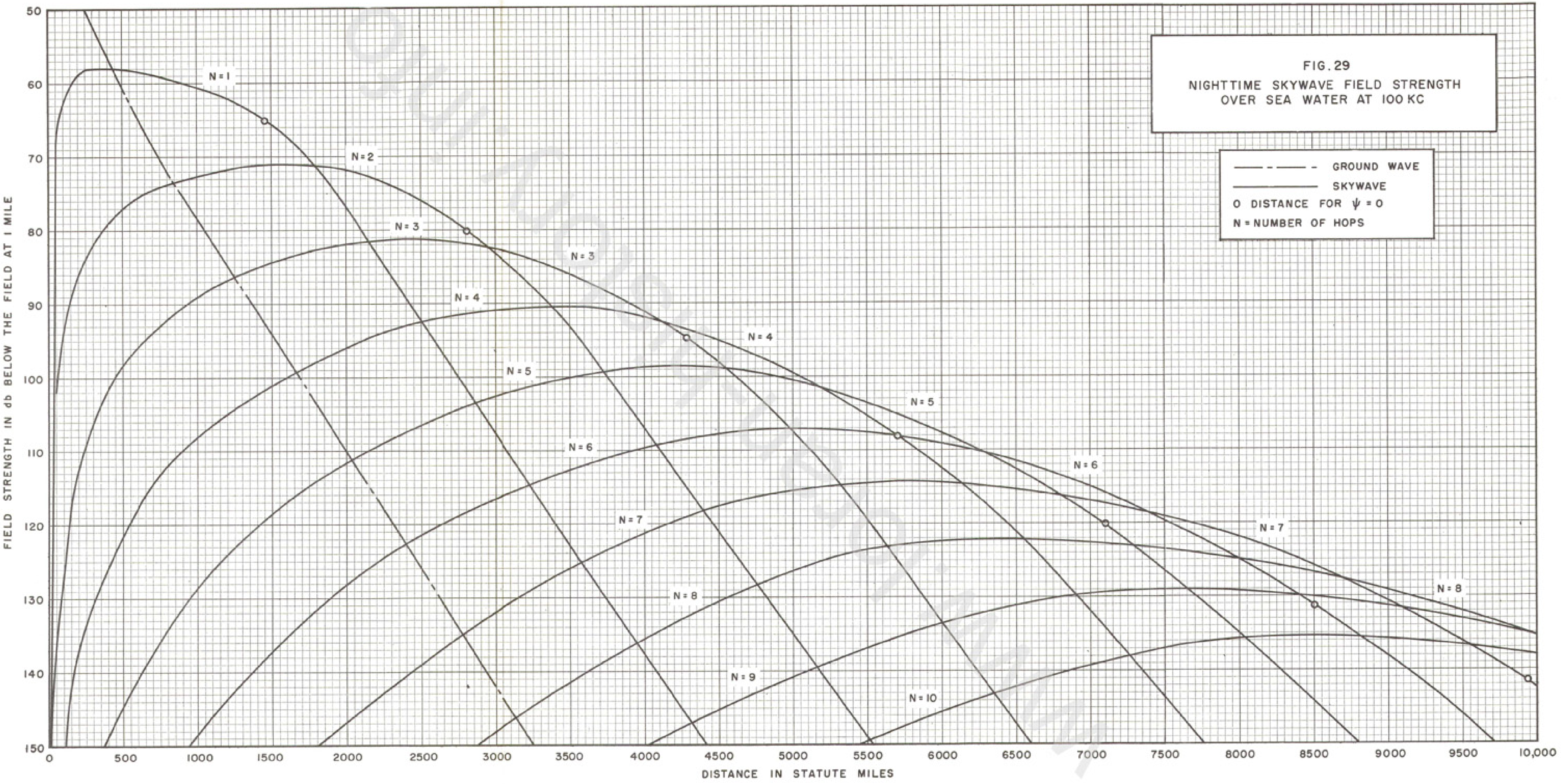

FIG. 29
NIGHTTIME SKYWAVE FIELD STRENGTH OVER SEA WATER AT 100 KC

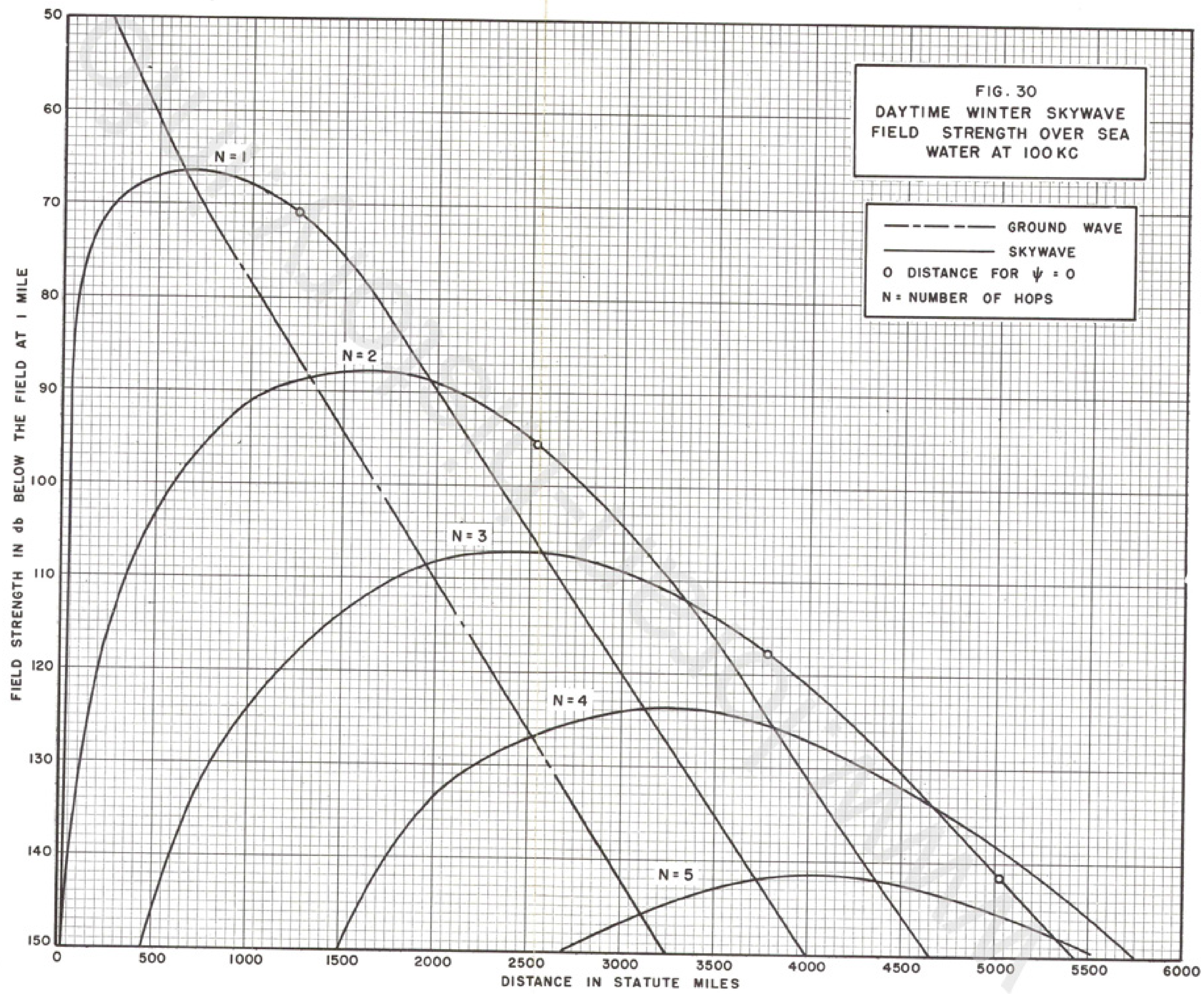
FIG. 30
DAYTIME WINTER SKYWAVE
FIELD STRENGTH OVER SEA
WATER AT 100KC
GROUND WAVE
SKYWAVE
O DISTANCE FOR ψ = 0
N = NUMBER OF HOPS
N = 1
N = 2
N = 3
N = 4
N = 5
FIELD STRENGTH IN db BELOW THE FIELD AT 1 MILE
50
60
70
80
90
100
110
120
130
140
150
0
500
1000
1500
2000
2500
3000
3500
4000
4500
5000
5500
6000
DISTANCE IN STATUTE MILES

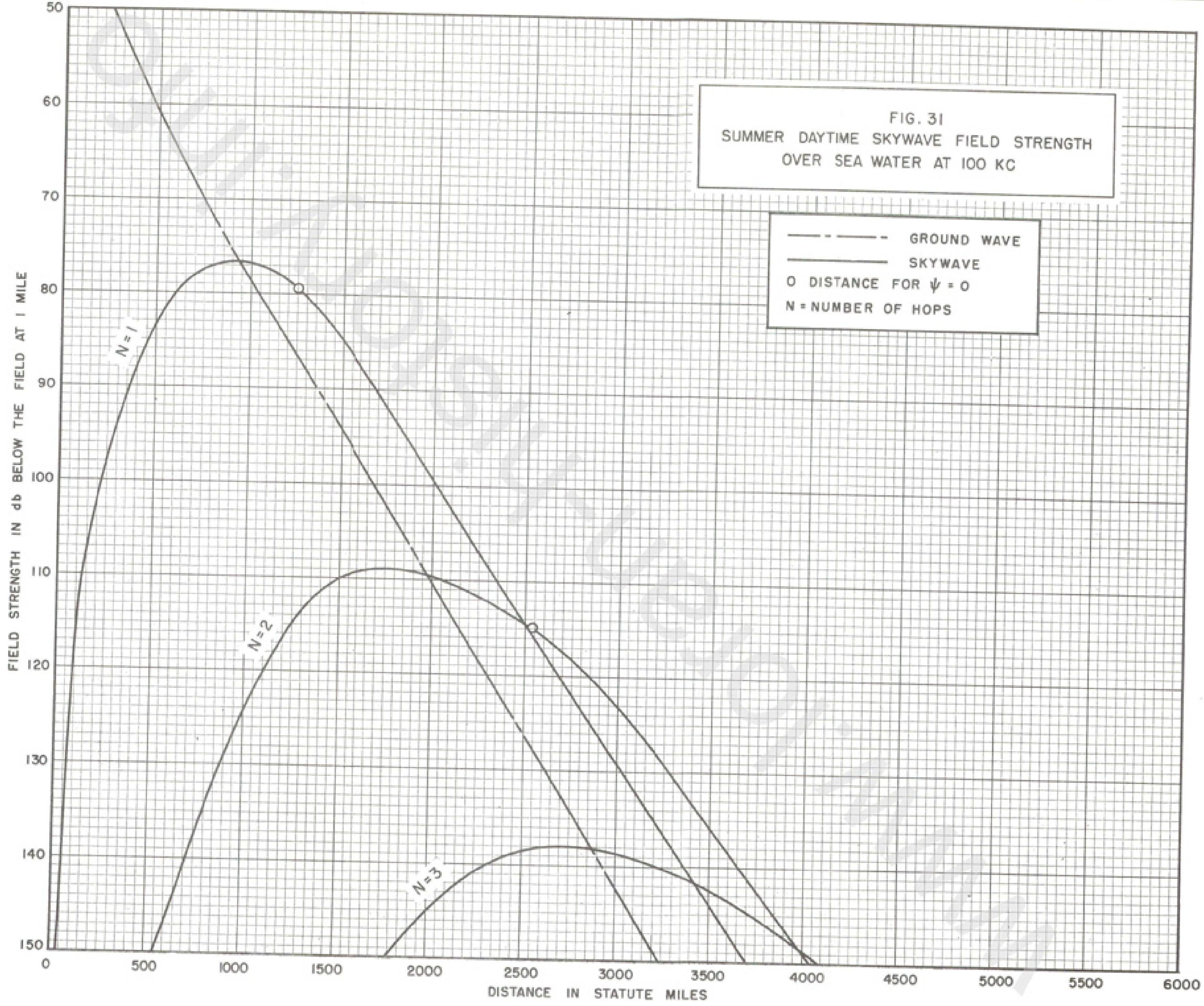
FIG. 31
SUMMER DAYTIME SKYWAVE FIELD STRENGTH
OVER SEA WATER AT 100 KC
GROUND WAVE
SKYWAVE
O DISTANCE FOR $\psi = 0$
N = NUMBER OF HOPS
N=1
N=2
N=3
FIELD STRENGTH IN db BELOW THE FIELD AT 1 MILE
DISTANCE IN STATUTE MILES
50
60
70
80
90
100
110
120
130
140
150
0
500
1000
1500
2000
2500
3000
3500
4000
4500
5000
5500
6000

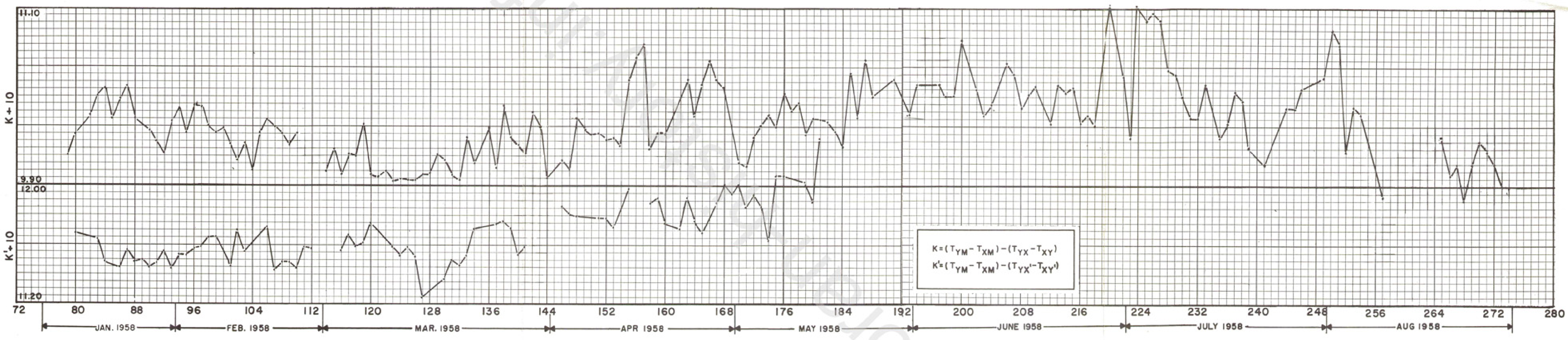

FIG. 32

K-FACTOR VERSUS OPERATING PERIODS

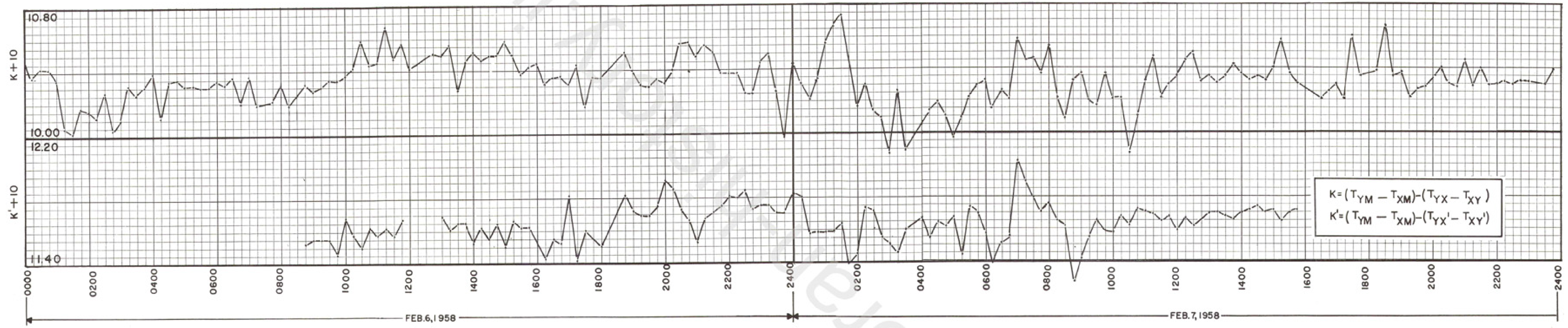

FIG. 33
15 MINUTE AVERAGE
K FACTORS FOR FEBRUARY 6, 7, 1958

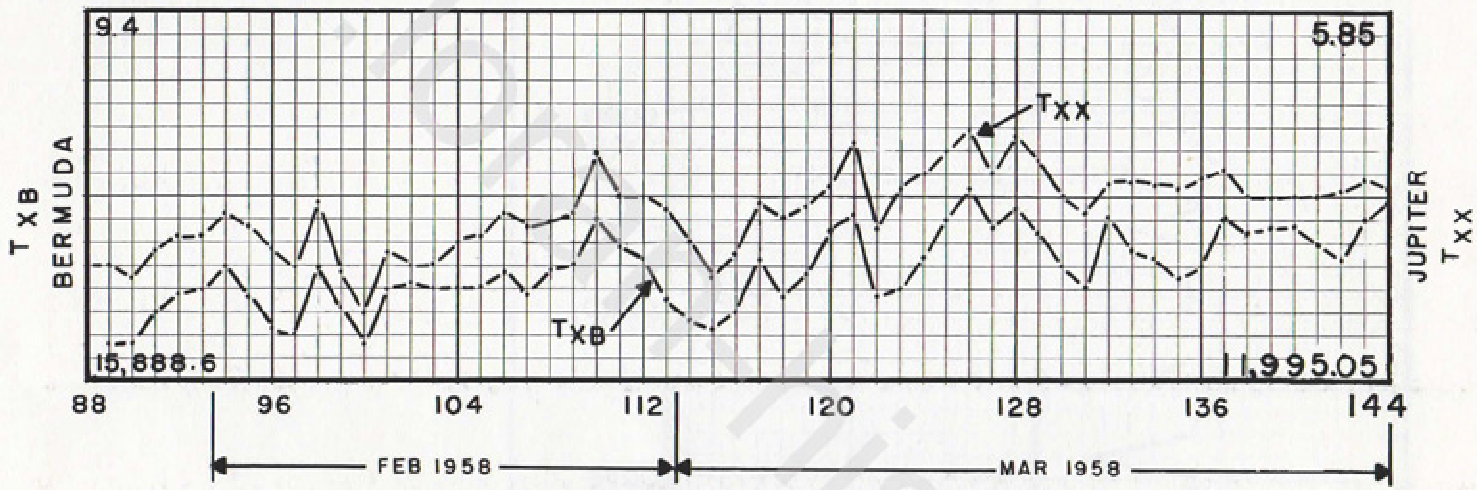

FIG. 34

COMPARISON OF T_{XB} AND T_{XX}

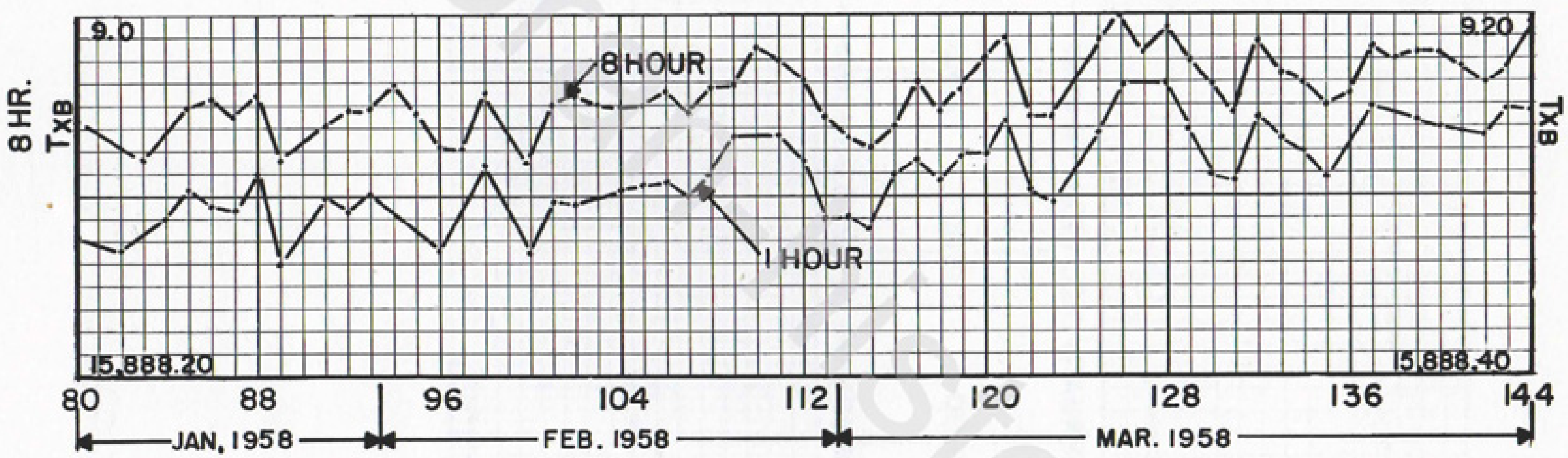

FIG. 35

COMPARISON OF 8 HOUR AND 1 HOUR
AVERAGES AT BERMUDA

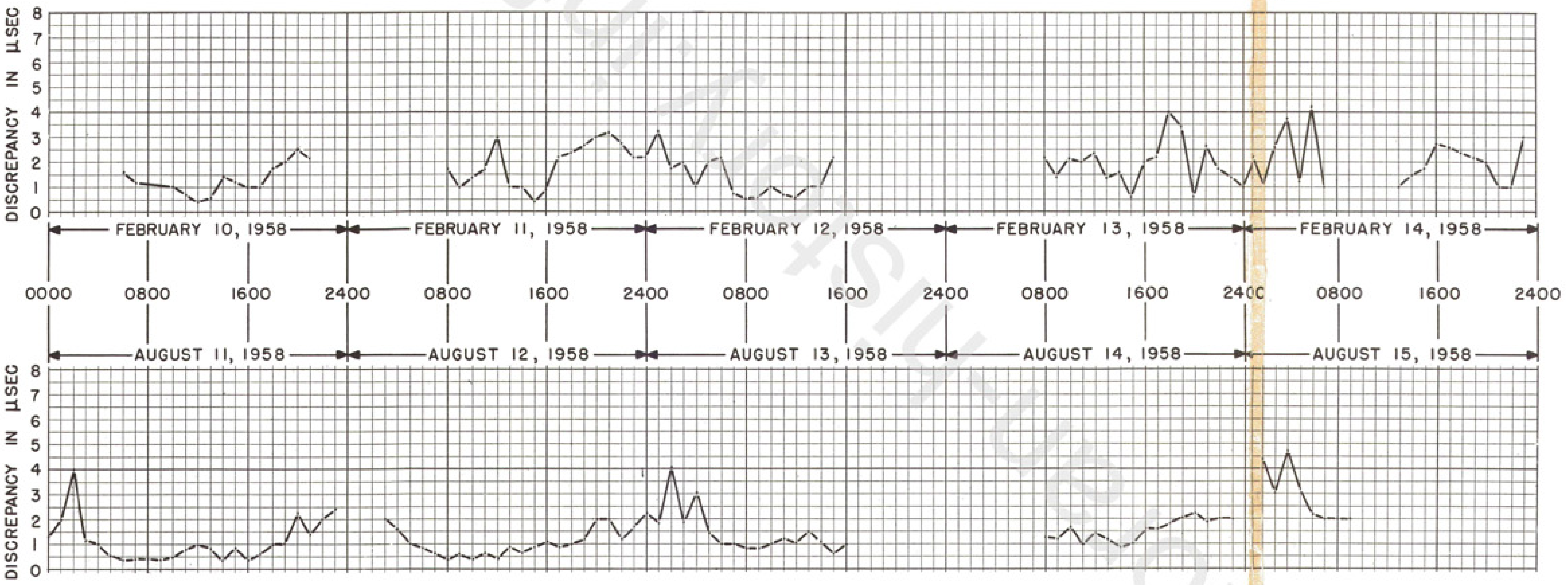

FIG. 36
VALUES EXCEEDED BY
X ENVELOPE-TO-CYCLE DISCREPANCY
FOR 10 PERCENT OF EACH HOUR

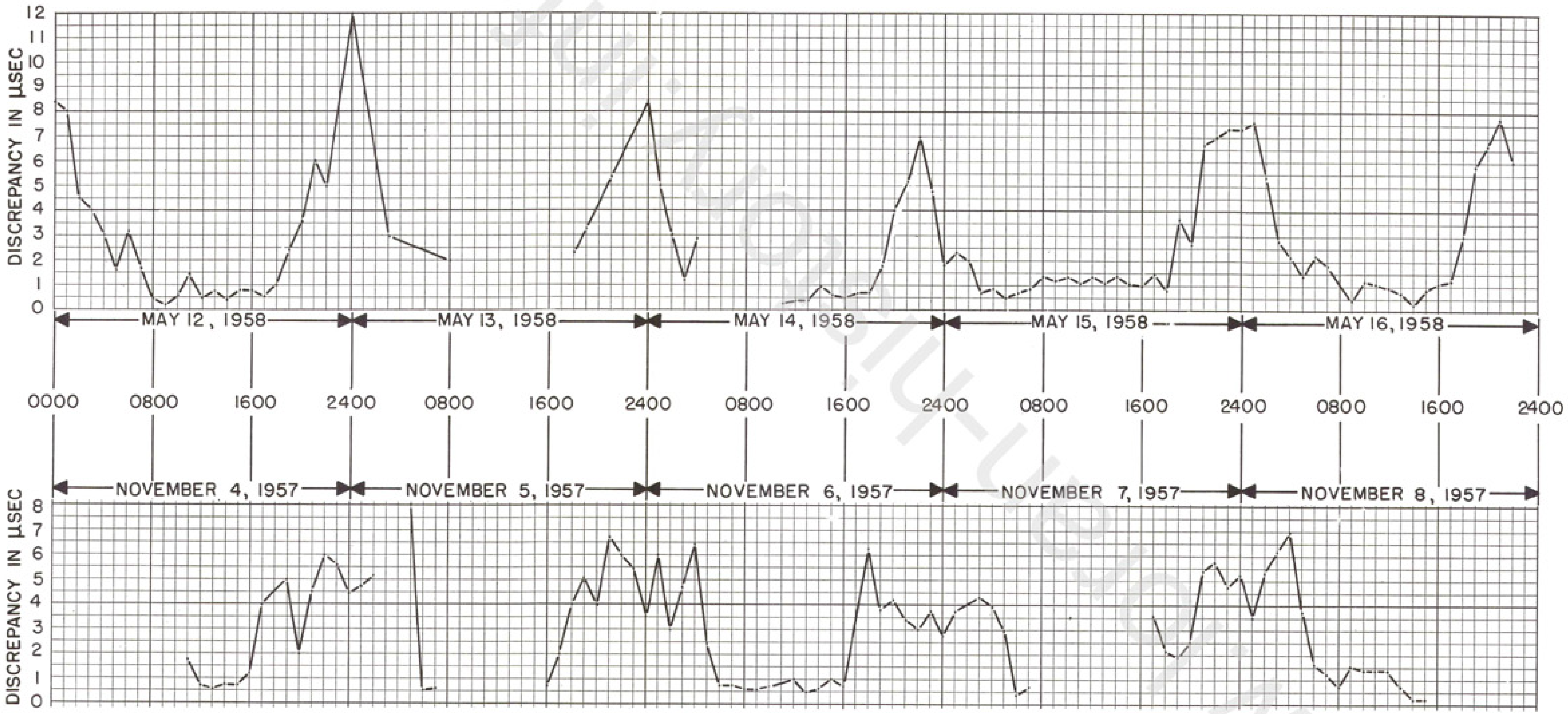

FIG. 37
VALUES EXCEEDED BY
X ENVELOPE-TO-CYCLE DISCREPANCY
FOR 10 PERCENT OF EACH HOUR

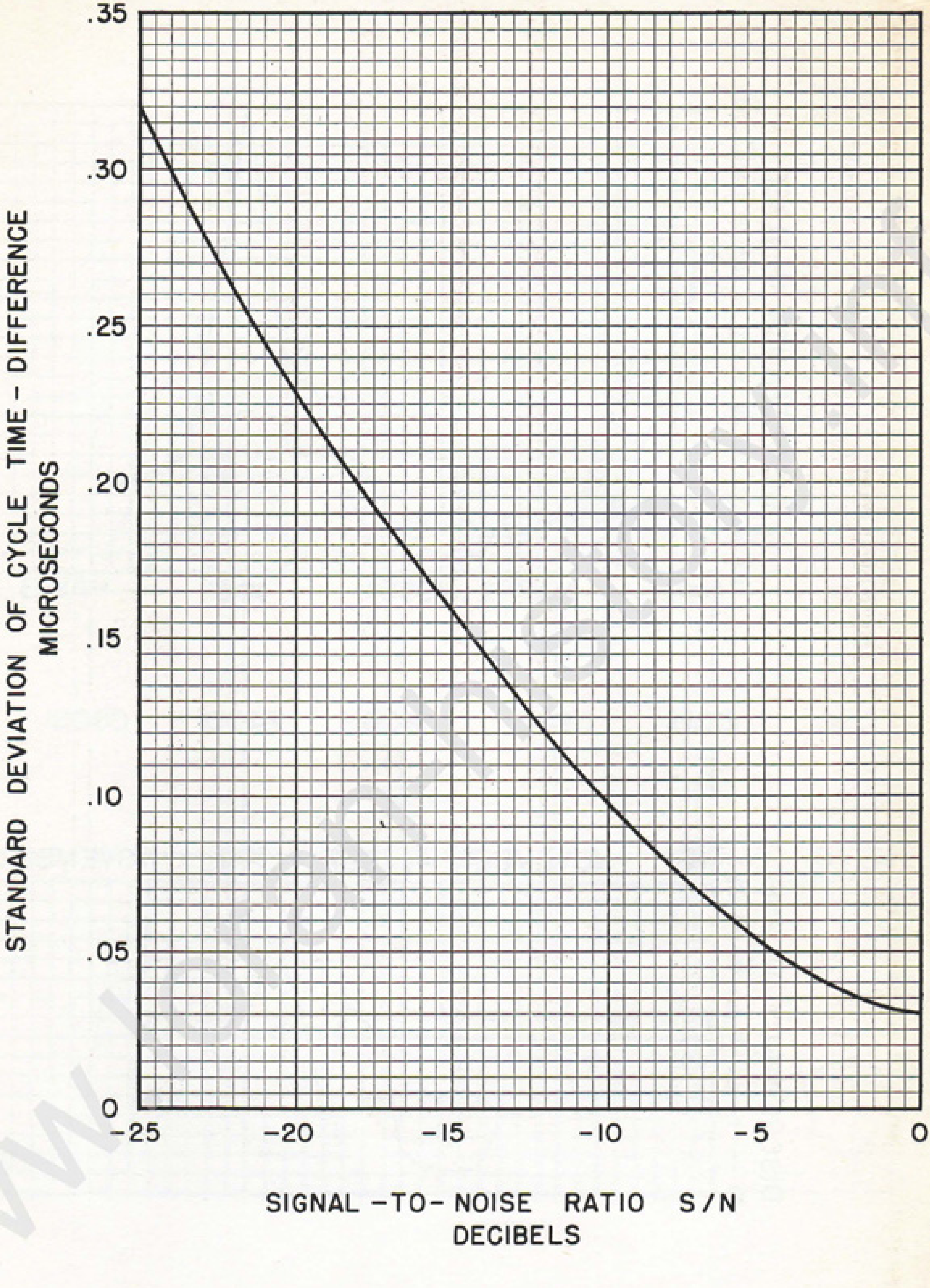

FIG. 38
LORAN-C RECEIVER AN/SPN-28 (XZ-1)
STANDARD DEVIATION OF CYCLE TIME-DIFFERENCE
DUE TO RANDOM NOISE

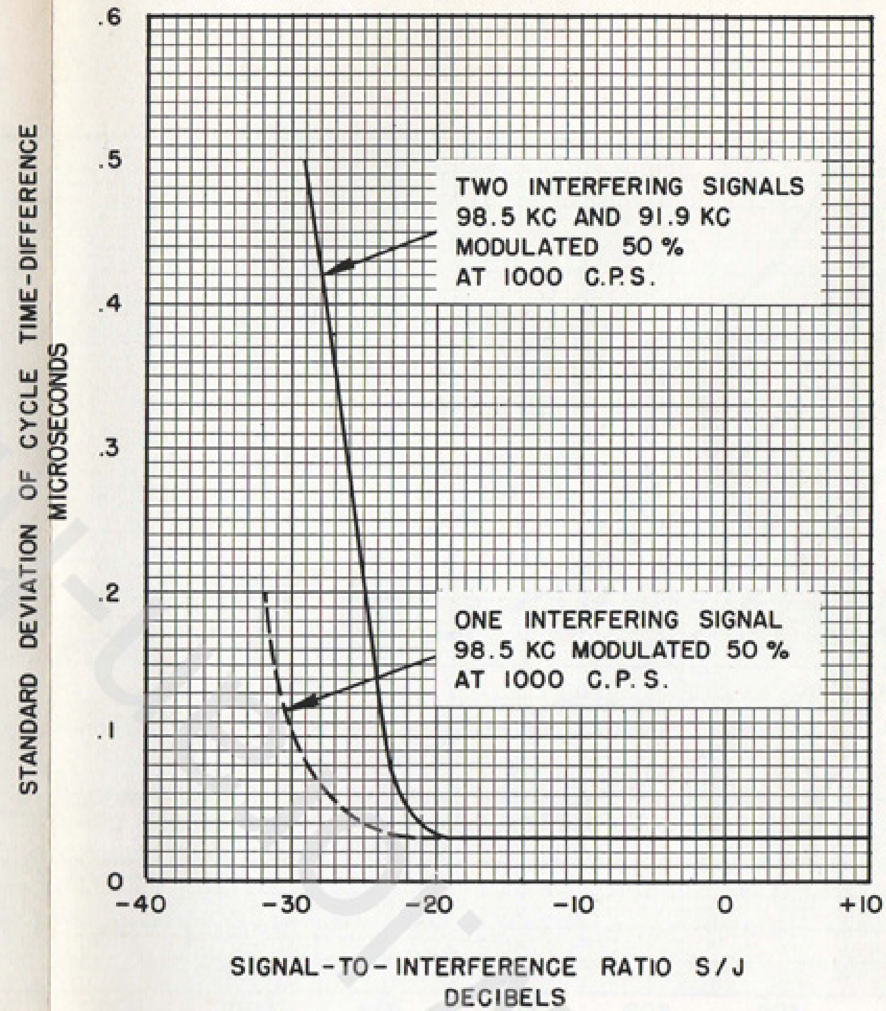

FIG. 39
LORAN-C RECEIVER AN/SPN-28 (XZ-1)
STANDARD DEVIATION OF CYCLE TIME-DIFFERENCE
DUE TO NON-SYNCHRONOUS INTERFERENCE

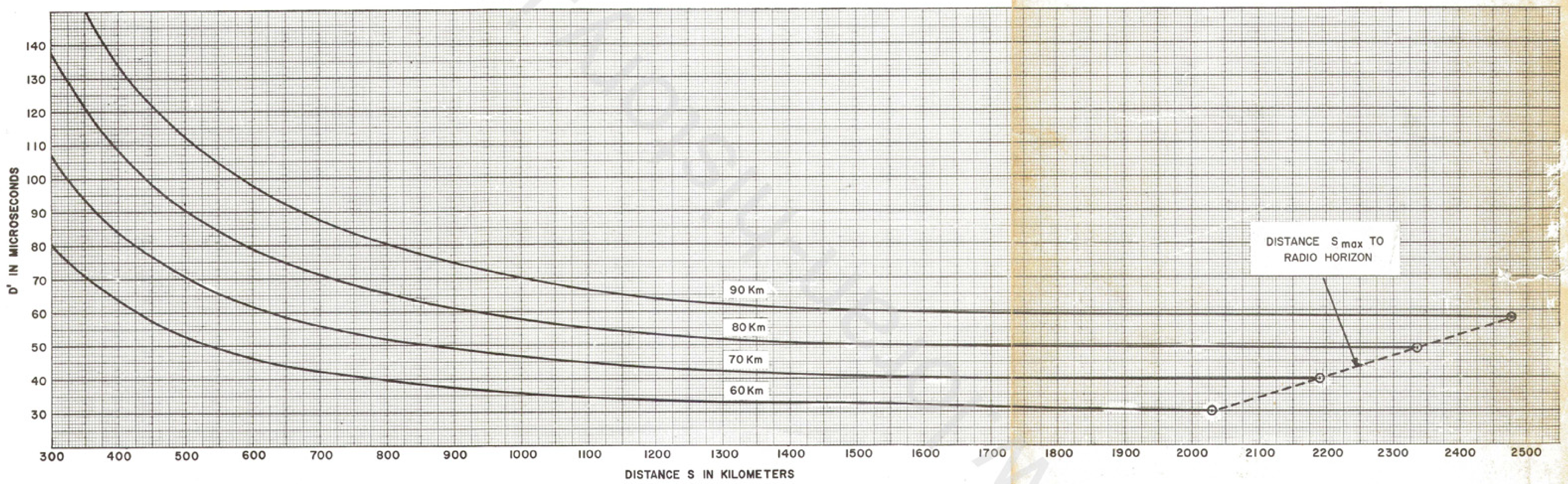

FIG. 40

PRINCIPAL PART OF SKYWAVE DELAY
D' IN MICROSECONDS (VS) S IN KILOMETERS